DESIGN AND CONSTRUCTION OF A SAMPLING SYSTEM THAT CAN COLLECT PM_{10}, $PM_{2.5}$ AND PM_1 SAMPLES SIMULTANEOUSLY FROM ATMOSPHERE

A THESIS SUBMITTED TO
THE GRADUATE SCHOOL OF NATURAL AND APPLIED SCIENCES
OF
MIDDLE EAST TECHNICAL UNIVERSITY

BY

ÖMER ATEŞ

IN PARTIAL FULFILLMENT OF THE REQUIREMENTS
FOR
THE DEGREE OF MASTER OF SCIENCE
IN
ENVIRONMENTAL ENGINEERING

SEPTEMBER 2019

Approval of the thesis:

DESIGN AND CONSTRUCTION OF A SAMPLING SYSTEM THAT CAN COLLECT PM10, PM2.5 AND PM1 SAMPLES SIMULTANEOUSLY FROM ATMOSPHERE

submitted by **ÖMER ATEŞ** in partial fulfillment of the requirements for the degree of **Master of Science in Environmental Engineering Department, Middle East Technical University** by,

Prof. Dr. Halil Kalıpçılar
Dean, Graduate School of **Natural and Applied Sciences** _____

Prof. Dr. Bülent İçgen
Head of Department, **Environmental Eng.** _____

Prof. Dr. Gürdal Tuncel
Supervisor, **Environmental Eng., METU** _____

Examining Committee Members:

Assoc. Prof. Dr. Tuba Hande Ergüder Bayramoğlu
Environmental Eng., METU _____

Prof. Dr. Gürdal Tuncel
Environmental Eng., METU _____

Prof. Dr. Eftade Gaga
Environmental Eng., Eskişehir Technical University _____

Assist. Prof. Dr. Ebru Koçak
Environmental Eng., Aksaray University _____

Assoc. Prof. Dr. Fatma Öztürk
Environmental Eng., Abant İzzet Baysal University _____

Date: 03.09.2019

I hereby declare that all information in this document has been obtained and presented in accordance with academic rules and ethical conduct. I also declare that, as required by these rules and conduct, I have fully cited and referenced all material and results that are not original to this work.

Name, Surname: Ömer Ateş

Signature:

ABSTRACT

DESIGN AND CONSTRUCTION OF A SAMPLING SYSTEM THAT CAN COLLECT PM_{10}, $PM_{2.5}$ AND PM_1 SAMPLES SIMULTANEOUSLY FROM ATMOSPHERE

Ateş, Ömer
Master of Science, Environmental Engineering
Supervisor: Prof. Dr. Gürdal Tuncel

September 2019, 147 pages

In this study, a particulate matter (PM) sampling system that can collect PM_{10} (particulate matter with diameter of less than 10 μm), $PM_{2.5}$ and PM_1 samples simultaneously with a single pump on separate filters was constructed and validated. The sampler consisted of a F&J Specialty DF-1E carbon vane vacuum pump, with a flowrate of 115 L/min, and 3 channels connected to the pump through a manifold. Each channel had a cyclone, a filter holder of 47 mm diameter, a micro-orifice (critical orifice) for velocity control and a flowmeter. Diameter of the particles were controlled by the cyclones. The particles passing through the cyclones was collected at the filters. The sampler was first constructed with MFCs, then MFCs were replaced with critical orifices. Afterwards, components were placed into the permanent shelter and data logger system was installed and flow rate stability tests were carried out using Nuclepore and Teflon filters. Teflon filters were selected for better stability. Validation was carried out through parallel sampling of the new sampler against 1 SFU, 2 Hi-vol samplers and 1 Grimm EDM164 laser spectrometer for 24 days. Average concentrations were found for PM_{10}, $PM_{2.5}$ and PM_1 as 25 ± 10, 13 ± 4.4 and 7.6 ± 2.9 μg m^{-3} respectively, which were in a good agreement with other samplers. The sampler constructed in this study is not currently available in the market and the

final configuration cost around 57,000 ₺ (~$15,700) which is less than half of dichotomous sampler or 3 pcs. of single channel samplers that can fulfill the same sampling task.

Keywords: Particle Sampler, Cyclone, Critical Orifice, PM_{10}, $PM_{2.5}$, PM_1

ÖZ

ATMOSFERDEN PM_{10}, $PM_{2.5}$ VE PM_1 PARÇACIKLARI EŞ ZAMANLI OLARAK TOPLAYABİLECEK, EKONOMİK BİR ÖRNEKLEME SİSTEMİNİN GELİŞTİRİLMESİ

Ateş, Ömer
Yüksek Lisans, Çevre Mühendisliği
Tez Danışmanı: Prof. Dr. Gürdal Tuncel

Eylül 2019, 147 sayfa

Bu çalışma kapsamında; atmosferden PM_{10} (çapları 10 μm'dan küçük parçacıklar), $PM_{2.5}$ ve PM_1 parçacıkları eş zamanlı olarak ayrı filtrelerde toplayabilen bir örnekleme sistemi geliştirilmiştir. Örnekleyici; 1 adet karbon paletli vakum pompası (F&J Specialty DF-1E), ve manifold aracılığıyla bağlanan 3 kanal içermektedir. Her kanalda; 1 siklon, 1 filtre tutucu (47 mm filtre için), hız kontrolü için 1 kritik orifis ve 1 akış ölçer (flow metre) bulunmaktadır. Parçacıkların boyutları siklonlar tarafından kontrol edilmektedir ve siklonlardan geçen parçacıklar filtre tutucuların içindeki filtrelerde toplanmıştır. Örnekleyici, ilk olarak MFC'ler kullanılarak kurulmuş, daha sonra MFC'ler kritik orifislerle değiştirilmiştir. Ardından örnekleyici bileşenleri dayanıklı bir kabine kutulanarak veri kaydedici (data logger) sistemi kurulmuş. Nuclepore ve Teflon filtreler kullanılarak akış stabilite testleri yapılmış, teflon filtrelerin daha stabil olduğu gözlenmiş bu nedenle tercih edilmiştir. Validasyon çalışmalarında; yeni örnekleyici, 1 SFU 2 yüksek hacimli (Hi-vol) örnekleyici ve 1 Grimm EDM164 lazer spektrometre ile 24 gün boyunca paralel örnekleme yapılmıştır. Bu süreçte; PM_{10}, $PM_{2.5}$ ve PM_1 için ortalama konsantrasyonlar sırasıyla 25 ± 10, 13 ± 4.4 ve 7.6 ± 2.9 μg m^{-3} olarak bulunmuş ve bu sonuçların diğer örnekleyicilerden alınan sonuçlarla uyum gösterdiği tespit edilmiştir. Bu çalışmada geliştirilen

örnekleyici piyasada mevcut olmayıp, nihai konfigürasyonun yaklaşık maliyeti 57,000 ₺ (~$15,700) olmuştur, bu miktar; dichotomous örnekleyicinin veya aynı örnekleme işini yapabilecek 3 adet tek kanallı örnekleyicinin maliyetinin yarısından daha az bir miktara karşılık gelmektedir.

Anahtar Kelimeler: Partikül Örnekleyici, Siklon, Kritik Orifis, PM_{10}, $PM_{2.5}$, PM_1

In the hope of a world, where all these efforts matter…

ACKNOWLEDGEMENTS

First and foremost, I would like to express my deepest gratitude to my advisor Prof. Dr. Gürdal Tuncel for his guidance, advice, support and patience throughout this study. I feel grateful to have the opportunity to work with him.

I would like to sincerely thank my examining committee members Prof. Dr. Eftade Gaga, Assoc. Prof. Dr. Tuba Hande Ergüder Bayramoğlu, Assoc. Prof. Dr. Fatma Öztürk and Assist. Prof. Dr. Ebru Koçak for their evaluations and contributions.

I would like to specially thank to İlke Çelik, Dr. İlker Balcılar and Assist. Prof. Dr. Ebru Koçak for sharing their knowledge and endless support on theoretical and laboratory works throughout this study.

I would like to thank to former and current members of our Air Pollution and Quality Research Group Elif Sena Uzunpınar, Tayebeh Goli, Ezgi Sert, Sema Yurdakul, Tuğçe Bek and Gizem Yücel for their friendship, support and cooperation.

Finally, I would like to express my deepest gratitude and love to my family for their unconditional love and everything they have done for me through my life.

This study was financially supported by The Scientific and Technological Research Council of Turkey (TÜBİTAK) under project no 114Y160.

TABLE OF CONTENTS

ABSTRACT v

ÖZ vii

ACKNOWLEDGEMENTS x

TABLE OF CONTENTS xi

LIST OF TABLES xv

LIST OF FIGURES xvi

CHAPTERS

1. INTRODUCTION 1

1.1. Purpose of the study 1

1.2. Action plan of the study 1

1.3. Rationale behind the study 2

2. LITERATURE REVIEW 5

2.1. General information about PM 5

2.1.1. Sources of PM 8

2.1.2. Health & Environmental Effects of PM 14

2.1.2.1. Health effects of atmospheric particles 14

2.1.2.2. Impacts of particles on haze formation 17

2.1.2.3. Impacts of particles on hydrologic cycle 18

2.1.2.4. Climate change effects of atmospheric particles 20

2.2. Particulate matter sampling systems 21

2.2.1. High volume samplers 21

2.2.1.1. Total suspended particulate matter (TSP) sampler 21

2.2.1.2. In-Stack Particulate Filtration 22
2.2.1.3. Trichotomous Sampler 23
2.2.2. Low volume samplers 25
2.2.2.1. In-Stack Particulate Filtration 25
2.2.2.2. Beta attenuation monitoring (BAM) samplers 27
2.2.2.3. Tapered Element Oscillating Microbalance (TEOM®) 29
2.2.2.4. Dichotomous Air Sampler 31
2.2.2.5. Laser Aerosol Spectrometry 32
2.2.2.6. GENT Stacked Filter Unit 33
2.3. Flow rate control in PM sampling 34
2.3.1. Mass flow controllers (MFC) 35
2.3.2. Critical orifices 35
2.3.3. Filters used in air pollutant sampling 37
2.3.3.1. Membrane filters 37
2.3.3.2. Glass and quartz fiber filters 37
2.3.3.3. Polycarbonate filters 37
3. MATERIALS AND METHODS 39
3.1. Location of the study 39
3.2. Strategy followed in development of the sampler 41
3.2.1. Development of general structure of the device 42
3.2.2. Determination of the constituents to be used 43
3.2.3. Procurement of the constituents 43
3.2.4. Construction of the device using MFC 44
3.2.5. Physical & electrical controls and operation of the device 45

3.2.6. Replacement of MFCs with critical orifices 45
3.2.7. Composing a data acquisition system to record air flow rates 46
3.2.8. Assembling of the constituents into a shelter 47
3.2.9. Validation studies 47
3.3. Components of the Sampler 47
3.3.1. Cyclones.....48
3.3.2. Filter Holders 52
3.3.3. Mass Flow Controllers.....53
3.3.4. Pump 54
3.3.5. Critical Orifices.....55
3.3.6. Manifold and pneumatic connections 56
4. RESULTS AND DISCUSSION 59
4.1. Construction of the sampler with mass flow controllers 59
4.1.1. Installation of the sampler.....59
4.1.2. Installation of the sampler using mass flow controllers and monitoring of the flow rates.....62
4.1.3. Installation of feedback system.....63
4.1.4. Comparison of the sampler with MFCs against the “Stack Filter Unit” ..65
4.2. Construction of the sampler with critical orifices 66
4.3. Variation of air flow rate with respect to various filter types.....69
4.4. Repeatability tests.....76
4.5. Construction of data logger and control unit.....78
4.5.1. Sampling system micro controller software 79
4.6. Flow rate stability tests.....80

4.6.1. Flow characteristics of the sampler when mass flow controllers are used in channels 81
4.6.2. Sampler configured with critical orifices 85
4.6.3. 1-channel and 3-channel comparison 91
4.7. Assembling of the sampler into a shelter 95
4.8. Validation studies 97
4.9. Comparison of cost of the sampler developed in this study with available samplers 104
5. CONCLUSION 115
REFERENCES 119
APPENDICES
A. Literature where SFU was used in sampling of atmospheric particles 129
B. Data logger system user manual 145

LIST OF TABLES

TABLES

Table 3.1. List of equipment purchased for construction of the sampler.....43
Table 4.1. Concentrations of PM_1, $PM_{2.5}$ and PM_{10} measured by different samplers operated side-by-side (concentrations are in $\mu g\ m^{-3}$).....100
Table 4.2 Prices of the components used in the sampler 105
Table 4.3. Cost of the sampler with MFC configuration 107
Table 4.4. Cost of the sampler with critical orifice configuration 108
Table 4.5. Market research for samplers comparable to the sampler designed in this study 110
Table 4.6. Cost of the sampler with solely $PM_{2.5}$ sampler configuration 113

LIST OF FIGURES

FIGURES

Figure 2.1. Typical aerosol size distribution in the atmosphere 7
Figure 2.2. Size classification of typical aerosols..... 7
Figure 2.3. National $PM_{2.5}$ emissions by source sector 8
Figure 2.4. $PM_{2.5}$ source contribution for seven US cities 11
Figure 2.5. Results of a PM_{10} source apportionment study performed at a roadside location in New York City in April 1992 12
Figure 2.6. Global sources of $PM_{2.5}$ components and precursors..... 14
Figure 2.7. Exposure extent of particulate matter by their sizes 15
Figure 2.8. Summary of relative risks for mortality by different air pollutants 17
Figure 2.9. The three ways pollutants can visually degrade a scenic vista 18
Figure 2.10. Total Suspended Particles (TSP) Sampler 21
Figure 2.11. High Volume PM_{10} Sampler 23
Figure 2.12. $PM_{1.0/2.5/10}$ Trichotomous Sampler..... 25
Figure 2.13. Andersen RAAS10-100 PM_{10} sampler 26
Figure 2.14. Tisch Environmental Model TE-Wilbur2.5 Particulate Sampler..... 27
Figure 2.15. Schematic diagram of a BAM device 29
Figure 2.16. TEOM® sampler schematic diagram..... 30
Figure 2.17. Dichotomous Air Sampler..... 31
Figure 2.18. Grimm EDM180 Laser Aerosol Spectrometer..... 32
Figure 2.19. Schematic Diagram for GENT Stacked Filter Unit 33
Figure 2.20. Stack Filter Unit (SFU) sampling system 34
Figure 2.21. Operation principle of critical orifices 36
Figure 3.1. Location of the study..... 40
Figure 3.2. Station where the studies are carried out..... 41
Figure 3.3. Sketch of the system presented in project proposal 42

Figure 3.4. Preliminary installation of the sampler.....44
Figure 3.5. Calibration curve for PM_{10} cyclone (from URG user manual).....49
Figure 3.6. Calibration curve for $PM_{2.5}$ cyclone (from URG user manual).....50
Figure 3.7. Calibration curve for PM_1 cyclone (from URG user manual).....51
Figure 3.8. The pump used in this study.....55
Figure 3.9. The critical orifices used in this study.....56
Figure 3.10. The manifold and quick-connect fittings used in this study.....57
Figure 4.1. Schematic flow diagram of the sampler constructed with mass flow controllers.....60
Figure 4.2. Calibration curves obtained by the sampler with MFCs.....63
Figure 4.3. MFC feedback system.....64
Figure 4.4. Electrical Diagram of MFC feedback system.....65
Figure 4.5. Sampler located inside the temporary shelter.....66
Figure 4.6. Comparison of PM_1, $PM_{2.5}$ and PM_{10} concentrations from the new sampler and $PM_{2.5}$ and PM_{10} concentrations from stack filter unit.....67
Figure 4.7. Technical drawing of the sampler with critical orifices.....69
Figure 4.8. Electron microscope pictures of PTTF and Nuclepore filters.....71
Figure 4.9. Variation of air flowrate wrt time 1: Teflon filter.....72
Figure 4.10. Variation of air flowrate wrt time 2: Nucleopore filter.....73
Figure 4.11. Variation of air flowrate wrt time 3: Nucleopore filter, 1 channel and 1 pump.....75
Figure 4.12. Variation of air flowrate wrt time 4: Nucleopore filter, 3 channel and 2 pumps.....76
Figure 4.13. Repeatability tests results.....77
Figure 4.14. View of the control unit installed on the sampler.....78
Figure 4.15. Electronic and process flow diagram of the control unit.....79
Figure 4.16. 72 hours of sampling with 3 MFCs connected to 1 pump using Nucleopore filters.....81
Figure 4.17. 24 hours of sampling with 3 MFCs connected to 1 pump using Nucleopore filters.....82

Figure 4.18. 72 hours of sampling with 3 MFCs connected to 1 pump using PTFE filters 82
Figure 4.19. 24 hours of sampling with 3 MFCs connected to 1 pump using PTFE filters 83
Figure 4.20. Flow comparison for PM_1 84
Figure 4.21. Flow comparison for $PM_{2.5}$ 84
Figure 4.22. Flow comparison for PM_{10} 85
Figure 4.23. 72 hours of sampling with 3 critical orifices on Nucleopore filters 86
Figure 4.24. 72 hours of sampling with 3 critical orifices on PTTF filters 87
Figure 4.25. 24 hours of sampling with 1 critical orifice on PTFE filter 88
Figure 4.26. 24 hours of sampling with 1 critical orifice on PTFE filter 88
Figure 4.27. 24 hours of sampling with 1 critical orifice on PTFE filter 89
Figure 4.28. Flow comparison for PM_1 89
Figure 4.29. Flow comparison for $PM_{2.5}$ 90
Figure 4.30. Flow comparison for PM_{10} 90
Figure 4.31. 1 channel & 3 channel comparison for PM_1 with MFCs 91
Figure 4.32. 1 channel & 3 channel comparison for $PM_{2.5}$ with MFCs 92
Figure 4.33. 1 channel & 3 channel comparison for PM_{10} with MFCs 93
Figure 4.34. 1 channel & 3 channel comparison for PM_1 with critical orifices 94
Figure 4.35. 1 channel & 3 channel comparison for $PM_{2.5}$ with critical orifices 94
Figure 4.36. 1 channel & 3 channel comparison for PM_{10} with critical orifices 95
Figure 4.37. Drawing of the sampler shelter 96
Figure 4.38. Image of the sampling shelter 96
Figure 4.39. Sampler constituents installed in the shelter 97
Figure 4.40. Comparison of PM_1, $PM_{2.5}$ and PM_{10} concentrations measured with sampler designed in this study, SFU, two HiVol samplers and Grimm laser spectrometer operated side-by-side in March 2017 102
Figure 4.41. Linear regression of PM_1, $PM_{2.5}$ and PM_{10} measured by the new sampler compared to SFU, two HiVol samplers and Grimm laser spectrometer 103
Figure 4.42. Cost distribution of the sampler with MFC configuration 108

Figure 4.43. Cost distribution of the sampler with critical orifice configuration 110
Figure 4.44. Market research for comparable samplers.....111

CHAPTER 1

INTRODUCTION

1.1. Purpose of the study

This study is dedicated to fulfilling the objective of enabling the researchers carry out sampling of atmospheric particles with different sizes simultaneously and at a reasonable cost. The terms “simultaneously’, and “at a reasonable cost” constitute the major keywords of the study.

For the accomplishment of the purpose, a particulate matter (PM) sampling system, which is capable of collecting PM_{10}, $PM_{2.5}$ and PM_{1} particles from the atmosphere was designed and constructed.

1.2. Action plan of the study

Tasks within the scope of this study was carried out in four phases;

- Constructing the sampler with best available components
- Replacing expensive components with low cost alternatives
- Establishing sampling protocol
- Validation of the sampler against well documented commercial PM samplers

In the 1st phase of the study, the sampling system was constructed with the advanced technology devices and appliances available in the market. Such a sampler is intended to achieve the sampling task with the greatest precision and consistency, regardless of the high costs that yields.

In the 2nd phase of the study, the components that has major contribution to the cost of the sampler were replaced with low-cost alternatives. Here, the term “low cost” does not refer to lower quality equipment, rather different techniques than

conventional that can achieve the same task at the same or similar quality, with lower costs.

In the third phase sampling protocol was established by monitoring flow characteristics against parameters like sampling duration, filter type, types of components used in construction of sampler.

Finally, in the fourth phase performance of the designed sampler was tested against widely-used commercial samplers. Two high volume samplers and one GENT stacked filter unit (SFU) was used for this test.

1.3. Rationale behind the study

In aerosol sampling studies in Turkey, two issues have always been challenging for researchers. The former, and the prominent one is the extremely high costs of sampler devices in Turkey. The latter is difficulties associated with the maintenance of devices. These are the issues that every researcher in this field could face.

The costs required for sampler devices are extremely higher in Turkey than other countries. To illustrate, a mass flow controlled high volume air sampler costs around 35,000₺. Similarly, cost of a dichotomous sampler, which can separate particles as coarse (>2.5μ) and fine (<2.5μ) and collect them on different filters, can exceed 40,000₺.

Besides initial costs, maintenance costs are another aspect of economic problems related with aerosol sampling. Even though the devices could operate smoothly for several years following the purchase, when maintenance is required, it becomes evident that maintenance services are expensive and supply of spare parts necessary for maintenance may be difficult. In addition to that, vendors and resellers, especially small-scale ones, are known to be reluctant for providing maintenance services. In some cases, it may be impossible to get maintenance services even though budget is available for that. For this, proposed sampling system with less electronic dependence is considered to demand less technical support and yield less maintenance costs.

Considering that electronic automation used in the devices mostly accounts for the huge cost, the rationale of the project can be summarized as decreasing the electronic automation where applicable without sacrifice from the performance and quality, which is intended to decrease the cost of the sampler. Under Turkey's circumstances, where budget constraints in research activities are stringent, to initiate a sampling project is a troublesome issue for researchers and device costs even sharpens the problem. Therefore; by the economic revenues intended to be gained by this study, it is envisioned that sampling tasks will require less budget and become more feasible. This, in turn, will encourage more research activities in the field and increase competitiveness of the researchers in Turkey in the international area.

CHAPTER 2

LITERATURE REVIEW

2.1. General information about PM

Particulate matter (PM) is a complex mixture of pollutants suspended in the atmosphere, which is composed of microscopic scale solid particles and liquid droplets. Composition of particulate matter in the atmosphere varies in a wide range of species; acids, organic chemicals, heavy metals and soils (EPA, 2013), whereas the most commonly encountered ones are sulfate, nitrates, ammonia, sodium chloride, black carbon, mineral dust and water (World Health Organisation, 2014).

Particulate matter has great significance in air pollution studies, being one of the six common air pollutants (a.k.a. criteria pollutants) designated by U.S. Environmental Protection Agency (EPA), along with ground-level ozone (O_3), carbon monoxide (CO), sulfur dioxide (SO_2), nitrogen dioxide (NO_2) and lead (Pb). By this designation, particulate matter, along with other criteria pollutants, is subject to National Ambient Air Quality Standards (NAAQS), as mandated by the Clean Air Act (EPA, 2015b) and corresponding national standards.

As can be recalled from incidences that caused severe casualties in the past and also epidemiological and toxicological information heritage, it may be well stated that particulate matter has remarkable health effects on humans and the environment as well. As the World Health Organization (WHO) defines PM-sourced air pollution as the 13^{th} leading cause of mortality worldwide, is a token of recognition of its significance and severity (Anderson et al., 2012).

Understanding the particulate matter size distribution in the atmosphere is utterly crucial for understanding the sources, behavior and the generation mechanism. Besides, the level of threat the PM poses to human health is directly related with its

size. The smaller the particles, the more likely they enter and travel through the respiratory system and cause more hazard. Most generally, atmospheric particles are categorized into two (EPA, 2013);

- ✓ Inhalable coarse particles, with diameter 2.5 μm <d < 10 μm
- ✓ Fine particles, with diameter less than 2.5 μm

PM_{10} and $PM_{2.5}$ particles have long been measured and monitored for compliance with ambient air quality standards. However, particles smaller than 1 μm (PM_1) have been receiving greater attention in recent years since epidemiological studies reveal that the hazard of atmospheric particles on human health is inversely related with the particle size. Which means, as the particle size decreases, the particles can penetrate deeper into the respiratory system and becomes more and more hazardous. Therefore, a need for a new convention that represents even finer particles arise and PM_1 is becoming accepted as the convention needed.

Unlike common conception that classifies particles as coarse (PM_{10}) and fine ($PM_{2.5}$), (Whitby, 1978) defined them as trimodal; fine mode (PM_1), intermediate mode ($PM_{2.5}$) and coarse mode (PM_{10}) (Marple et al., 2014).

A typical representation of aerosol size distribution along with sources and generation mechanism, as shown by Whitby is depicted below; (Whitby, 1978)

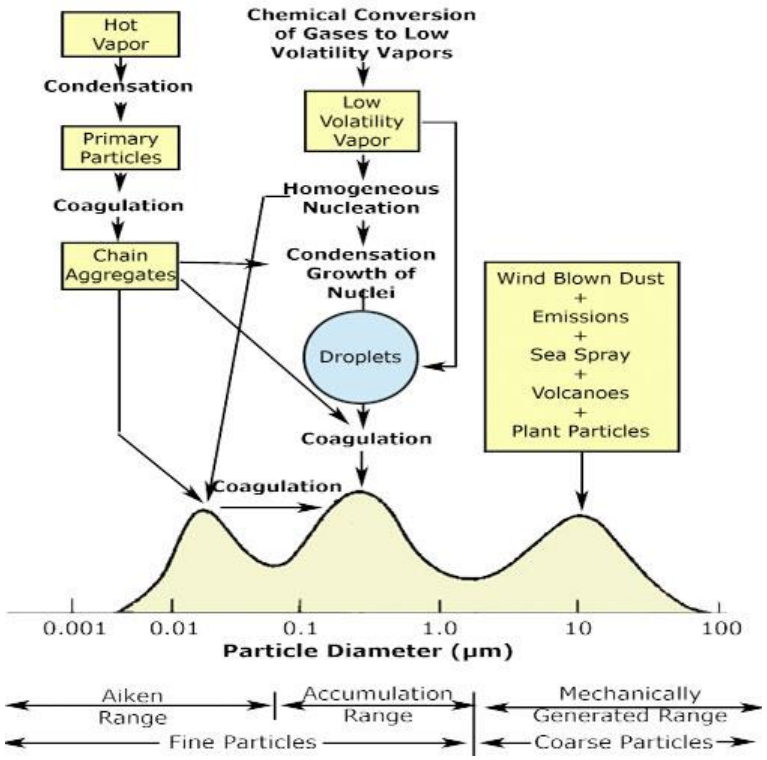

Figure 2.1. Typical aerosol size distribution in the atmosphere (Whitby, 1978)

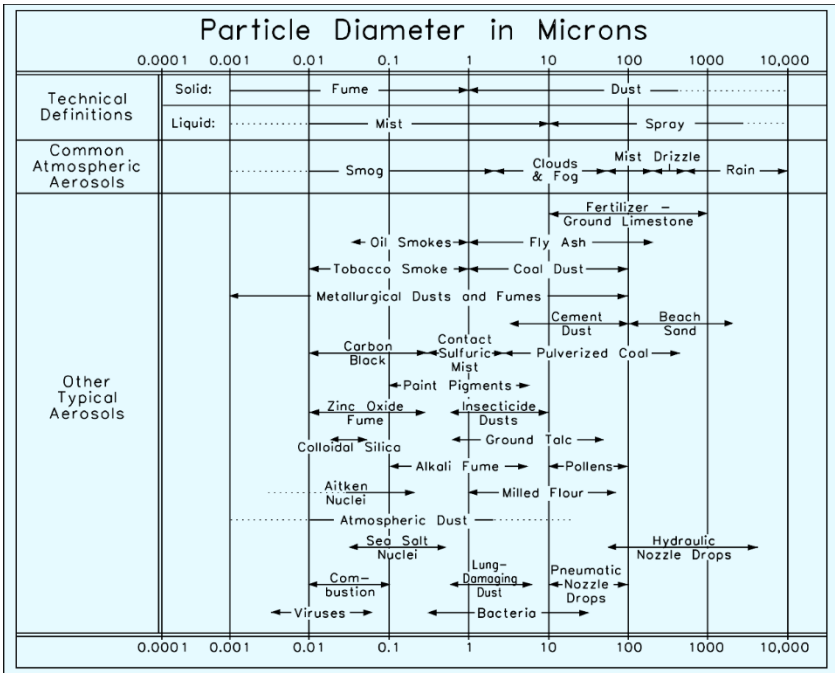

Figure 2.2. Size classification of typical aerosols (Malm, 1999)

2.1.1. Sources of PM

Particulate matter pollution arises from both natural and anthropogenic sources and these sources can either be primary (directly emitted to the atmosphere) or secondary (formed in the atmosphere). (National Research Council, 2010)

US National Emissions Inventory, prepared by EPA indicates $PM_{2.5}$ emissions by source sector in 2011 (EPA, 2016c). The results are depicted below.

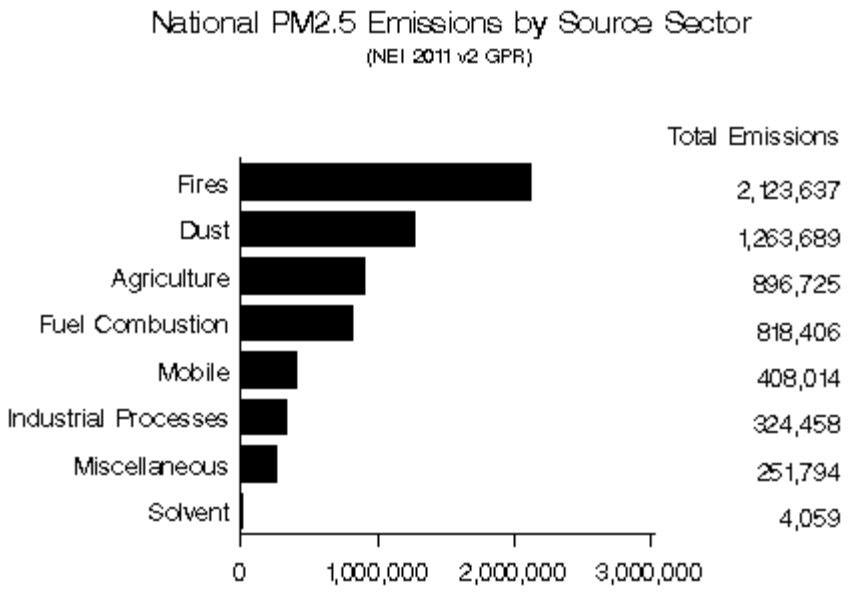

Figure 2.3. National $PM_{2.5}$ emissions by source sector (EPA, 2016c)

The most common natural sources are windblown dust, volcanic emissions, salt and mineral dust from oceans and seas, and wildfires. (NSW EPA, 2013)

Mineral dust, which is one of the two most significant natural sources of PM, arises from various sources; soil erosion, dust storms, resuspension of soil particles from the road surface and unpaved roads. The largest known source of emission is Sahara region (Fuzzi et al., 2015). These emissions contribute to PM pollution, consisting the largest portion of PM_{10} emission. (EPA, 2016c; NSW EPA, 2013) This type of sources results in emission of mineral oxides and crustal trace elements such as Fe, Al, Si, Ca, K, Mg and Mn. (Appel et al., 2013; Houghton et al., 2001; Perraud et al., 2012) It is

estimated that 75% of mineral dust is of natural origin, while the remaining 25% is anthropogenic (Fuzzi et al., 2015). Mineral dust emissions have been receiving an increasing attention due to Saharan dust transport episodes over Europe, which is responsible for exceedances of PM limits in the atmosphere (Fuzzi et al., 2015).

Sea and/or ocean derived particles, in other name, sea spray aerosols (SSA) are also a significant component of atmospheric studies due to both their contribution to global PM budget as the largest mass source at an emission rate of of 3–30 Pg yr^{-1}(Lewis & Schwartz, 2004) and their effect on global radiative budget as a climate forcer by scattering and absorbing solar radiation and influencing cloud-condensation nuclei (CCN) formation (Grythe et al., 2014; Houghton et al., 2001). Main constituent of sea spray aerosols is NaCl, however, ions like K^+, Mg^{2+}, Ca^{2+}, SO_4^{2-} etc. are also found, along with significant amount of organic matter. (O'Dowd et al., 2004) Main generation mechanisms for sea-spray aerosol are; bubble bursting during whitecap formation, which generates fine particles that are smaller than 1μm; jet filling by the bubble at the ocean surface, which creates particles in the range of 1–10μm; ripping of the froth at the wave crests in the times of strong winds, which creates even larger particles and therefore, shorter atmospheric lifetime (Grythe et al., 2014; Houghton et al., 2001; Monahan et al., 1986).

Volcanic eruptions are another natural source of aerosols in the atmosphere. They mainly release two species: volcanic ash – that is rich in iron and magnesium, and sulphur in gaseous form. (mainly SO_2) (Houghton et al., 2001) Ashes emitted from volcanoes is transported to the free troposphere, even to the stratosphere, depending on the strength of eruption. Besides eruptions, the winds are also known to mobilize volcanic ashes from where they are deposited. (Langmann, 2013)

Wildfires, which is, naturally occurred by the combustion of wood and other organic materials, causes emissions of gases and fine particles complex. (NSW EPA, 2013) Wildfire emissions constitute a significant portion of combustion emissions, as (Hinds, 1999) estimates annual forest-fire related PM emissions as 20 Tg yr^{-1}.

Wildfires causes emissions of products of incomplete combustion of trees, and other organic materials (Franzi et al., 2011) and mostly contribute to organic carbon and elemental (black) carbon fraction of particulate matter budget (Radke et al., 1991; Urbanski et al., 2009).

Anthropogenic sources are generally classified into two – stationary sources; which accounts for most of the point and non-point sources, like residential, commercial, industrial and agricultural emission sources, and mobile sources like motor vehicles, aircraft, rail, and marine vessels (EPA, 2015a; European Commission, 1997).

Anthropogenic contribution to particulate matter in the atmosphere is mostly associated with fossil fuel combustion; in the forms of, motor vehicle emissions, combustion for electricity generation in power plants, residential heating and industrial processes (EPA, 2015a; National Research Council, 2010)

Traffic emissions include both direct emissions from exhausts of motor vehicles and side emissions from tires and brakes and also from resuspension of road dust (European Commission, 1997). Figure 2.4 represents contributions to $PM_{2.5}$ from various exhaust and non-exhaust emissions in the cities of Albany, Birmingham, Houston, Long Beach, El Paso and Westbury (Gertler, 2005).

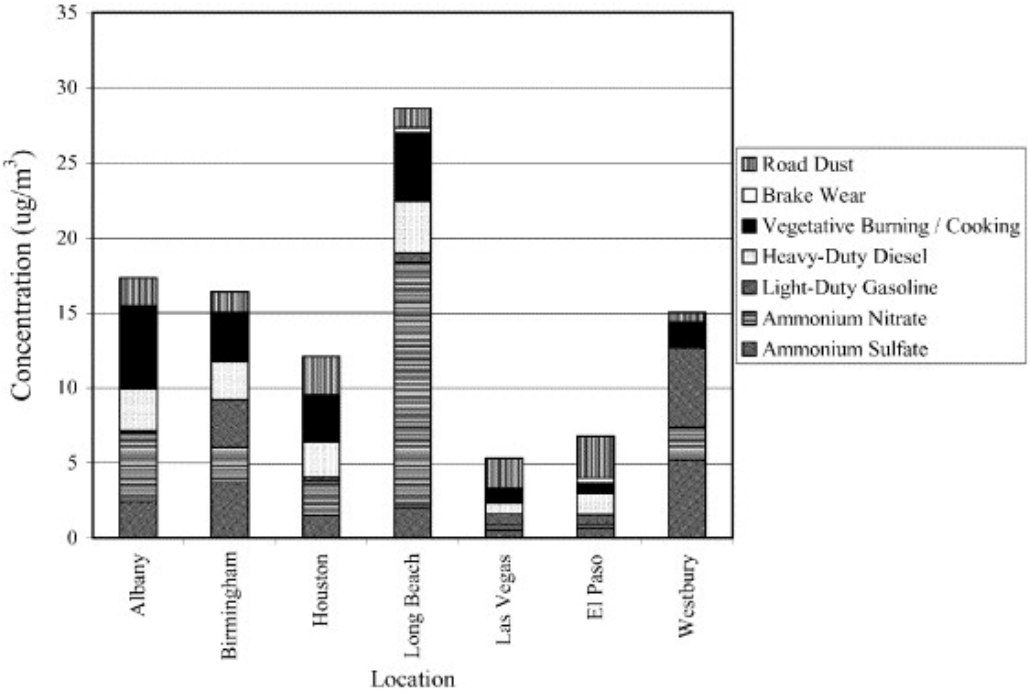

Figure 2.4. $PM_{2.5}$ source contribution for seven US cities (Gertler, 2005)

Most prominent of them is, clearly, exhaust gas emissions from vehicles, as they are the main source of particulate matter, along with many other products of incomplete combustion of fossil fuels such as diesel, gasoline etc. Studies reveal that emissions from diesel vehicles dominate the particulate matter emissions (Gertler, 2005). One example for these studies is depicted in Figure 2.5; a particulate matter monitoring study conducted at a roadside location in New York City in 1992 (Gertler, 2005).

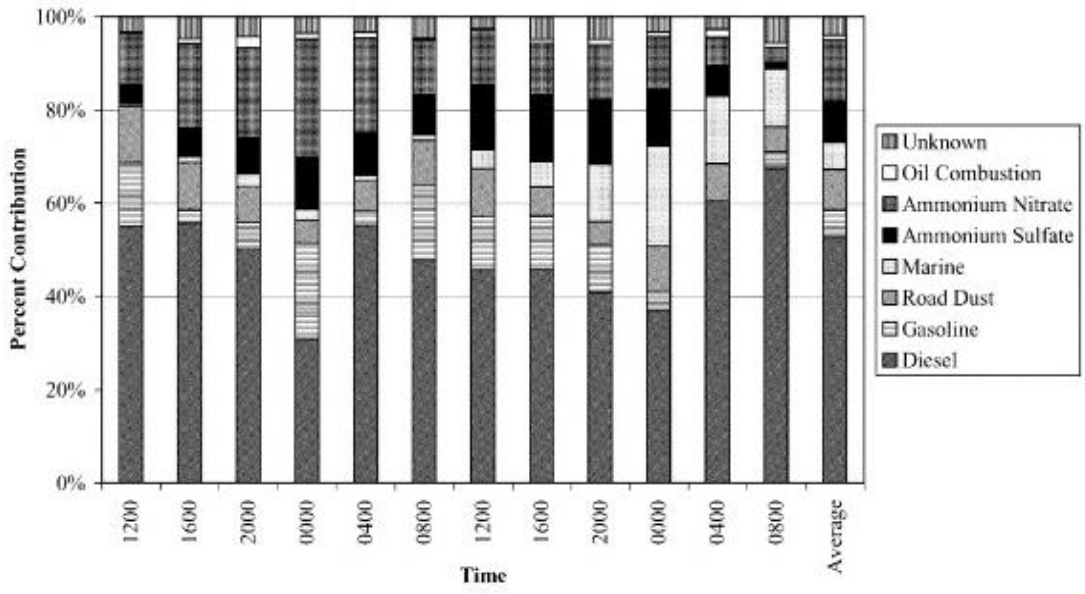

Figure 2.5. Results of a PM_{10} source apportionment study performed at a roadside location in New York City in April 1992 (Gertler, 2005)

Motor vehicles account for emission of trace elements like Fe, Al, Ca, Na, K, Ba, Se, S, Mn, and Pb (Hung-Lung and Yao-Sheng, 2009; Omidvarborna et al., 2014; Robert et al., 2007).

Power plants, as one of the major sources for all types of air emissions, contribute to fine fraction of particulate matter emissions significantly (European Commission, 1997). Most of these emissions arise from coal-fired power plants; as reported in (Commission for Environmental Cooperation, 2005), among 250 largest $PM_{2.5}$ emitting power plants in USA, 96.4% utilizes coal, while for heavy fuel oil and natural gas is responsible for 2.8% and 0.8% respectively. Main composition for PM emissions from coal-fired power plants are SiO_2, Al_2O_3, Fe_2O_3 (Zhang et al., 2005).

Domestic heating, as based on combustion of fossil fuels, shows similar characteristics with power plant emissions. Major portion of heating emissions is associated with coal and wood burning, due to their complex structure and high carbon and sulfur content, they cause higher amounts of PM emissions as products of incomplete combustion and fly ash (Energy Information Administration, 1999). Natural gas, on the other side,

is known to release much less amounts of particulate matter, along with other criteria pollutants (EPA, 1995). Emissions of particulate matter from fossil fuels per billion BTU energy is estimated as 7 lbs. for natural gas, while this figure is 84 lbs. for oil and 2744 lbs. for coal, which reveals natural gas as 392 times cleaner than coal in terms of particulate matter emissions (Energy Information Administration, 1999).

Emissions from industries is another contributor to particle pollution in the atmosphere, which constituted 23% of PM emissions in the UK in 1999 (Passant et al., 2002). Major industries associated with PM emission are; sinter plants, blast furnaces, iron & steel foundry, cement production, lime production, glass production, construction and quarrying (Passant et al., 2002).

As a result of these industrial activities, elements like arsenic, cadmium, chromium, copper, lead, zinc, mercury, nickel, selenium and vanadium etc. are emitted to the atmosphere (Passant et al., 2002).

Even though the natural sources constitute 90% of particulate matter by mass (Voiland, 2010), sources that are of anthropogenic origin, the remaining 10%, can dominate urban air and yield more impacts on both human and environment (National Research Council, 2010; Voiland, 2010). The rationale behind this is that abundancy of an aerosol is inversely proportional with its aerodynamic diameter, which means, anthropogenic sources release particles of smaller diameter and therefore with higher atmospheric lifetime (Carruthers et al., 2005; National Research Council, 2010). Besides, particles with smaller diameter yields greater health and environmental effects, as will be covered in detail in the following chapters.

Contribution of sources to particulate matter, specifically fine particles, can be summarized below (National Research Council, 2010). In the figure, the size of the dots represents proportion of contribution from that source, such that, total area in each column represents the same total area.

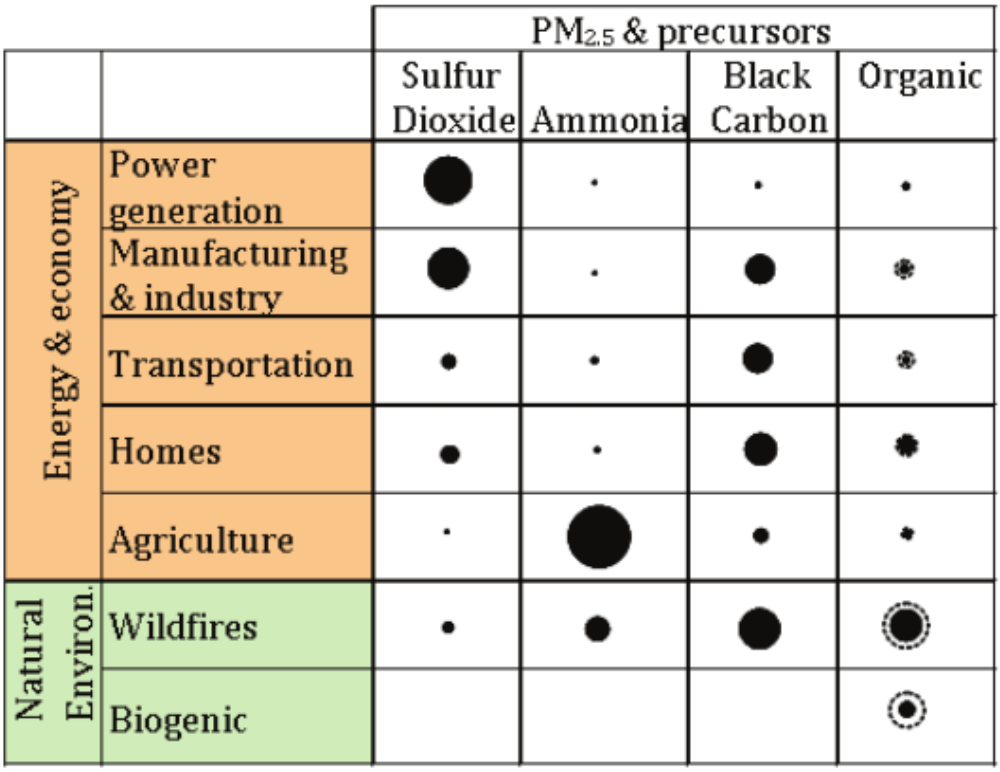

Figure 2.6. Global sources of $PM_{2.5}$ components and precursors

2.1.2. Health & Environmental Effects of PM

Particulate matter pollution has impacts both on human health and the environment, which can be briefly introduced as visibility degradation, affecting hydrologic cycle by cloud condensation nuclei (CCN) formation and climate change (EPA, 2016b; World Health Organisation, 2003)

2.1.2.1. Health effects of atmospheric particles

Poor air quality has always been a token of poor health; however, in the last century it has been a serious concern and gained serious attention especially after fatal air pollution episodes throughout the world in the 20th century (Anderson et al., 2012). The Meuse Valley episode in Belgium is the first known major episode example. Between Dec 1 and Dec 5, 1930, a thick fog covered the area, which was a heavily industrialized zone, and caused casualties of 60 people due to respiratory symptoms

(Nemery et al., 2001). In 1952, the most well-known air pollution episode in the history – the Great Smog – occurred in London. A dark and intense smog of sulphur dioxide and black smoke appeared and lasted for more than a week, leading to ~4,000 deaths (Timms, 2012). This catastrophic event became a breakthrough in atmospheric studies, as recognition of lethality of air pollution led to introducing measures to reduce air pollution. The Clean Air Act, which was introduced in 1956 in UK and in 1970 in USA are legacies of this episode (Anderson et al., 2012; Timms, 2012).

The most significant criteria in assessing the health impacts of particulate matter is aerodynamic diameter of particles, since it determines the extent of exposure (EPA, 2016b). Particles that are greater than 10 μm in diameter have relatively short atmospheric lifetime and mostly captured by the nose and upper respiratory system; therefore, yield low health impact (Anderson et al., 2012). On the other hand, fine particles, that are defined as smaller than 2.5 μm and ultrafine particles that are smaller than 0.1 μm in diameter, poses greater threat to human health, since they can penetrate deep into the lungs and even reach the bloodstream (EPA, 2016b).

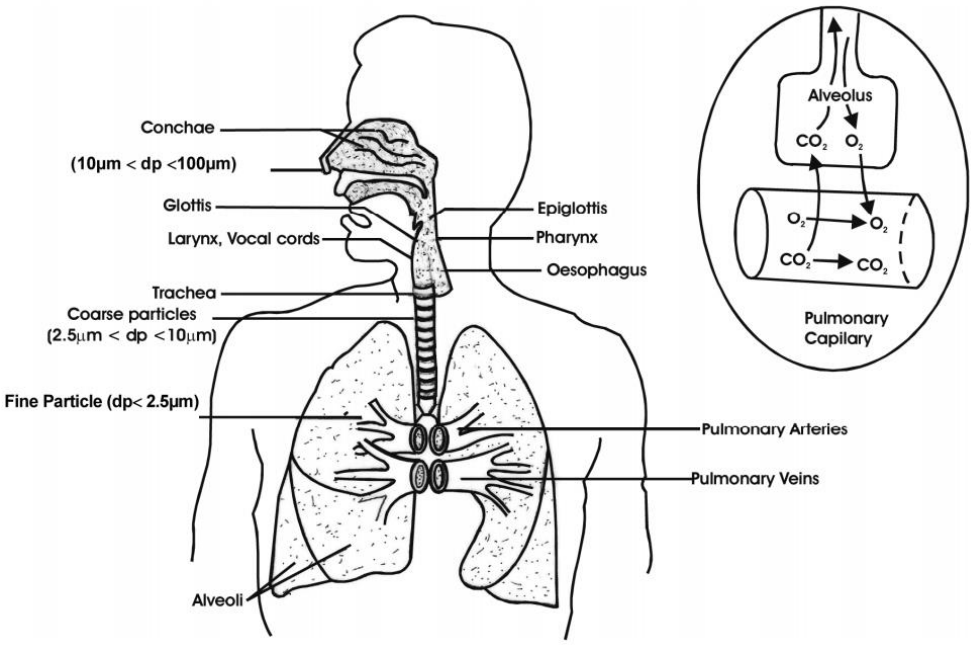

Figure 2.7. Exposure extent of particulate matter by their sizes (Jimoda, 2012)

Particulate matter is the key factor for air pollution impacts on human health, since it poses more threat to human health than any other criteria pollutants, i.e. carbon monoxide, ozone etc. (Kim et al., 2015). Since size and chemical composition of PM varies widely so as to contain nitrates, sulfates, acids, organics and heavy metals, which has serious potential for deterioration of human health (World Health Organisation, 2003). Particular matter exposure is known to cause symptoms like premature deaths (especially ones with heart or lung diseases), non-fatal heart attacks, irregular heartbeat, aggravated asthma, decreased lung function, shortage of breath, irritation of air canals (Anderson et al., 2012; EPA, 2016b; Kim et al., 2015; World Health Organisation, 2003).

Increase in particulate concentration by 10 $\mu g\ m^{-3}$ is associated with 6% increase in mortality or more than 40,000 imputable cases in an epidemiology-based exposure-response function (Künzli et al., 2000). 10 $\mu g\ m^{-3}$ of increase in PM_{10} concentration is also found responsible for 25,000 adult bronchitis cases, 290,000 children bronchitis episodes, 500,000 asthma attacks and 16 million person*day of restricted activities in European countries. More recent studies reveal that; increase in PM_{10} by 10 $\mu g\ m^{-3}$ is related to increase in mortality rate per day by 0.21%, whereas increase in $PM_{2.5}$ by 10 $\mu g\ m^{-3}$ accounts for long-term mortality risk increase by 4 – 8% (National Research Council, 2010).

Figure 2.8 represents relative casualty risks for various species including PM_{10}, $PM_{2.5}$, black smoke and ozone, caused by a 10 $\mu g\ m^{-3}$ increase, with 95% confidence interval (World Health Organisation, 2003).

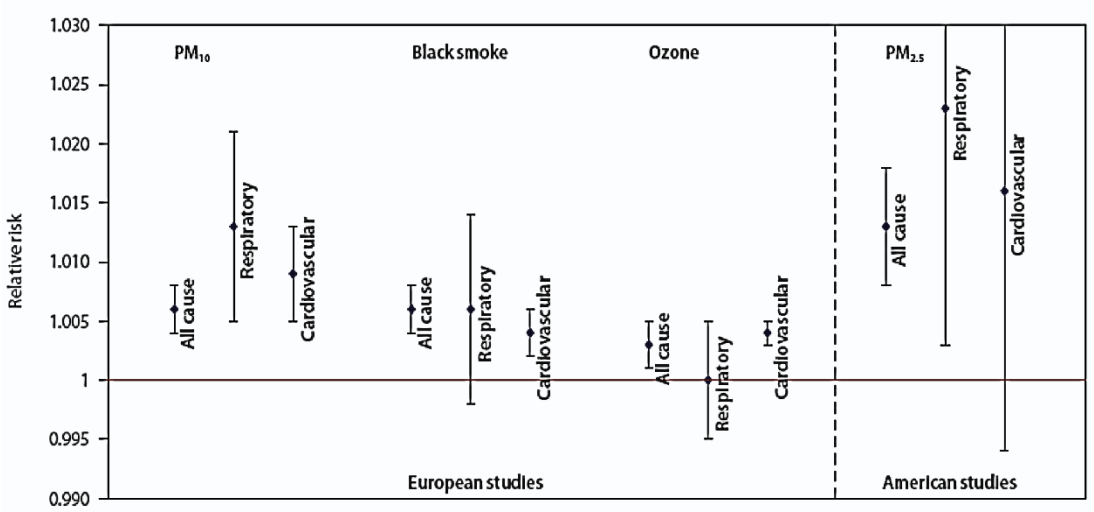

Figure 2.8. Summary of relative risks for mortality by different air pollutants

2.1.2.2. Impacts of particles on haze formation

Beside human health, particulate matter has considerable environmental impacts as well (EPA, 2016b). These impacts are mainly visibility impairment caused by specifically fine ($PM_{2.5}$) particles, impacts on hydrological cycle by cloud condensation nuclei (CCN) formation and climate change contributed by the black carbon content of PM (World Health Organisation, 2003).

Visibility can be defined as the furthest distance that can be seen with naked eye (Zhao et al., 2013). Particulate matter in the atmosphere is known to interfere with the visibility, either in the form of absorbing or scattering the light (Cheng et al., 2013; Malm, 1999). In three ways the haze formed by pollutants can appear in the atmosphere (Malm, 1999);

- ✓ When there is enough sunlight to cause atmosphere to become turbulent and pollutants are well-mixed, a uniform haze will occur,
- ✓ During cold winter months, if there is a wind present, emitted pollutants will appear as a coherent plume,
- ✓ If there is no wind or pollutants are emitted into stagnant air, a layer of haze appears and builds up as the stagnant conditions continue.

These conditions are represented schematically in Figure 2.9.

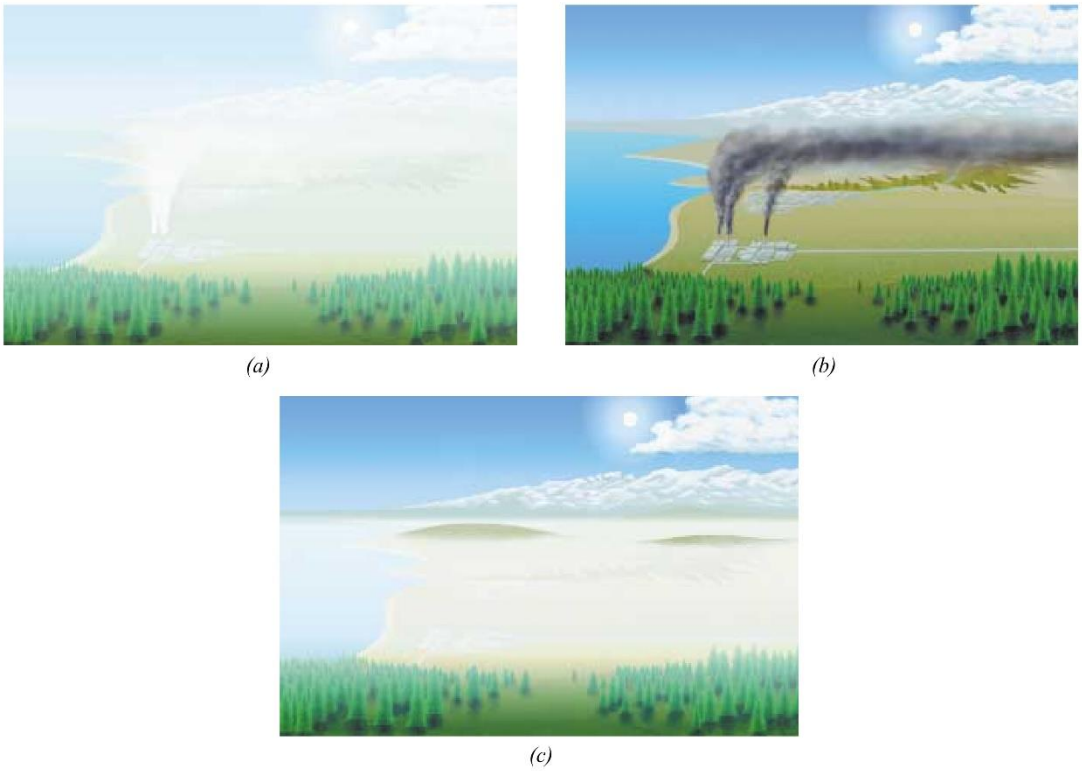

Figure 2.9. The three ways pollutants can visually degrade a scenic vista (Malm, 1999).

2.1.2.3. Impacts of particles on hydrologic cycle

Although particles can arise from both natural and anthropogenic sources; since fine fraction plays a greater role in visibility reduction, man-made sources have greater contribution to haze (EPA, 2016d; Zhao et al., 2013). Diesel and gasoline emissions, power plant emissions (specifically coal-fired) and industries like oil refineries, smelters etc. are known to be major sources of visibility impairment (Malm, 1999). Major components of PM such as sulfate, nitrate and organic matter are actively responsible in haze formation; therefore, regions that encounter intense urban emissions experience severe haze pollution (Zhao et al., 2013). Study conducted by (Zhao et al., 2013) support this claim, Yangtze River Delta, Beijing, which is, one of the largest city clusters in the world, has experienced a visibility reduction from ~25 km to less than 20 km from 1980s to 2010s.

In particle-free atmosphere, water vapor requires around 400% supersaturation for the formation of water droplets, which leads to rainfall. In order for this to occur in ambient atmosphere, particles that will serve as a nucleus for water droplet formation are needed. Particles that can initiate cloud condensation at a given supersaturation are defined as cloud condensation nuclei (CCN) for the given supersaturation (Seinfeld & Pandis, 2006)

Although fresh soot particles are known to be hydrophobic and thus not good CCN, as they are aged to become sufficiently hydrophilic, they can act as a CCN (Ma & Kim, 2014). As the laboratory-scale study conducted by (Ma & Kim, 2014) suggested, CCN activation time for the fed soot particles is 40 minutes and soot particles are observed to act as a cloud condensation nuclei.

In addition to direct emissions to the atmosphere from natural and anthropogenic sources, particles acting as CCN can also be formed in the atmosphere by primary and secondary aerosols (Kalivitis et al., 2015; Kerminen et al., 2012; Merikanto et al., 2009). New particles are initially formed at the size of 1 – 2 nm, however grow rapidly by coagulation to become a cloud condensation nuclei (Fuzzi et al., 2015; Kerminen et al., 2012). Model studies reveal new particle formation accounts for a large portion of cloud condensation nuclei in the global atmosphere (Fuzzi et al., 2015; Kalivitis et al., 2015; Kerminen et al., 2012).

(Merikanto et al., 2009) reported that 45% of global low-level cloud CCN at 0.2% supersaturation originates from nucleation (ranging 31 – 49%, considering the uncertainties). Besides, model suggested that in the marine boundary layer 55% of CCN (0.2%) are from nucleation, with 45% from the free troposphere and 10% nucleated directly in the boundary layer (Merikanto et al., 2009). Another study found that nucleation contributes to CCN (0.2%) significantly at the boundary layer, within a range of 49 to 78%, depending on the choice of simulation scenario (Westervelt et al., 2014).

2.1.2.4. Climate change effects of atmospheric particles

Emissions of air pollutants to the atmosphere undoubtedly can result in climate change, and particular matter does not bring an exception to this statement (EPA, 2016a). The most obvious impact of particulate matter on the climate is associated with the earth's radiative budget (EPA, 2016a). However; the way particles effect the global radiative budget is highly case specific, depending on size, shape and composition and also subject to spatial and temporal variation (National Research Council, 2010). Aerosols can interact with solar radiation either directly, which is called direct radiative forcing effect; or, with terrestrially reflected infrared radiation, which is called indirect radiative forcing effect (Jimoda, 2012).

Aerosols can affect atmospheric radiative budget either by reflecting or absorbing solar radiation. The former occurs when particles with low carbon content, such as sulfate particles and sea salt spray. These type of particles have a net negative impact on radiative budget, which means, they cool the earth by reflecting sunlight (UCSUSA, 2015). The latter situation is valid for particles like desert dust particles and black carbon, which is typically a product of combustion processes. According to IPCC; black carbon is the second most important anthropogenic source of global warming (Fuzzi et al., 2015).

In addition to direct effect as radiative forcer, aerosols with high black carbon content alters the climate by albedo effect. Black carbon, when deposited on snow and ice, darkens the surface and decreases its albedo, so that snow/ice surfaces absorb more radiation and melting of ice caps and glaciers are accelerated (Fuzzi et al., 2015; National Research Council, 2010).

Studies suggest radiative forcing for several aerosol types are; −0.26 to −0.82 W/m^2 for sulfate aerosols, +0.16 to +0.42 W/m^2 for black carbon, +0.9 to -0.46 W/m^2 for mineral dust (Haywood & Boucher, 2000)

2.2. Particulate matter sampling systems

2.2.1. High volume samplers

2.2.1.1. Total suspended particulate matter (TSP) sampler

Total suspended particulate matter (TSP) sampler is used to measure the total amount of suspended particles in the atmosphere, without classifying with respect to size fractions. Intended to meet U.S. EPA reference method for determination of total suspended particulate (TSP) concentrations. The sampler typically draws around 1500 m^3 of air per 24 hours, which corresponds to around 1000 L/min of flowrate and flowrate is controlled by mass flow controllers (MFC). Particles are collected on cellulose fiber filters and weighed before and after sampling, so as to determine the mass collected on filters and then divided by the volume of air drawn to reach the TSP concentration (Hart et al., 1992; Park et al., 2009; Queensland Government, 2013).

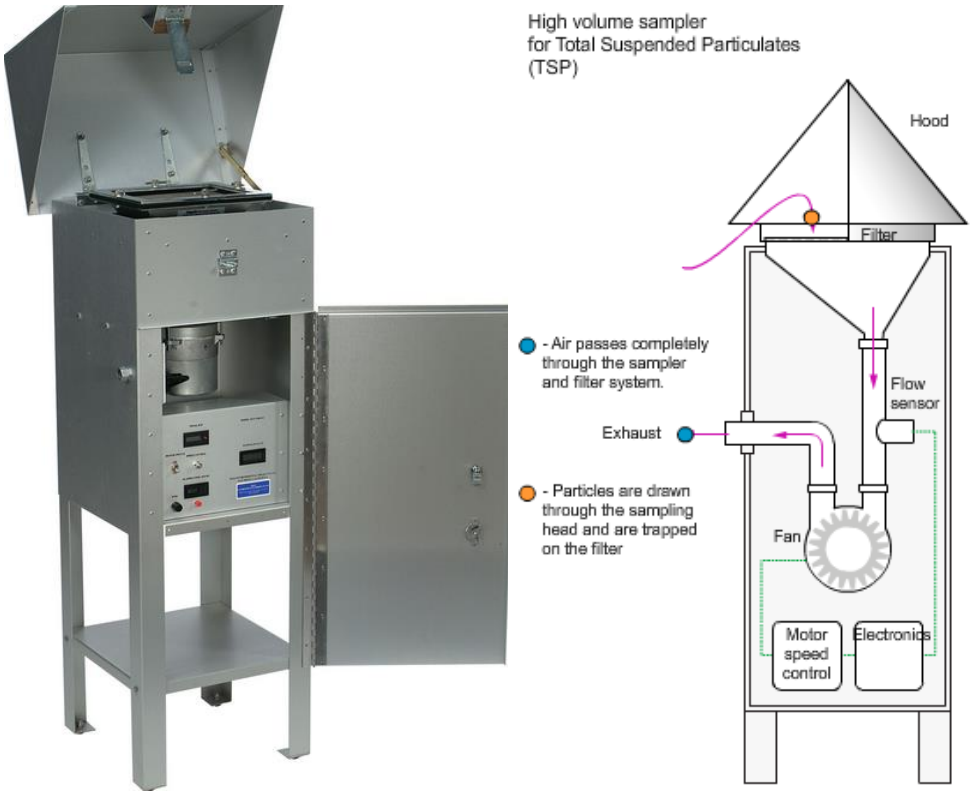

Figure 2.10. Total Suspended Particles (TSP) Sampler (Queensland Government, 2013).

2.2.1.2. In-Stack Particulate Filtration

In-stack particulate filtration technique is a Federal Reference Method (FRM) by EPA for sampling of PM_{10} particles, as described in Appendix J of 40CFR, Part 50 (Gilliam & Hall, 2016).

Quite similar operation principle with TSP sampler, except for PM_{10} inlet head that allows particles smaller than 10 μm. Greater particles have greater inertia, so these particles are trapped by the inlet based on this property. As a result, only particles smaller than 10 μm are collected on the filter. The pump of the sampler, like TSP sampler, operates at a flowrate around 1000 L/min and vacuums around 1500 m^3 of air in a 24-hour interval. Particles are collected on cellulose fiber filters and weighed before and after sampling. The gravimetric procedures described in the previous section are applied to obtain PM_{10} concentration (K. M. Hart et al., 1992; Park et al., 2009; Queensland Government, 2013).

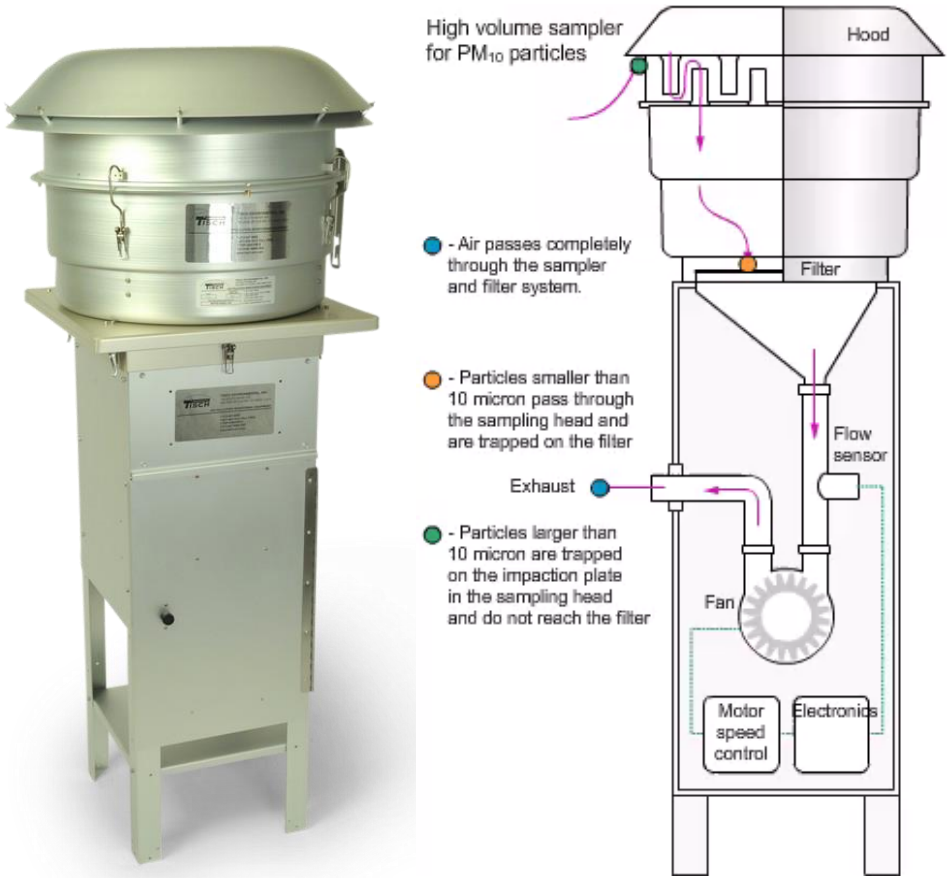

Figure 2.11. High Volume PM_{10} Sampler (Queensland Government, 2013)

2.2.1.3. Trichotomous Sampler

Trichotomous sampler is a virtual impaction-based sampler that is designed to collect three particle groups; PM_{10}, $PM_{2.5}$ and PM_1 by Dr. Virgil A. Marple at the University of Minnesota (Lundgren et al., 1996). This trichotomous sampler can collect particles for both indicated cutpoints and intermediate cutpoints, $PM_{1\text{-}2.5}$, $PM_{2.5\text{-}10}$ (Lundgren et al., 1996).In the sampler, two High Volume Virtual Impactors (HVVIs), with cutpoints of 2.5 µm and 1.0 µm are placed between the PM10 size selective inlet and a standard PM_{10} sampler filter of 8×10 inch (20×25 cm). The sampler is designed as a high volume sampler and operates at a flowrate of 40 cfm, corresponding to around 1133 L/min (Marple et al., 2014). By using sufficient number of 47 mm filters, it possible to collect the particles in the ranges of sampler, concentration and

composition of particles could be obtained for particulate matter in five size ranges of PM_{10}, $PM_{2.5–10}$, $PM_{2.5}$, $PM_{1–2.5}$, and PM_1 (Marple et al., 2014).

Operation of the dichotomous sampler occurs in the following steps;

- Sample air reaches to 2.5 μm impactor and $PM_{2.5-10}$ particles are collected on two filters by a minor flow.
- Air with particles smaller than 2.5 μm flows to 1 μm impactor, while a branch of stream is collected on a filter as $PM_{2.5}$
- Particles that continues to 1 μm impactor, is collected on two filters as $PM_{1–2.5}$, while another branch of stream is collected on a filter as PM_1,
- The remaining air with PM_1 particles are collected on the rectangular filter at the base of the impactor chamber and leaves the system (Lundgren et al., 1996).

Trichotomous sampler is shown in Figure 2.12; where, a) Shows assembled sampler, b) 2.5 μm HVVI and c) 1.0 μm HVVI. Also, component marked with “A” represents PM_{10} inlet; “B” intermediate chamber; “C” base; “D” 2.5 μm HVVI; “E” 1.0 μm HVVI; and “F” after filter (Marple et al., 2014).

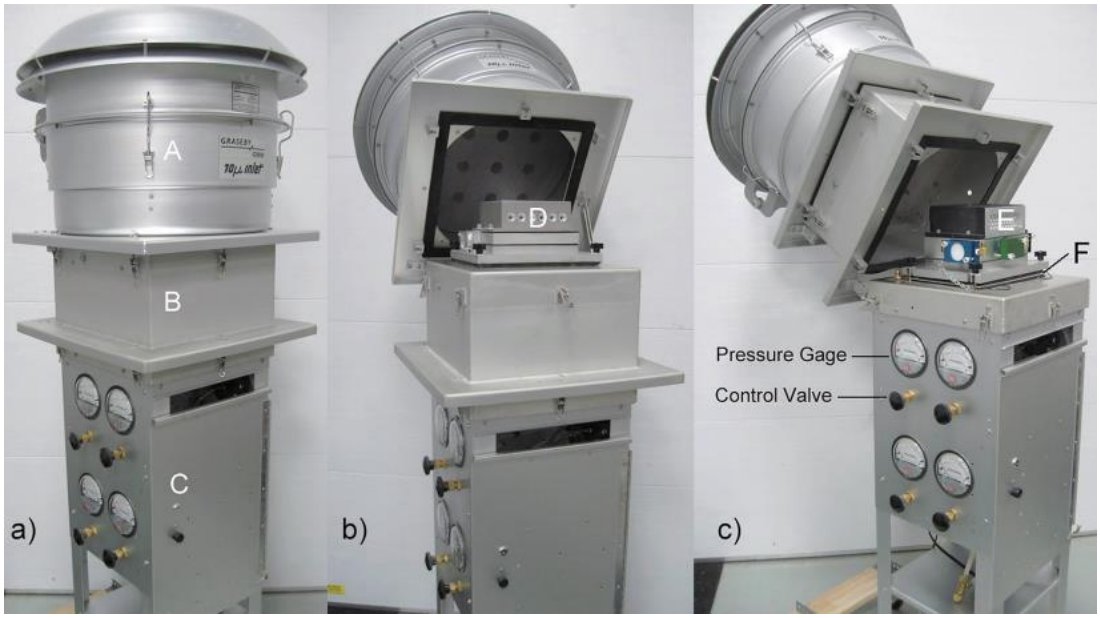

Figure 2.12. $PM_{1.0/2.5/10}$ Trichotomous Sampler

2.2.2. Low volume samplers

2.2.2.1. In-Stack Particulate Filtration

In-stack particulate filtration technique is a Federal Reference Method (FRM) by EPA for sampling of PM_{10} particles, as described in Appendix J of 40CFR, Part 50 (Gilliam & Hall, 2016).

One of the approved FRM devices for the measurement of PM_{10} using in-stack particulate filtration, "Andersen Model RAAS10-100 PM_{10} Single Channel PM_{10} Sampler (RFPS-0699-130)", is displayed in Figure 2.13.

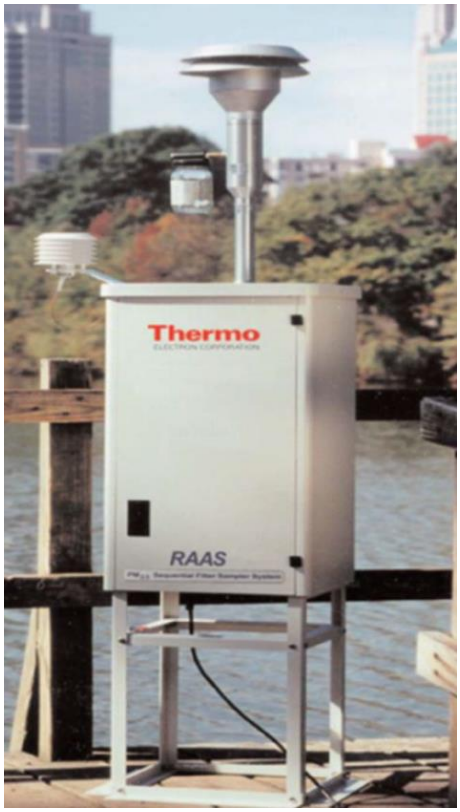

Figure 2.13. Andersen RAAS10-100 PM_{10} sampler

In this technique, ambient air is drawn at a constant rate into the sampler's inlet that is specifically designed for inertial separation of particulate matter into PM_{10} or more than one fractions within PM_{10} range. In addition, $PM_{2.5}$ can be collected by combining PM_{10} head with a Very Sharp Cut Cyclone (VSCC) or Well Impactor Ninety-Six (WINS) with this technique. "Tisch Environmental Model TE-Wilbur2.5 $PM_{2.5}$ Low-Volume Air Particulate Sampler" can be exampled as such a $PM_{2.5}$ Federal Reference Method (FRM) (Gilliam & Hall, 2016; Tisch Environmental, 2014).

Figure 2.14. Tisch Environmental Model TE-Wilbur2.5 Particulate Sampler

Particles are collected on filter media during sampling for a specified period. Each filter is conditioned for moisture removal before and after sampling and weighed before and after sampling so that the net mass collected during sampling period is obtained. Following, total volume of air during the sampling is determined by the flow rate and sampling time and corrected to EPA reference conditions (25 °C, 101.3 kPa). PM concentration is calculated by the division of total mass collected on filter and total volume of air passed through the filter and is expressed as $\mu g/m^3$. (Gilliam & Hall, 2016)

This method is a relatively inexpensive method for particulate matter sampling and is commonly used. Despite these advantages, only one particle size fraction can be sampled at one device. Therefore, the costs will increase as the quantity of devices will increase in multiple particle groups sampling.

2.2.2.2. Beta attenuation monitoring (BAM) samplers

Beta attenuation monitoring (BAM) is a Federal Equivalent Method (FEM) designated by EPA. In this method, ambient air is drawn at a constant flow rate into the sampler and particles are collected on filter tape which intermittently moves between the

sample inlet and the detector before and after every sampling (Gilliam & Hall, 2016). Prior to particle collection, beta rays are emitted by a carbon-14 (^{14}C) element on top of the clean filter tape and the attenuation is detected by a scintillation counter, that is mostly a Geiger-Müller (GM) counter or a photodiode detector (Thermo Scientific, n.d.). The procedure is repeated after sampling in order to determine the difference in the attenuation before and after sampling, thus, the mass collected on the filter. As the volume of air drawn on the filter is known, particle concentration can be calculated (Gilliam & Hall, 2016; Liberti, 1975).

This method is based on Beer's law; that is, the attenuation by the particles is related only to the mass of the particles collected, regardless of other properties like density, elemental or chemical composition, which makes BAM a robust, reliable sampling technique (D. Hart, 2009; Liberti, 1975). Typical sampling scheme using a BAM device is shown in Figure 2.15 (Washington State Department of Ecology, 2017).

BAM samplers are partially advantageous over filter based FRM samplers in terms of sampling continuity, hourly data generation and remote operation up to 60 days, as the most manufacturers provide 60-day filter tapes (Gilliam & Hall, 2016).

As a reliable and proved method, BAM samplers are widely used in Turkey as well. Almost all air quality monitoring stations (AQMS), operated by the Ministry of Environment and Urbanism and some by private facilities, are equipped with PM_{10} sampler, which are mostly BAM devices. Air Quality Assessment and Management Regulation of Turkey designates EN 12341 as the reference method for sampling and measurement of PM_{10}.

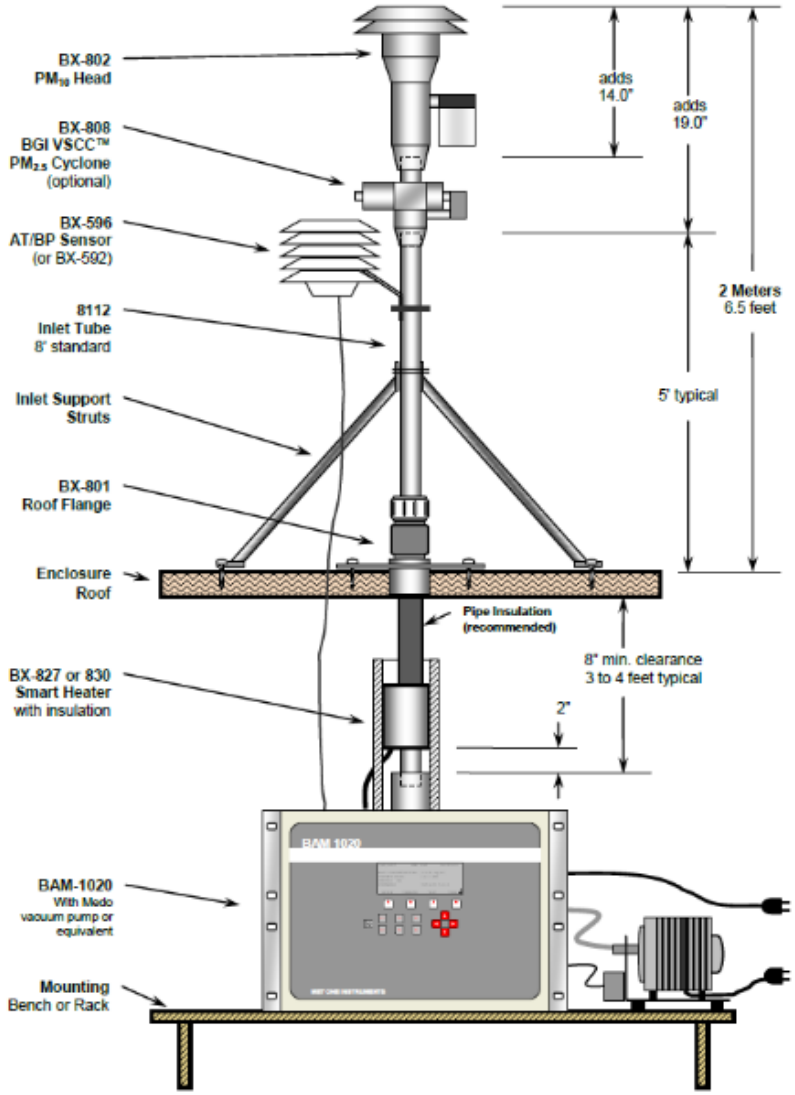

Figure 2.15. Schematic diagram of a BAM device

2.2.2.3. Tapered Element Oscillating Microbalance (TEOM®)

Tapered element is a hollow glass tube, of which base is fixed but tip is unattached so that vibrates at a frequency. As the air is sampled and the particle mass is collected on the filter at the tip of the tapered element. As the mass is accumulated, the oscillation frequency decreases and based on this difference, the mass is determined, and the concentration is then calculated by division of mass by sample volume (Gilliam &

Hall, 2016). A process flow diagram of TEOM® sampler is given in Figure 2.16 (Queensland Government, 2017).

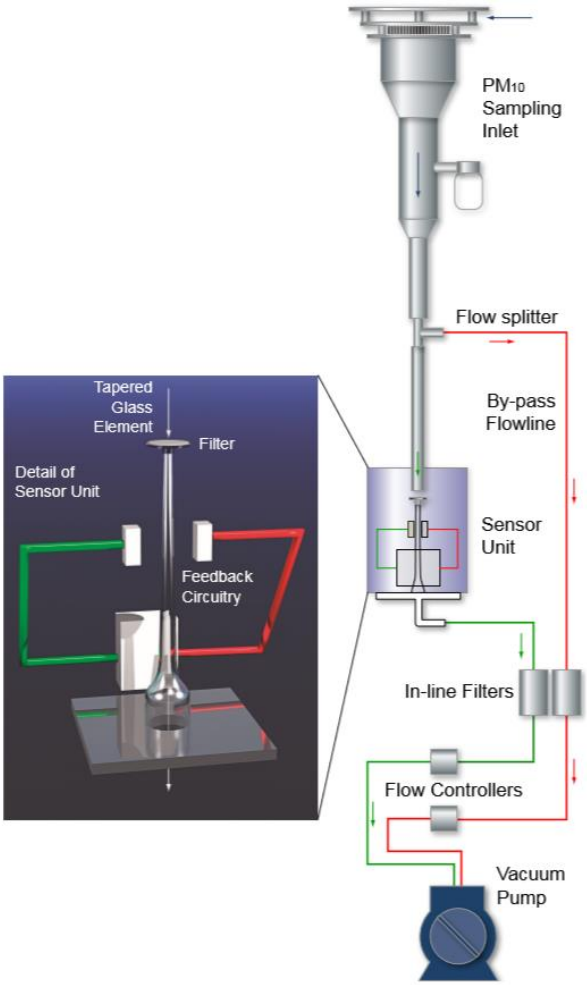

Figure 2.16. TEOM® sampler schematic diagram

As a continuous real time measurement device, TEOM® provides useful data under ideal conditions; however, its sensitive measurement mechanism may causes errors as it is highly vulnerable against external conditions and mechanical interferences (Gilliam & Hall, 2016).

2.2.2.4. Dichotomous Air Sampler

Dichotomous sampler is a Federal Equivalent Method (FEM) designated by EPA for $PM_{2.5}$ and PM_c ($PM_{10-2.5}$) particle fractions (Gilliam & Hall, 2016). The sampler separates particles by a virtual impactor and simultaneously collects coarse and fine ambient particles on separate filters. The pump draws 24 m^3 per 24 hours, which corresponds to 16.7 L/min flow rate. This flow is split after the main inlet such that primary sample ($PM_{2.5}$) is adjusted to 15 L/min and secondary sample (coarse) is adjusted to 1.67 L/min of the air flow. As the collection media, polytetrafluoroethylene (PTFE) filters that has a diameter of 47 mm and pore size of 2 µm (Queensland Government, 2013; ThermoScientific, 2015).

Figure 2.17. Dichotomous Air Sampler (ThermoScientific, 2015)

2.2.2.5. Laser Aerosol Spectrometry

Laser Aerosol Spectrometry (LAS) is a recent equivalent method (FEM) approved by EPA. In this method, sample air is drawn into a measurement chamber through a narrow inlet, where the sample air is exposed to laser. The particles exposed to laser scatter the light, which is, then reflected by a mirror to a detector. Based on the intensity of the reflected light, particle size is determined. This process occurs for a small sampling volume of air, which statistically contains one particle and repeated sequentially in order to determine the quantity of the particles in the sample air, with corresponding particle sizes. The mass concentration of the particles are then derived based on the assumption of uniform density and spherical shape. (Gilliam & Hall, 2016; Grimm Aerosol Technik, 2019)

Figure 2.18. Grimm EDM180 Laser Aerosol Spectrometer

This method offers several advantages over filter-based methods. The prime difference is that there is no need for filter. This provides operation versatility as the device can operate remotely for prolonged periods without maintenance and in the long term, cost revenues as there is no need of consumables. Besides, data resolution

is much higher as the particle concentration is measured instantly and data acquisition intervals can be set as minutes and even seconds, whereas BAM devices typically conduct measurements per hour and high-volume samplers per 24 hours.

2.2.2.6. GENT Stacked Filter Unit

In this sampler unit, air flows through a virtual impactor that allows particles smaller than 10 μm and then reaches to a filter holder. Particles are collected on two separate filters that are stacked in a single filter holder. Particles first reaches to coarse filter, which has 8 μm pore size, and coarse fraction of the particles are trapped here. The remainder particles reach to the fine filter, which has 0.4 μm pore size, and are trapped in this layer. As the virtual impactor is calibrated as a PM_{10} impactor at 16.7 L/min flowrate, the pump is operated at this flowrate. Coarse particles are collected on 8 μm pore sized filters while fine particles are collected on 0.4 μm pore sized filters.
Both are Nucleopore membrane filters, with a diameter of 47 mm (Maenhaut et al., 1994).

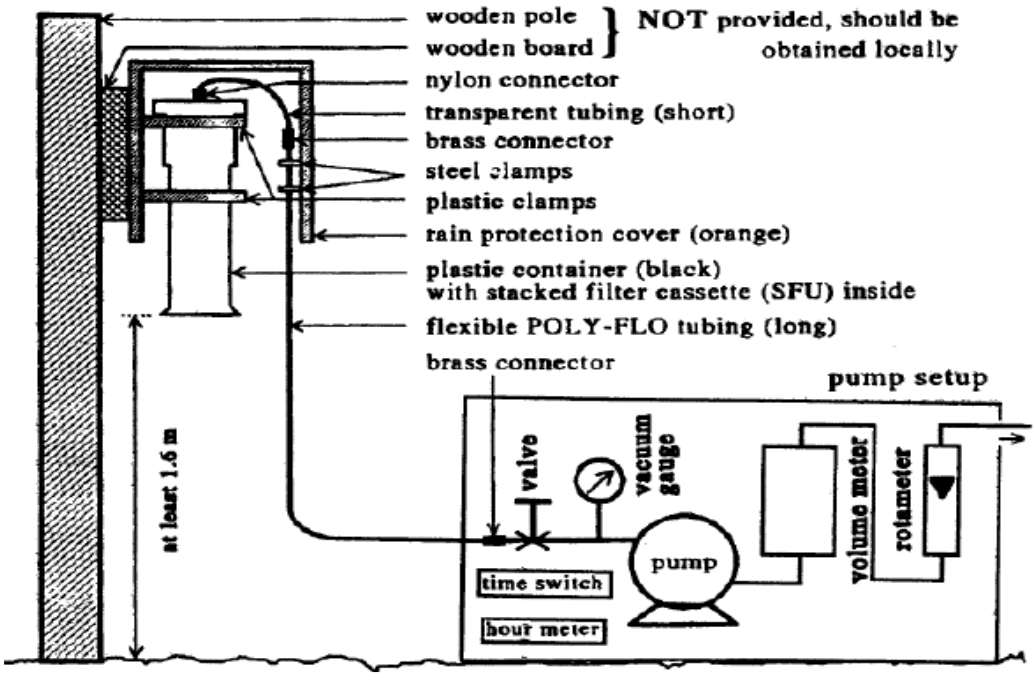

Figure 2.19. Schematic Diagram for GENT Stacked Filter Unit (Maenhaut et al., 1994)

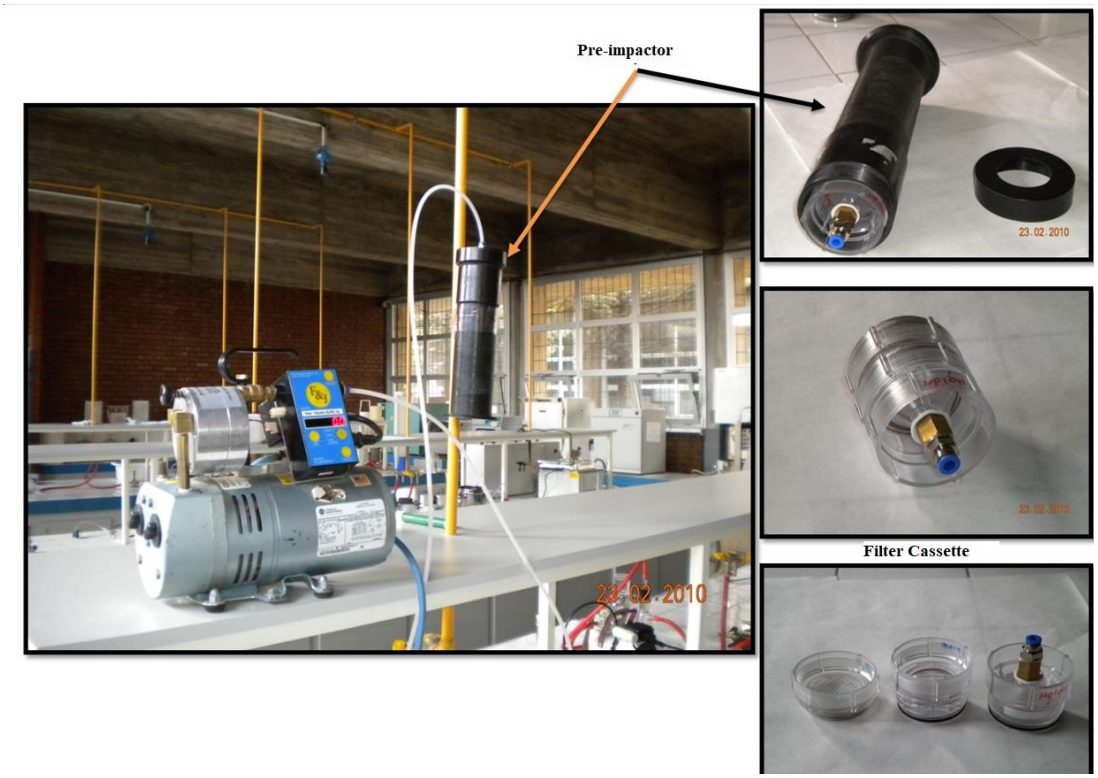

Figure 2.20. Stack Filter Unit (SFU) sampling system

2.3. Flow rate control in PM sampling

An air pollutant can be effectively sampled and determined provided that the air flow rate is controlled precisely. The equipment used in particulate matter sampling is designed to collect desired range of particles by drawing air at a constant flow rate. This means, for both impactor-based systems and cyclone-based systems, air flow control is crucial in order to achieve accurate sampling. Otherwise, deviation from the ideal flow rate will lead to deviation from the desired size range of particles and result in inaccurate results.

In this study, two instruments were used for flow rate control. In the 1st phase of the study, mass flow controllers (MFC), in the 2nd phase, critical orifices were used. The instruments were calibrated against rotameter.

2.3.1. Mass flow controllers (MFC)

Mass flow controllers are flow rate control instruments that are used in liquids and gases. In general, mass flow controllers are calibrated for specific liquid(s) or gas(es); therefore, selection of appropriate mass flow controllers is vital for accurate sampling.

Mass flow rate controllers stabilize the flow at the desired rate by assigning a setpoint between 0% and 100% of its full scale. Thus, eliminating air flow rate fluctuations caused by pumps or other elements of the system. MFCs are available with and without display and do not need any further gauge, which makes them easy and practical to use.

Mass flow controllers are composed of an inlet port, outlet port, a mass flow sensor and proportional control valve. This way, it checks the flow rate signal received from mass flow sensor against the desired flow rate (setpoint) and adjusts the control valve in order to maintain the flow rate within minimal deviation from the setpoint.

In this study, Sierra Instruments SmartTrak® 50 Series mass flow controllers are used.

2.3.2. Critical orifices

Critical orifices are instruments that control the air flow rate by mechanical means, which basically constitutes an inlet and outlet, with a very small hole (orifice plate) in order to restrict the flow. Similar to a Venturi nozzle, critical orifice operation is based on Bernoulli Principle; which means, air flow rate is proportional to pressure difference.

In order to fully understand critical orifices, understanding of the concept of critical flow (a.k.a. choked flow) is prerequisite. Air flow rate increases as the differential pressure between the edges increases; however, once the air velocity reaches to sonic velocity, it reaches to maximum and no longer increases. This flow rate is called critical flow, and the orifices are called critical orifices (O'Keefe Controls Co., 2010; Stockham & Plante, 2004).

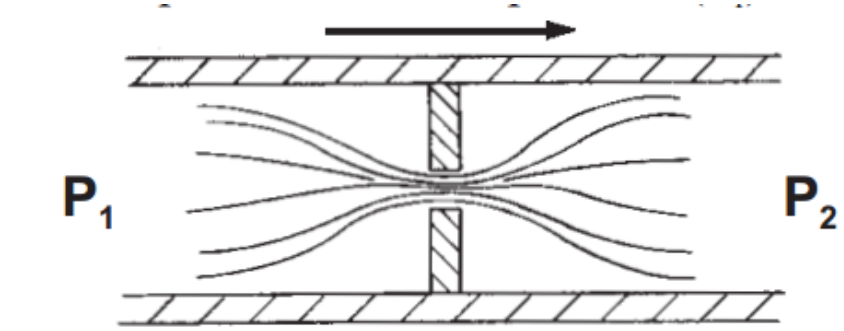

Sonic velocity occurs for air flow when $P_2/P_1 \leq .528$.

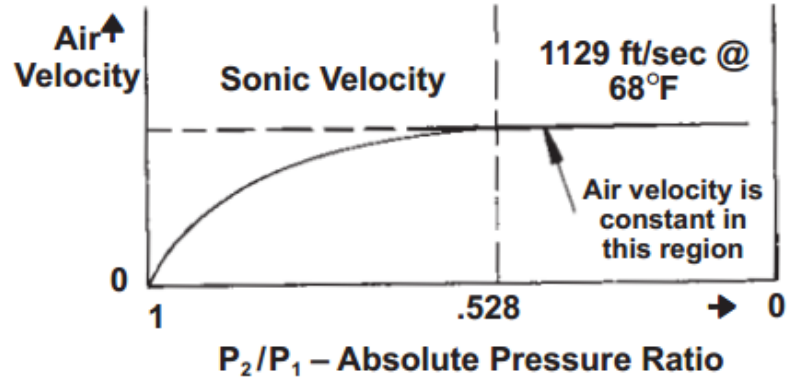

The air flow velocity is limited once the absolute pressure ratio is $\leq .528$.

Figure 2.21. Operation principle of critical orifices

Critical flow occurs when the ratio of absolute pressure in the inlet of the orifice and that of the outlet is 0.528 or greater. In other words, pressure difference between two edges is 15 – 18" Hg, under normal conditions. The pressure that this occurs is called critical pressure. At that condition, air velocity through the orifice is equal to sonic velocity and cannot increase any further. Considering that flow rate is a function of velocity and surface area, flow rate also will not increase any further. This enables critical orifices to provide stable air flow and greatly reduces fluctuations (O'Keefe Controls Co., 2010; Parkinson & Day, 1979).

Critical orifices are greatly advantageous over mass flow controllers by means of small size, compactness and lower repair & maintenance need much less price.

However, MFCs can be adjusted to any value within operation range in seconds, whereas critical orifices can only operate on one fixed flow rate. Besides, as critical orifices are analog devices, real time data monitoring and data logging is not possible, unlike mass flow controllers.

In this study, Swagelok - 6LV-4-VCR-6-DM-055P critical orifices are used. The hole diameter is selected as 0.055" (1.397 mm).

2.3.3. Filters used in air pollutant sampling

Filters are the media that the analyte particles are collected. For proper sampling and measurement of particles, selection of the filters is essential. Most commonly used type of filters are as follows (Mccammon et al., 1998).

2.3.3.1. Membrane filters

Membrane filters are the most popular type of filters used in air sampling. PTFE (Polytetrafluoroethylene – Teflon®), MCE (Mixed Cellulose Esters), silver and PVC (Polyvinylchloride) filters are common examples of membrane filters. With this type of filters, particulate matter, asbestos, PAHs, minerals and trace elements for ICP analysis can be sampled (Mccammon et al., 1998).

2.3.3.2. Glass and quartz fiber filters

This class of filters are suitable for applications like mercaptans and diesel emissions sampling. The quartz filters have been more widespread for having low blank values (Mccammon et al., 1998).

2.3.3.3. Polycarbonate filters

Polycarbonate filters are mostly preferred when the analyte collected on filters are to be analyzed by electron microscopy and X-ray fluorescence due to its specific characteristics (Mccammon et al., 1998).

CHAPTER 3

MATERIALS AND METHODS

3.1. Location of the study

Although the study is mostly research & development-based laboratory study, a field sampling for validation was carried out. For this reason, characterization of the study area is important.

Both laboratory studies and field studies are conducted at Environmental Engineering Department of the Middle East Technical University. The university is located at suburban region of Ankara, approximately 10 km away from the city center. The Department of Environmental Engineering is located at southern end of the campus, with an approximate distance of 2.5 km to Eskişehir Blvd and 3.5 km to Konya Blvd, which are, two heavy – traffic roads in Ankara.

In general, location of the university is not a densely populated residential area. In 1960s, the university was completely outside of the city. Through the years, the city had expanded towards the west (along the Eskişehir Blvd) and Middle East Technical University lost its rural characteristic. Despite the university is no longer outside of the city, the residential density is not as high as in the city center; therefore, "suburban" would be a relevant definition for the location of the university.

The design studies were carried out at laboratories of the department, while the sampling studies were carried out at the station established on backyard of the department building. Location of the study is shown in Figure 3.1.

Figure 3.1. Location of the study

The station used in this study had been used in a number of other monitoring projects in the past. The outcomes reveal that METU Environmental Engineering Station shows typical suburban AAQMS (Ambient Air Quality Monitoring Station) characteristics. The pollutant concentrations measured in this station (trace elements, volatile organic compounds, organic particles etc.) is generally lower than that of city center of Ankara (Goli, 2017; Koçak et al., 2017; Kuntasal et al., 2013). However, compared to data generated at rural areas in Turkey, pollutant concentrations measured at METU ENVE station is generally higher. General view of the study station is displayed in Figure 3.2.

Figure 3.2. Station where the studies are carried out

3.2. Strategy followed in development of the sampler

General description of the sampler and the rationale behind this study was discussed at the beginning. In construction of the device, 9-stage strategy was followed.

i. Development of general structure of the device
ii. Determination of the constituents to be used
iii. Procurement of the constituents
iv. Construction of the device using MFC
v. Physical & electrical controls and operation of the device
vi. Replacement of MFCs with critical orifices
vii. Design and construction of a data acquisition system to record (capture) sampling parameters such as air flow rates ın each channel, sampling duration, total volume of air that passes from each filter.
viii. Assembling of the constituents into a shelter
ix. Validation studies

3.2.1. Development of general structure of the device

The first stage in development of the sampler is, to design and construct the skeleton of the sampler. Although the study is initiated with a well-defined objective of developing a sampler with three channels that can simultaneously collects different PM fractions, a preliminary work is still required on how to reach this end. For example, particle size to be collected can be selected by cyclones, or pre-impactors. Similarly, the air flow rate which passes through the system can be adjusted by methods and/or products ranging from simple rotameters to complicated mass flow controllers. All these options are variables in this study and each selection leads to a different design of the sampler. And naturally, each design will have a different success rate regarding accomplishment of the targets defined at the beginning of the study. Therefore, primary knowledge of the main framework of the sampler and its constituent is a prominent first step to reach the desired results at the end of the study.

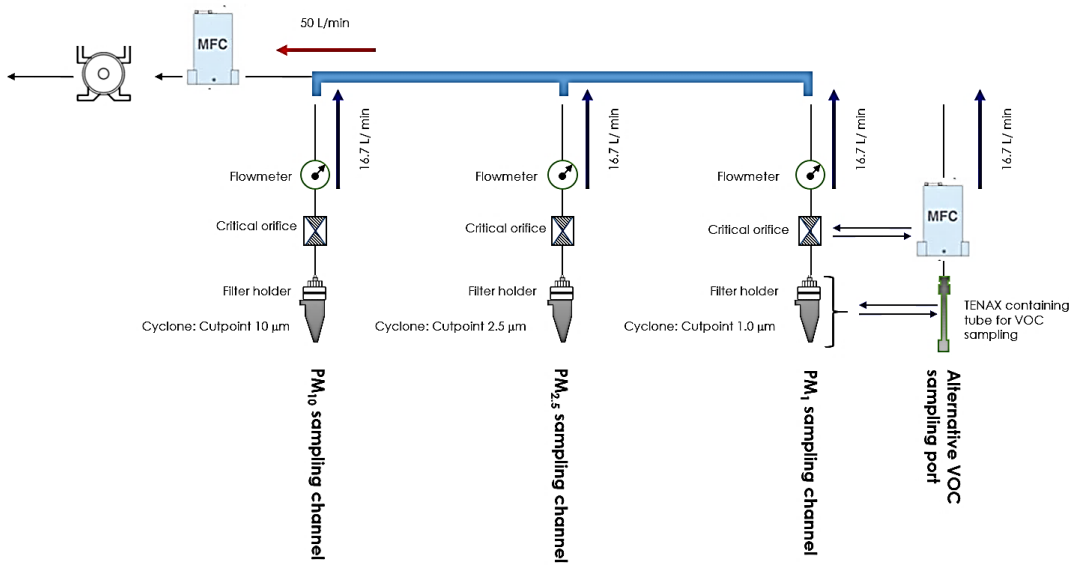

Figure 3.3. Sketch of the system presented in project proposal

The main framework of the sampler was determined prior to study, at the project proposal stage and even a roughly sketched process flow diagram was presented with the project proposal. The diagram can be seen in Figure 3.3. Throughout the study, the

framework has been subject to alterations and modifications, in line with problems faced during practical application of the study. The differences between the initial target and the end-product is evaluated at the discussion part.

3.2.2. Determination of the constituents to be used

The main framework of the sampling system and main constituents are certain; however, countless options are available in the market for each of the constituents. For instance, cyclones are determined as the PM size fractions selector and many types of cyclones are available in the market for this purpose. Similarly, a vast variety of options are available for filters/filter holders, air flow rate control and measuring devices and vacuum pumps. The preference of the equipment and justifications are discussed in detail in following chapters.

3.2.3. Procurement of the constituents

In the third stage of the study, the preferred constituents of the sampler were procured. Within this scope, three pieces of cyclones, filter holders, mass flow controllers (MFC), mass flow meters (FM) and critical orifices were purchased. Information regarding the instruments purchased for this study is presented in Table 3.1;

Table 3.1. *List of equipment purchased for construction of the sampler*

Item	*Qty*	*Product Information*	*Origin Country*
PM_1 cyclone	1	URG-2000-30EHB	US
$PM_{2.5}$ cyclone	1	URG-2000-30EH	US
PM_{10} cyclone	1	URG-2000-30ENB	US
Filter holder	3	URG-2000-30FG-2	US
Manifold	1	URG-2000-30HD-1	US
Mass Flow Controller (MFC)	3	SIERRA model C50L-AL-DD-2-PV2-V1-5POINTCAL-50-C9(0)-50 T8D	US
Mass Flow Meter (FM)	3	SIERRA model M50L-AL-DD-2-PV2-V1-5POINTCAL-50-C9(0)-50 T8D	US
Critical Orifice	3	Swagelok 6LV-4-VCR-6-DM-055P	US

Detailed information on the equipment used in the sampler is provided in the following sections.

3.2.4. Construction of the device using MFC

The step following the procurement of equipment is, to set up the system, providing necessary pneumatic and electric connections. Preliminary installation and operation studies were carried out at laboratory bench, where 3 cyclones are connected to the mass flow controllers. Initial construction phase of the system is displayed in Figure 3.4.

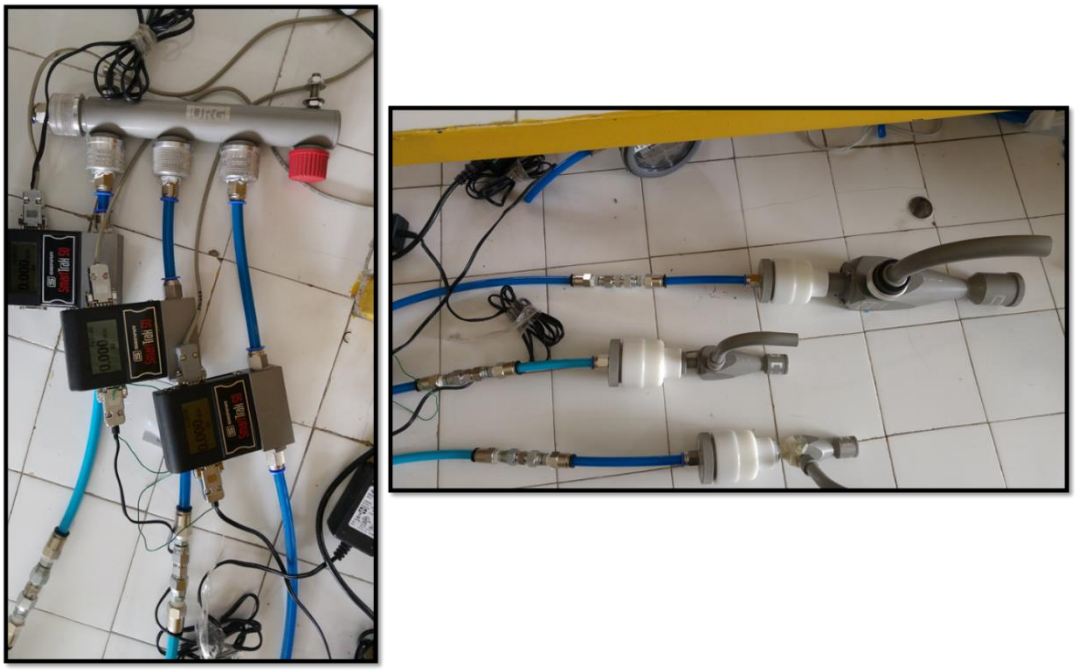

Figure 3.4. Preliminary installation of the sampler

During early phases of the study it was observed that, during sampling, pores on filters are clogged by the particles collected, which causes filter resistance (pressure drop across filters) to increase. As a result of this, the pump power required to keep flow rate steady at desired rate increases, thus, the stability of the flow rate controlled by mass flow controllers is disturbed and flow rate starts to decrease. In order to overcome this problem, a signal feedback unit is built to keep flow rate stable, by

increasing or decreasing the revolution of the pump via electric signals. This way, the air flow rate through the filters that particles are collected, can be stabilized. Detailed information on the feedback system is provided in the following chapters.

3.2.5. Physical & electrical controls and operation of the device

Following the construction of the system and getting into operation, mass flow controllers are calibrated with a rotameter to ensure accurate measurements.

Mass flow controllers and flow meters operate accurately provided that input or output is open to atmosphere. However, in this system, mass flow controllers and flow meters are installed between the pump and the filters, hence, they operate under mild vacuum. Due to vacuum conditions, the volume of the air under vacuum will be different than that of under 1 atm pressure. In this study, pressures are measured at points where mass flow controllers and flow meters are to be installed and reported to the manufacturer prior to purchase. Therefore, MFCs were calibrated to operate precisely under reported pressures, and calibration curves are plotted for validation of measurements in device displays, as in the following stages, the study will proceed with the presumption that the measurements on the display of mass flow controllers and flow meters are accurate.

In the first phase of the study, where, the sampler is operated with mass flow controllers, a temporary shelter was built to install components of the sampler equipment, in order to operate the sampler in parallel with stack filter unit (SFU), which collects PM_{10} and $PM_{2.5}$ particles. This way, the measurements of the sampler constructed can be compared to a known sampler. The shelter used in this part is not final shelter that is built by service procurement, a simple, temporary shelter to protect equipment against outside conditions during its test runs outside the building

3.2.6. Replacement of MFCs with critical orifices

So far in this study, the sampler has been constructed using available techniques and best available equipment, without worrying about the cost. The next stage was, as

mentioned in the action plan of the study, to reduce the costs of the sampler and to increase its competitiveness in atmospheric aerosol studies.

In order to fulfil this purpose, mass flow controllers were replaced with critical orifices. Mass flow controllers are the costliest constituent of the sampler, therefore, removing mass flow controllers from the system reduced the cost significantly.

As mentioned in a number of times in the manuscript, air flow rate control and stability is the primary concern for accurate sampling. Critical orifices are considered a low-cost alternative for keeping the flow rate constant. Detailed information on critical orifices and operation principles are provided in the following chapters.

Air flow rate is observed to decrease during sampling due to clogging of the filter surface by the particulate pollutants. The duration which flow rate decreases and the rate of decrease is observed to depend on the type of filter and filter material. Each filter type exerts different resistance to air flow, for this reason, the period for flow rate to decrease is determined experimentally. Details of this optimization will be discussed later in the manuscript.

3.2.7. Composing a data acquisition system to record air flow rates

The next phase of the study is to design a control unit that can log air flow rate and total volume of air passing through each channel.

Flow rate and total volume are two critical operational parameters in this sampler; flow rate ensures that the desired particle fraction is collected by the cyclones, as the cyclones in this study are designed to operate at 16.7 LPM. Therefore, flow rate should be monitored to ensure specified performance of the sampler.

Total volume of air withdrawn in each channel is another operational parameter for this sampler to generate data. Since the samples are measured gravimetrically, the total volume of air from which the corresponding particulate mass collected is needed to convert particle mass collected on filter (in μg) to particle concentration in $\mu g\ m^{-3}$.

Therefore, a data acquisition system was designed, constructed and installed to sampler. The data acquisition unit consisted a software that receives real - time air flow rate signals from the MFCs or FMs for each channel in the sampler and record these along with time and date data. After the sampling is ended total volume of air for each channel is computed. The control unit logs flow rate data in 10 second – averages. Collected data including, sampling start and end date and times, sampling duration and interruptions in sampling are shown on a small computer screen installed on the sampler along with the total air volume passed through each filter and average air flow rate at each channel during sampling. 10-sec average air flow rate data are stored in a memory and can be withdrawn if needed. Collected data can be transferred to a computer through a USB connection.

3.2.8. Assembling of the constituents into a shelter

The last phase of the study is installation of all components, including the pump, flow meters, critical orifices and electronic hardware of the data acquisition system, into a protective shelter. Only the cyclones and the filter holders attached to them are left outside, as they are supposed to collect samples from outside air. The cyclones are installed such that the air inlet is 2 meters higher from the ground.

3.2.9. Validation studies

At the end of the study, developed sampler was operated in parallel with samplers that are widely used in the literature and PM_{10} and $PM_{2.5}$ concentrations measured with each system were compared. Validation measurements were performed against two high volume samplers (Hi-vol), one stack filter unit (SFU) and one laser aerosol spectrometer (LAS)

3.3. Components of the Sampler

The components used in construction of this sampler are given in the following sections.

3.3.1. Cyclones

As the separation of particle fractions with respect to size is the most important step in a size - separated PM sampling, therefore, as the size selector component of the sampler, cyclones play the most important role in the operation of the whole system.

In this study, cyclones manufactured by URG Corp. are procured and installed to the system. Cutpoints of the three cyclones are; 10 μm, 2.5 μm and 1 μm when air flow – rate passing through them is 16.7 LPM. Here, cutpoint refer to the particle sizes at which 50% of the particles are allowed through the cyclone and collected on filters and the larger particles are intercepted by the cyclone inner walls.

PM_{10} cyclone is the one that allows particles smaller than 10 μm and intercepts the larger, so that enables PM_{10} particles to be collected on the filter attached to it. Model number of PM_{10} cyclone is URG-2000-30ENB. The body of the cyclone is Teflon coated aluminum. The bottom is removable for cleaning of accumulated particles. The outlet is #30 male threaded, so that the filter holder can be attached directly. Since there is no external connections between the cyclone and the filter holder, and the interior of all equipment are non-stick, the probability of particles stick to the walls and result in underestimation of particles is highly reduced, which is a commonly encountered problem in particle sampling using cyclones. Dimensions of the PM_{10} cyclone is 29.8 cm x 26 cm x 6.4 cm, while the weight is 1.4 kg. Inlet arm is 90 degrees downward curved in order to prevent rain droplets to enter the cyclone.

Teflon coating of the interior is very beneficial in trace element analyses, as in the metal cyclones, particles are likely to be contaminated by metals while leaving the cyclones. However, in polymer or Teflon coated cyclones like the one used in this study, such a contamination does not occur. This property was the main reason why URG cyclones were used in the sampler. Unfortunately Teflon coated Al URG cyclones are the most expensive ones in the market.

We could replace these expensive cyclones with cheaper high - density polyethylene or polypropylene cyclones, but we avoided it at this development stage, because we

did not want to deal with an additional uncertainty arising from potential cut-point fluctuations or variations in cheap cyclones. Using cheaper cyclones can be an option if the sampler is commercialized, or widely used in our group.

The correlation between the air flow - rate and the cutpoint at which the cyclone operates is presented by the manufacturer's chart in .

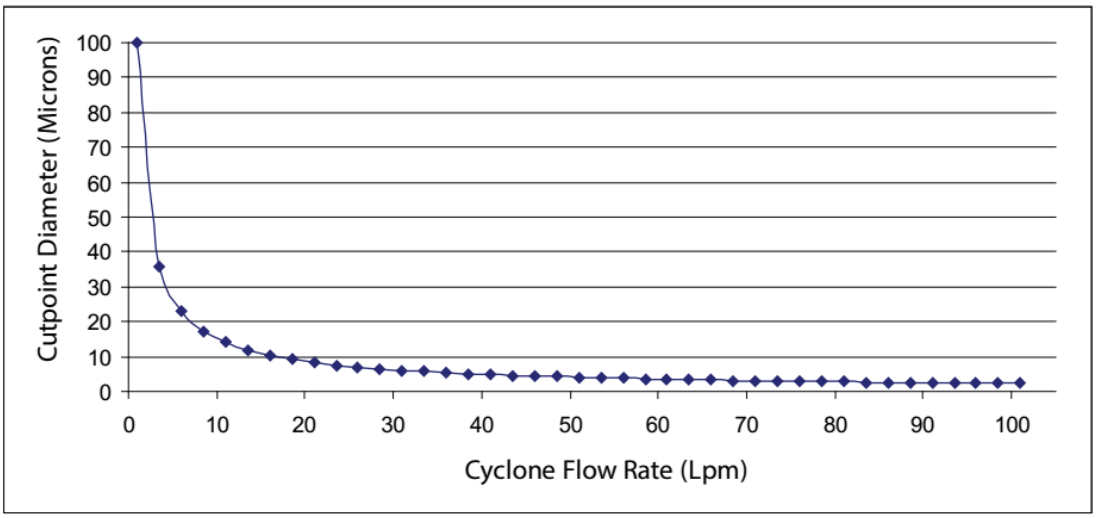

Figure 3.5. Calibration curve for PM_{10} cyclone (from URG user manual)

As seen in the figure, cutpoint diameter of the cyclone varies with air flow rate. This means, at flow rates lower than 16.7 LPM, particles larger than 10 μm can reach the filter, similarly, at flow rates higher than 16.7 LPM, some fraction of particles smaller than 10 μm cannot reach the filter. For this reason, in our sampler air flow rate at each channel was kept as close to 16.7 LPM as possible.

Cutoff diameter is more sensitive to air flow rate at air flows < 16.7 LPM than it is at air flows >16.7 LPM. For example, cutoff diameter we expect to use in this cyclone ia 10 μm at 16,7 LPM flow rate. It can be seen from the chart that cutoff diameter drops from 10 to 8 μm when flowrate increase from 16.7 LPM to 30 LPM. However, at lower flow-rate side; cutoff diameter increase form 16.7 μm to 23 μm when flow rate decrease from 16.7 LPM to 5 LPM.

Considering that the filter gets clogged with particles as the sampling proceeds, a shift in the flow rate toward lower values is much more likely to happen than the shift toward higher flow rate. Through an efficient flow rate control, this can be delayed but cannot be completely prevented. In this study, flow rate through PM_{10} is attempted to be sustained between 13 and 20 LPM for 24 hours, which is a typical sampling duration.

For $PM_{2.5}$ cyclone, the correlation between air-flowrate and cutoff diameter is given in . The cyclone used in $PM_{2.5}$ channel is model URG-2000-30EH manufactured by URG Corp. as the cyclones in other channels. $PM_{2.5}$ has dimensions of 16.5 cm x 15.6 cm x 3.8 cm and weight of 0.3 kg, which is relatively smaller than PM_{10} cyclone. However, operational principle and material properties are the same; having interior surfaces Teflon coated against metal contamination and threaded outlet to minimize particle loss on the way to the filter.

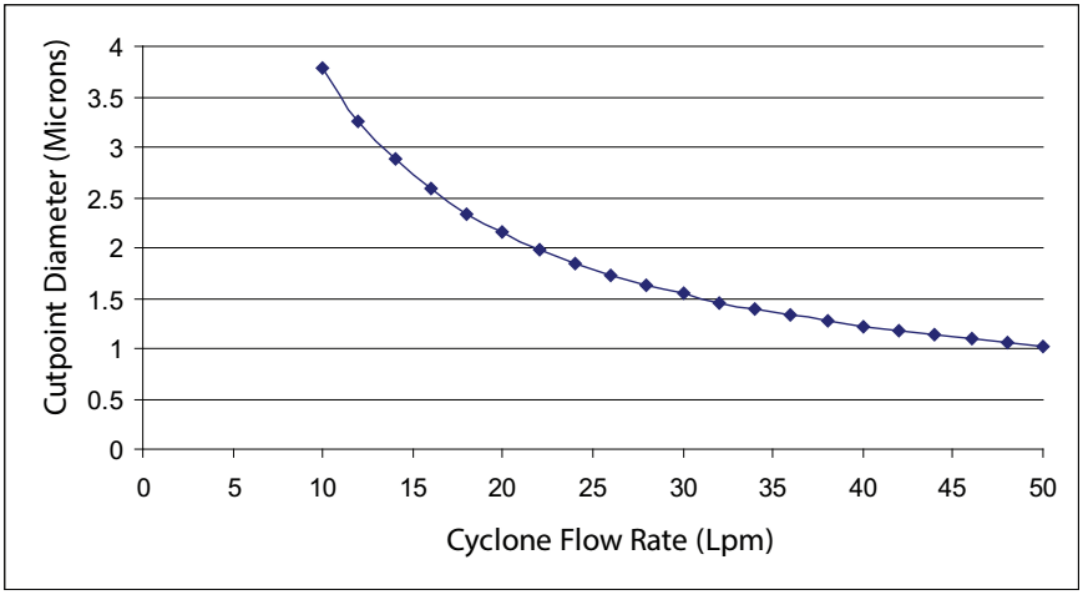

Figure 3.6. Calibration curve for $PM_{2.5}$ cyclone (from URG user manual)

Manufacturer's chart for cutoff diameter with respect to air flow rate reveals that the sensitivity of $PM_{2.5}$ cyclone to fluctuation in flow rate is higher than that of PM_{10} cyclone. The cutpoint is observed to be 2.5 μm at 16.7 LPM, while 2.8 μm at 13 LPM,

2.7 μm at 15 LPM and 2.2 μm at 20 LPM. In this study, the flow rate is attempted to be kept above 13 LPM for a 24- hour duration.

In PM_1 channel, URG-2000-30EHB model cyclone is used. Dimensions are 3.3 cm x 14.9 cm x 3.2 cm and the weight is 0.2 kg, which makes it the smallest of the cyclone among the three. Likewise, operational principle and material properties are the same; having interior surfaces Teflon coated against metal contamination and threaded outlet to minimize particle loss.

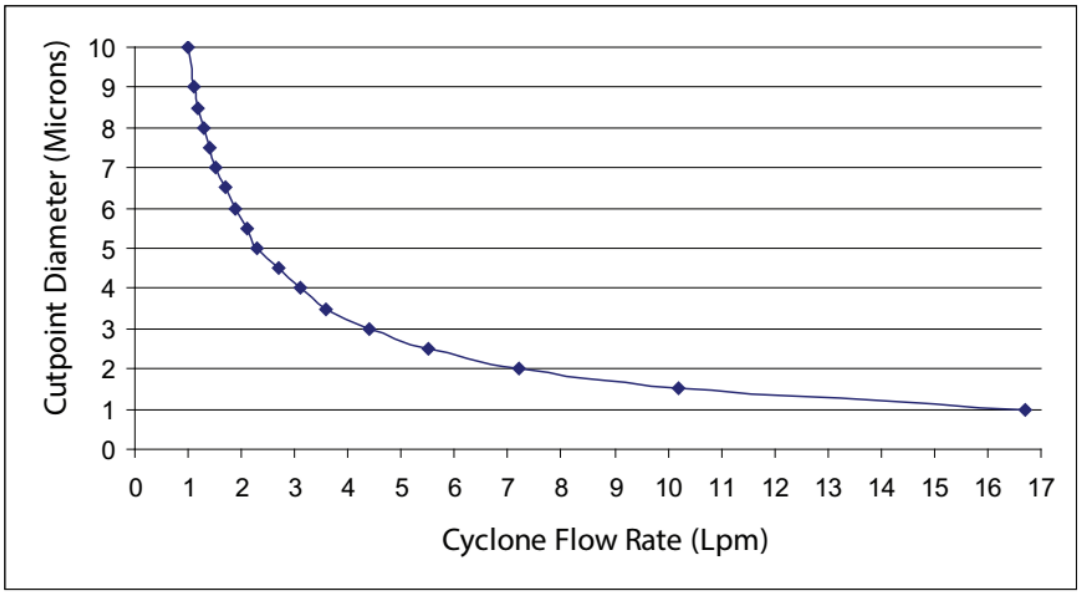

Figure 3.7. Calibration curve for PM_1 cyclone (from URG user manual)

Manufacturer's chart for cutoff diameter of PM_1 cyclone against air-flow-rate is displayed in . The chart reveals that the control of cutoff diameter, in other words, the control of the particles entering the cyclone and reaching the filter is relatively easier in PM_1 channel. At 16.7 LPM flow rate, the cutoff diameter is 1 μm, while this value becomes 1.5 μm at flow rates as low as 10 LPM. Therefore, assuming the flow rate is maintained above 13 LPM, the cutpoint will be maintained between 1 – 1.2 μm.

3.3.2. Filter Holders

Model 2000-30FG filter holders, manufactured by URG Corp. were preferred in this study in order to achieve the best fitting to the cyclones manufactured by the same company. Filter holders are directly connected to threaded cyclone outlet. Thus, air does not travel through any tubing, where particle loss is likely.

Outer diameter of the filter holder is 6.7 cm and height of 12.7 cm. These holders is appropriate for filters with 47 mm diameter. All components of the filter holder is made of Teflon, with a threaded inlet, so that the filter holder and the cyclone is connected without an external connection element. This way, as stated previously, the risk of particle loss along the sampling path due to sticking to interior surfaces can be greatly reduced; therefore, this specification is an important motive of preference in particle sampling tasks. For this reason, this filter holders are preferred in this study despite being relatively costly.

The outlet of the filter holder has a diameter of ¼" and of "quick connect" type, as the filter holders will be required to be plugged in and out before and after each sampling. Throughout the study, 2 drawbacks have been observed with the built-in quick connect fittings of the filter holders. (1) This type of quick connects and are not readily available in Turkey and should be imported upon purchase order. Considering that these quick connects will be used not only in filter holders, but in each connection nod throughout the system (MFCs, manifold connections, pump connection etc.), the procurement process may jeopardize the continuity of the study. Besides, preliminary sampling studies revealed that ¼" fittings are not appropriate for the sampler designed, as they cause too much resistance to air flow, which leads to difficulties in maintaining the desired air flow rate during the sampling. For these reasons, even though initially ¼" fittings were planned to be used, ½" diameter is determined as standard for all fittings and pipes in this sampler.

For the reasons mentioned; the outlet of the filter has been processed to be suitable for ½" fitting and the quick connect fittings are replaced with a different type of ½"

fittings that are easily available in Turkey. This type of fittings have been used in many applications in our group and are known to be reliable fittings. Leak tests are performed regularly in order to ensure that fittings are leak-free.

3.3.3. Mass Flow Controllers

In this study, SmartTrak 50 Series mass flow controllers, manufactured by Sierra Instruments were used. The instruments are denoted with model number C50M-AL-DD-3-PV2-V1-5POINTCAL-50-C9(0)-50 T10D. The order code refers to the following specifications;

- **C50M:** Mass Flow Controller
- **AL:** Aluminum Body
- **DD:** Digital Display (front mounted)
- **3:** 3/8-inch compression
- **PV2:** 24 VDC for all instruments
- **V1:** 0 to 5 VDC linear output signal and setpoint
- **5POINTCAL:** 5 Point calibration certificate
- **50-C9(0):** Communication cable with D9 mating connector
- **50 T10D:** 24 VDC power supply with D-connector, 1.5 Amps, 110-230 VAC,

Mass flow controllers consist of a measurement unit, by-pass unit, air flow rate control valve and necessary electronic units. Inlet air is first split into two parts such that one part of the air passes through flow rate measurement unit and the other part passes through by-pass unit. The air velocity is measured by velocity sensor and transferred to control valve as electrical signal. Control valve adjusts the flow rate such that the difference in set flow rate and actual flow rate reaches to zero and constant flow rate is maintained.

Mass flow controllers used in each channel are of the same model. In the initial design of the instrument, three MFCs; one at each channel and one between the manifold and pump (which is capable of controlling flow at higher flow-rates) was planned to be

used. However, this configuration is observed to increase air resistance in the system, thus affecting the flow rate stability in channels. For this reason, the idea of using MFC between manifold and pump was abandoned and rest of the work was carried out with one MFC in each channel. MFCs in channels was placed between filter holders and manifold.

In the second phase of the study, again SmartTrak 50 Series mass flow meters (not controllers), manufactured by Sierra Instruments were used. Model number of these devices is M50-AL-DD-2-PV2-V1-5POINTCAL-50-C9(0)-50 T8D. Mass flow meters are identical to the mass flow controllers in appearance and dimensions. The only difference is, flow meters do not include of a control valve, therefore cannot control flow rate.

3.3.4. Pump

In this study, an oil-less carbon vane vacuum pump, which is manufactured by F&J Specialty Products, with model number DF-1E was used. The pump is more expensive than some of the other brands in the market, but it has two main advantages.

1. there is a mass flow controller installed on the pump with which air flow rate through the filter can be adjusted between 14 and 115 LPM (the maximum flow can only be achieved while no filter holder is attached, in other words, while there is no resistance to air flow).
2. The pump includes a control unit, which stores information such as sampling duration, real-time and average air flow rate and total air volume passed through filters during sampling. However, since one pump is connected to all three channels in the sampler, this unit can only display the values for the sum of the channels, not individually.

A photo of the pump is depicted in Figure 3.8. In the past, this pump was used in many sampling studies in our group.

Figure 3.8. The pump used in this study

3.3.5. Critical Orifices

In the second phase of the study, critical orifices are used for the flow rate control, to reduce manufacturing cost of the sampler. Cost of a critical orifice is around $184, while for MFC, this is around $1280, which makes a remarkable difference in the cost of the sampler. Critical orifices are intended to accomplish the flow rate control task with less cost than mass flow controllers. Within this context, Swagelok model 6LV-4-VCR-6-DM-055P critical orifices are used. The orifice has a 316L stainless steel body, and hole diameter 0.055 inches (1.397 mm). Image and technical drawing of critical orifices are given in Figure 3.9.

As in the rest of the system, the critical orifices are connected to the system via ¼” quick-connect fittings. ½” fittings were preferred in all connections in sampler. However, ¼” fittings were used in critical orifices, because orifices come with ¼” threads and ones with ½” threads were not available. In Figure 3.8, the orifices are shown with quick connect fittings on them.

Figure 3.9. The critical orifices used in this study

3.3.6. Manifold and pneumatic connections

In this study, channels are connected to the pump via URG 2000-30HD manifold, and the pneumatic connections between elements of the sampler are via quick-connect fittings. Technical specifications of the manifold and the quick-connect fittings used in this sampler is shown in Figure 3.10.

Figure 3.10. The manifold and quick-connect fittings used in this study

The manifold is 27 cm long and has 4 ports, each placed with 7 cm intervals. The ports are threaded to fit the filter holders that are manufactured by URG Corp. However, since mass flow controllers or critical orifices are connected in between, adapters that converts #30 male threads to ½" quick connects are fabricated in order to connect the manifold with MFCs or critical orifices. Like other components by URG, the manifold is made of Teflon coated aluminum. Since 3 channels are used in this sampler, the 4th inlet of the manifold is sealed to prevent air leakage.

Air in all parts of the sampler, from sample holder to the pump, transported through ½" diameter, HDPE (High Density Polyethylene) tubing. As mentioned previously, all junctions throughout the system are connected to each other via quick-connect fittings. For this, the instruments that do not have quick-connect fittings or the ones that have quick connect fittings different than ½" are modified accordingly and in the end, fittings and pipes of same diameter is used through the system.

Quick-connect fittings constitute a significant role in development stage of the sampler in this study. The construction of the sampler requires hundreds of trials, experiments, controls and observations, and these require the elements of the sampler to be plugged and unplugged hundreds of times. In addition, even after construction of the sampler, through regular sampling, filter holders should be unplugged and plugged at the end of every sampling period to change the filers. For these reasons, quick connects save the user(s) a significant loss of time and effort.

The quick connect fittings that are used in this study are model PC ½-N03 manufactured by Eason Pneumatics. However, these type fittings are standard and available by many manufacturers and very easily supplied at very low cost. Yet, despite all these advantages, they are very reliable fittings and have long been used in similar studies efficiently. The fittings have stainless steel body and polyethylene ring that unlocks and locks the thread of the fitting. As the pipe pushed in, the thread fits to pipe and locks, thus makes the connection airtight. For the removal, as the blue ring is pushed, the thread unlocks and releases the pipe for easy removal.

CHAPTER 4

RESULTS AND DISCUSSION

4.1. Construction of the sampler with mass flow controllers

4.1.1. Installation of the sampler

The proposed sampler has the following characteristics;

- The device is a 3-channel system and in these channels, PM_1, $PM_{2.5}$ and PM_{10} particles will be collected simultaneously,
- Each channel consists of; a size selector to classify particles in the desired size range, which are cyclones in this study, a filter holder, a flow control unit to stabilize flowrate at 16.7 LPM and a flow measuring unit to display the instant flowrate.
- All three channels are connected to the same pump.

Although the final configuration of the sampler is in line with the initial design, it has been subject to minor alterations.

In the initial design, connection between the elements were planned to be through high-density polyethylene (HDPE) tubing with inner diameter of ¼“(8.4 mm). However, during the construction, it was observed that these pipes generate too much pressure on the pump and fail to provide the desired flow rate. Therefore, in final application, elements are connected through ½” (12.7 mm) inner diameter HDPE tubing.

The sampler is planned as a 3-channel sampler; however, the sampling manifold, where all three channels are connected to the pump, is selected to be of 4-channels, so that it can operate with up to four channels.

Scheme of the proposed sampler is illustrated in . To identify each component of the device, the numbers are assigned for each unit and briefly explained below;

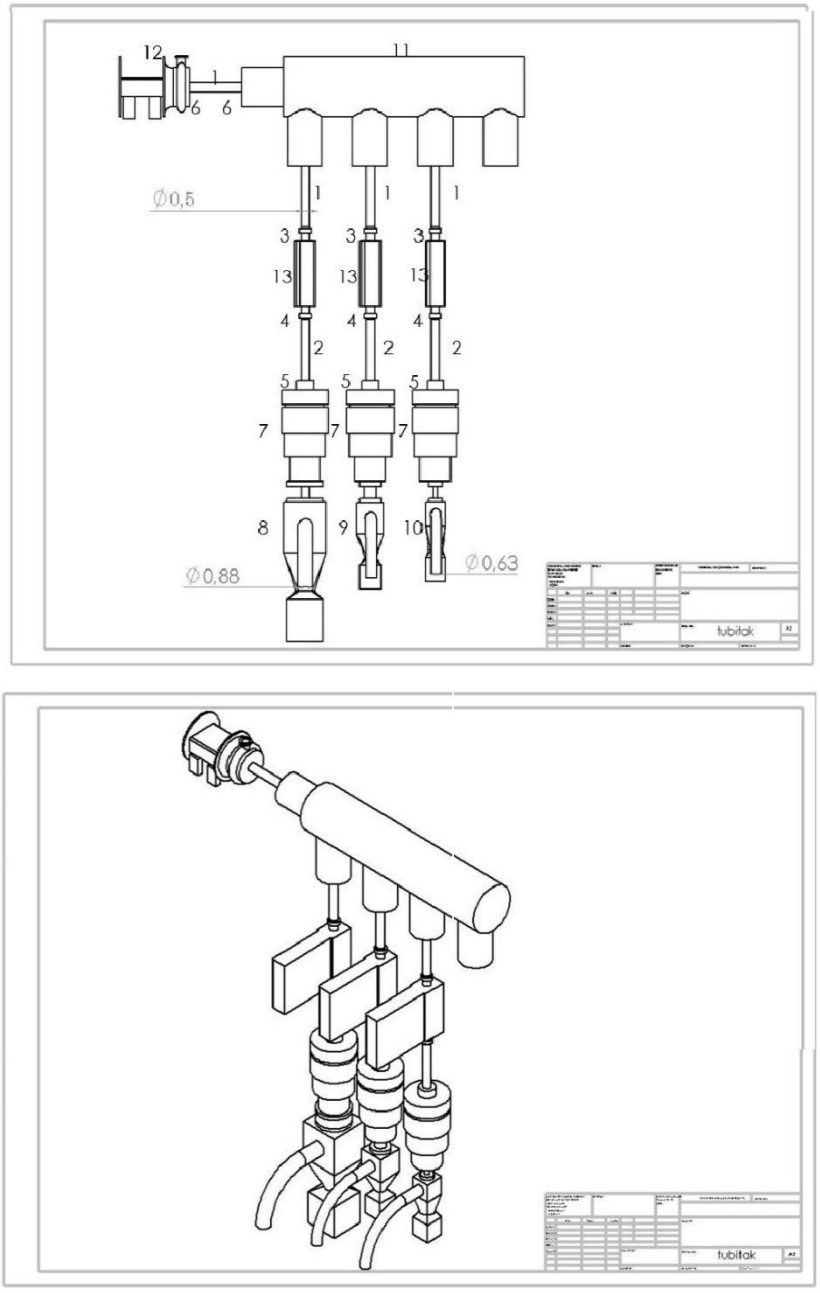

Figure 4.1. Schematic flow diagram of the sampler constructed with mass flow controllers

The connections #1 and #2 represent high density polyethylene (HDPE) tubing with inner diameter of ½" (12.7 mm).

Connections with number 3, 4, 5 and 6 are quick-connects which can be easily assembled & disassembled without any mechanical tools. These quick connects enable the system to be very modular and flexible to different configurations and thus significantly facilitated the development and production stage, where, many different configurations are tested.

The items #7 are filter holders, which are made of Teflon (PTFE). Items #8, #9 and #10 are PM_{10}, $PM_{2.5}$ and PM_1 cyclones, respectively. The cyclones are designed to operate at 16.7 LPM and collect the particles on the filter, which are smaller than 10 μm, 2.5 μm and 1 μm respectively. Since cutoff diameter of the cyclones are dependent on flow rate, it is crucial to provide a steady flow of 16.7 LPM (24 m^3/day) to achieve the desired particle collection.

As discussed before, for efficient operation of the sampler, a constant flow rate of 16.7 LPM should be supplied. Even though the desired flow rate is supplied at the beginning, as the filters are clogged with particles, the filter resistance increases, and the flow rate gradually decreases. This fall may be postponed but cannot be completely prevented. For this reason, in this study, flow rate is aimed to remain >13 LPM at the end of a 24-hour sampling in a polluted urban atmosphere.

The items designated with #13 are mass flow controllers (MFC), which set the flow rate and hold constant. In the further stages of the study, mass flow controllers are replaced by critical orifices in order to reduce the cost.

The item #11 is a manifold, which connects the three sampling channels to one air outlet, where the pump is connected. The manifold is made of Teflon-coated aluminum, as in cyclones.

The pump, which is designated with #12, is a highly stable and reliable pump. It has capacity of drawing 115 liters of air per minute when no filter is on. It can also display and record the flow rate, total air drawn and operation time.

4.1.2. Installation of the sampler using mass flow controllers and monitoring of the flow rates

The stage after designing the sampler is, physically assembling and carrying out tests on the sampler. The sampler is first assembled in the laboratory and flow rate of the mass flow controllers are controlled. The cyclones are connected with a calibrated rotameter and operated against different flow rates, which are adjusted through MFC's software in the computer. This way, flow rates displayed by the MFCs and the rotameter are compared.

The purpose of this comparison is to observe the precision of the flow rate controlled by MFCs under various conditions. Devices like mass flow controllers and flow meters operate precisely when input or output is open to atmosphere; however, in this system, they are installed between the filter holder and the pump. Therefore, they operate under vacuum, and the pressure of the air is not equal to 1 atm and measured volume is different. In the procurement stage of the MFCs and FMs, vacuum measurements are carried out at the junctions where the devices will be installed, and the results are reported to the manufacturer (Sierra). So that, the devices are calibrated to conduct the measurements precisely under the reported vacuum conditions, which means, flow rates displayed by mass flow controllers and flow meters are supposed to be precise. This condition is confirmed through a simple measurement with rotameters. Rotameters are placed in the beginning of the sampling train (instead of cyclone and filter) (because one end of the rotameter has to be open to atmosphere). Rotameter readings at 1 atm are compared with MFC and MF readings under vacuum in different flow rates.

Calibration curves obtained by flow rate values read by MFCs against the rotameter is given in Figure 4.2 for each sampling channel. As seen in the figure, when all three MFCs' data are plotted against rotameter data and resulted in around 1.1 slope value. This result corresponds to a 10% error. This difference is considered "acceptable". As

a result of this test, MFCs are considered to hold the flow rate constant properly. A similar test is conducted when MFCs are replaced with critical orifice – FM couple.

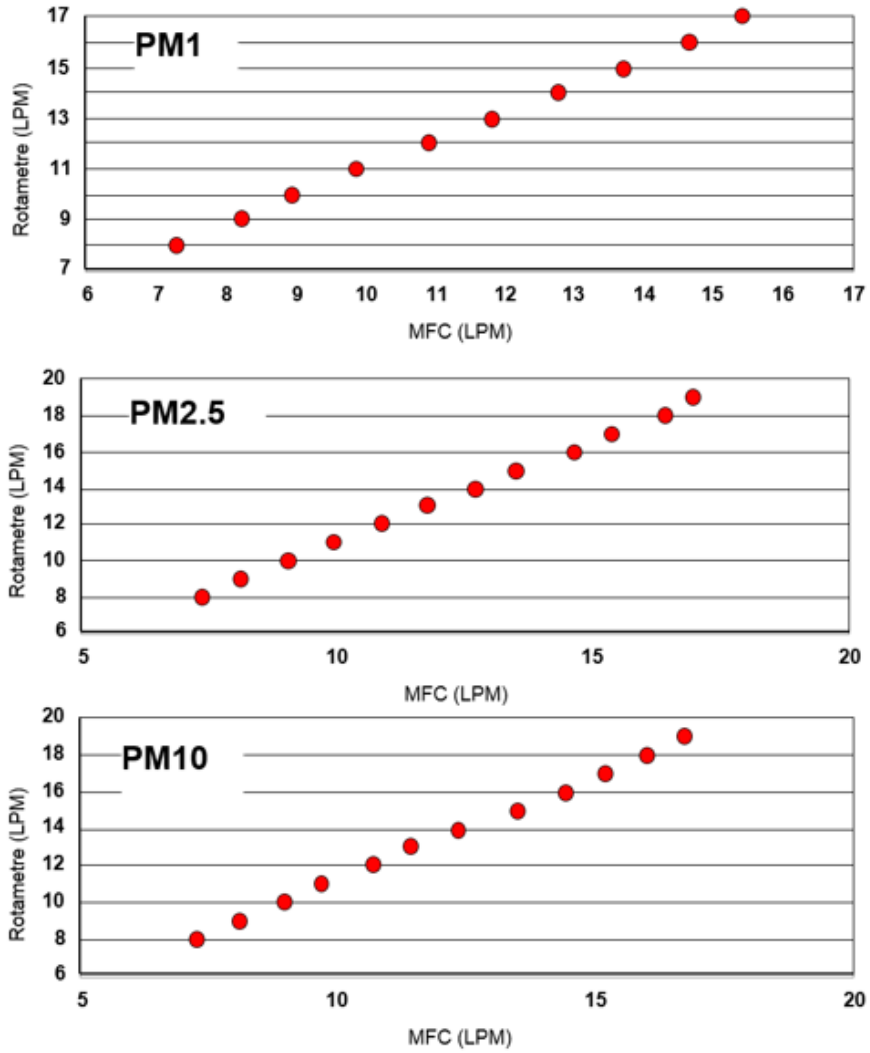

Figure 4.2. Calibration curves obtained by the sampler with MFCs

4.1.3. Installation of feedback system

As previously mentioned, MFCs keep the flow rate at a specified value. However, as the pores of the filters are clogged with particles, the flow rate decreases. Although MFCs keep the flow rate at 16.7 LPM to some extent, when the resistance of the filter

increases to a point, MFCs lose their control ability and starts to function as a flow meter.

In order to prevent this inconvenience, a feedback system is installed. The system receives flow rate data from MFC and evaluates with the current RPM (Revolutions per minute) value of the pump. When the flow rate decreases, the system responds and increases the revolution of the pump so as to sustain the flow rate at 16.7 LPM and when it exceeds 16.7 LPM, the system decreases the revolution of the pump, thus the flow rate of air. The system can be seen in Figure 4.3, and the electrical diagram of the system is given in Figure 4.4.

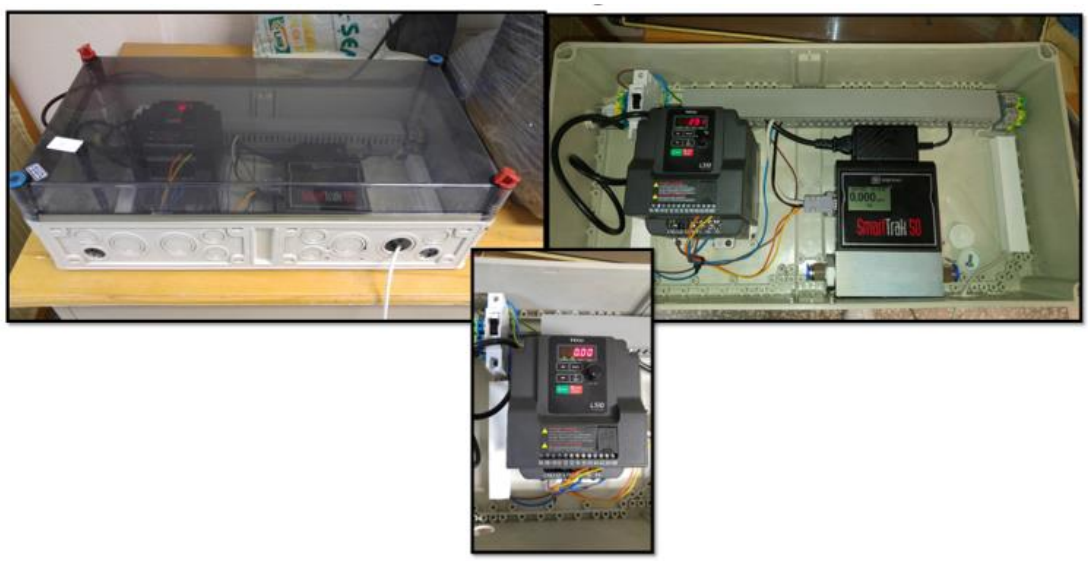

Figure 4.3. MFC feedback system

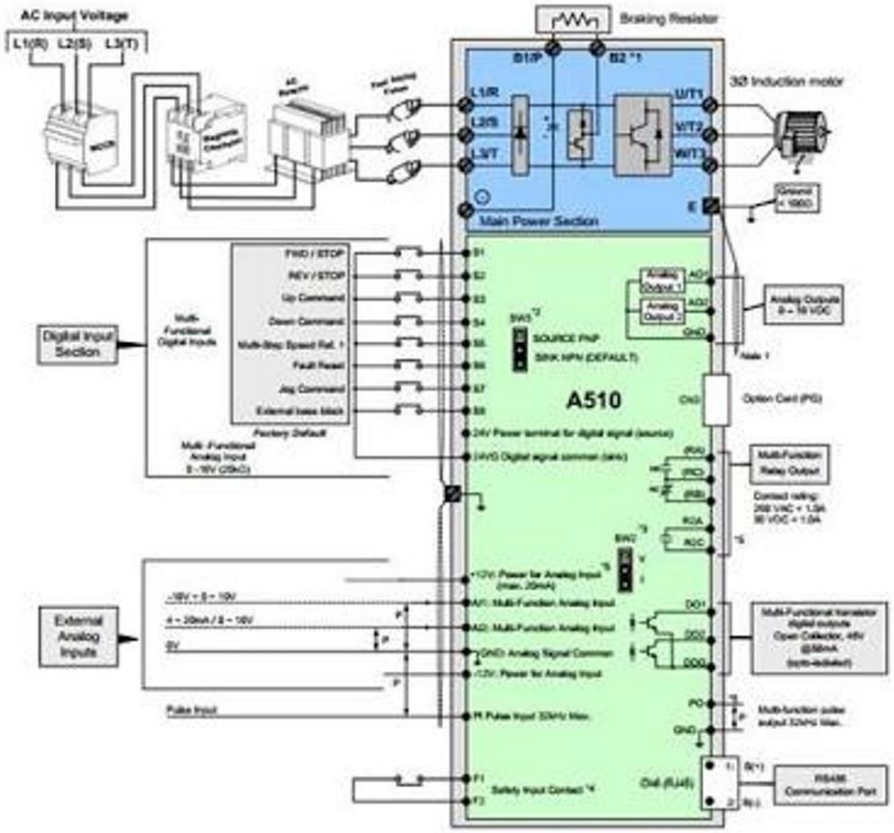

Figure 4.4. Electrical Diagram of MFC feedback system

4.1.4. Comparison of the sampler with MFCs against the "Stack Filter Unit"

In this phase of the study, the sampler assembled with MFCs were operated in parallel with a Stack Filter Unit (SFU, a.k.a. Gent Sampler), in which, $PM_{2.5\text{-}10}$ and $PM_{2.5}$ particles are collected in two separate filters. SFU is a widely used and validated (Hopke et al., 1997) sampling system. In both samplers, Nucleopore™ filters are used as particle collection media for durations 24 – 71 hours.

As the sampling was carried out outdoor, a temporary shelter was built for components of the sampler. This shelter was temporary and constructed for tests that must be conducted at the open air. Since the sampler was not in its final form at this stage a permanent shelter was not designed. The design and construction of permanent shelter

is described later in the manuscript. The shelter and the sampler inside the shelter can be seen in Figure 4.5.

Filters are conditioned for 24 hours under constant temperature and humidity, before and after sampling. Filter weights are measured by a microbalance (Mettler, XPR2U) with 1 μg precision. Mass concentrations obtained by the two samplers are compared and the results are demonstrated in Figure 4.6.

At the end of 12 days of sampling, the ratio of mass concentrations (SFU/new sampler) is found to be 1.0 for $PM_{2.5}$ fraction, and 1.1 for PM_{10} fraction. This result indicates that there is only 10% difference in coarse fraction of particles and the new sampler operates satisfactorily for field study.

Figure 4.5. Sampler located inside the temporary shelter

4.2. Construction of the sampler with critical orifices

In the previous section, operation of the designed sampler using mass flow controller units, which is the first phase of this study, is discussed. As previously stated, mass flow controllers are costly instruments. Considering that each channel needs MFCs, three MFCs are required for assembling of the sampler and this puts a heavy financial

burden on the sampling study. Since the rationale of the study is to develop an economical sampler, MFCs were replaced with lower cost flow-control devices, which are critical orifices. Definition and working principle of the critical orifice was mentioned in previous chapters.

Critical orifices are remarkably lower cost instruments compared to mass flow controllers. A set of three critical orifices cost around $480, whereas three MFCs cost approximately $9,000. This numbers indicate a notable cost reduction by this replacement.

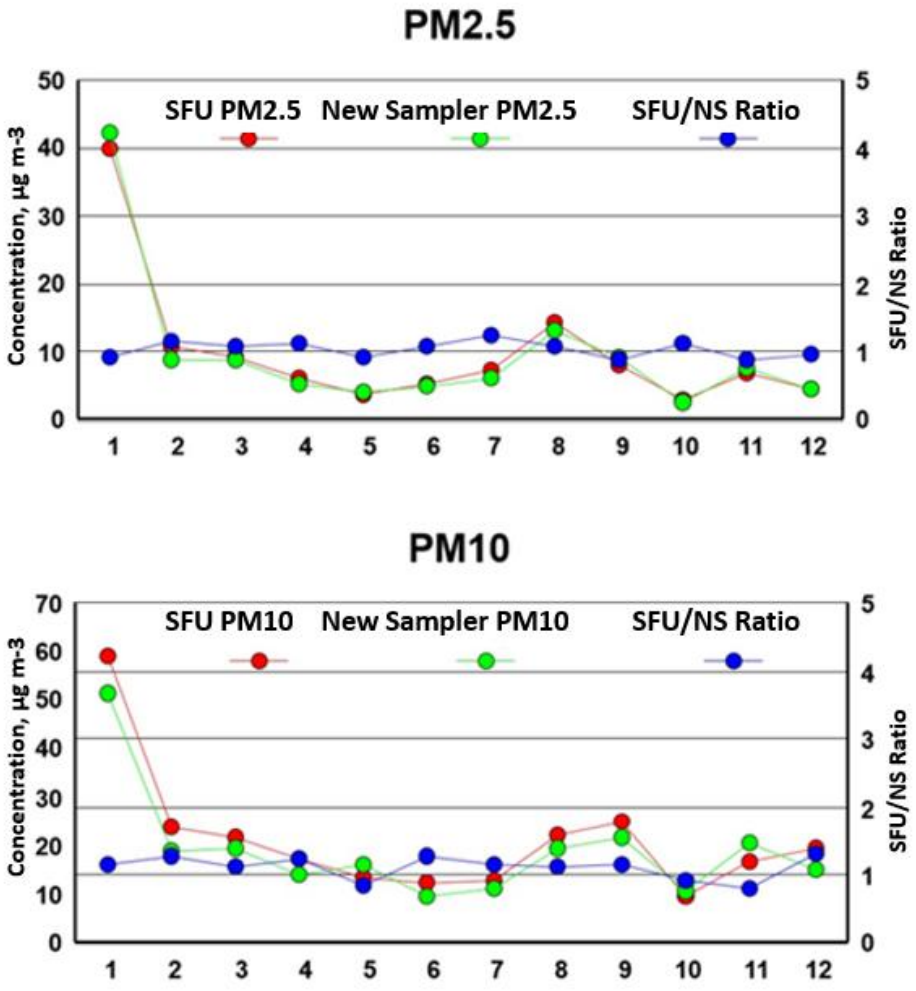

Figure 4.6. Comparison of PM_1, $PM_{2.5}$ and PM_{10} concentrations from the new sampler and $PM_{2.5}$ and PM_{10} concentrations from stack filter unit

Unlike mass flow controllers, critical orifices cannot measure air flow rate; therefore, each channel needed to be equipped with an air flowmeter. In this study, mass flow meters are used, which are, the most accurate, but also the most expensive flowmeters in the market. Technical specifications of the instruments used are mentioned in previous sections. In this phase of the study, mass flow meters are planned to be installed temporarily and then replaced with rotameters, which are, much cheaper than electronic flow meters. However, throughout time, monitoring of flow rate and recording of flow rate, sampling time and total volume of air data through PC connection turned out to be necessary and a control module is integrated to the system in order to receive data from the instruments and export to computer. Since rotameters are mechanical instruments and cannot transmit electronic signals, replacement of mass flowmeters, which can transmit real-time electronic flow rate signals to computer, with rotameters was given up.

Technical drawing of the sampling system with critical orifices installed is illustrated in Figure 4.7. The process flow is principally the same with the case where MFCs were on the system, the only difference is mass flow controllers are replaced with a critical orifice and flow meter. Connections between the elements of the system is, as in the previous installation, quick connections. Transport of air in the sampler is again through ½” (12.7 mm) HDPE tubing.

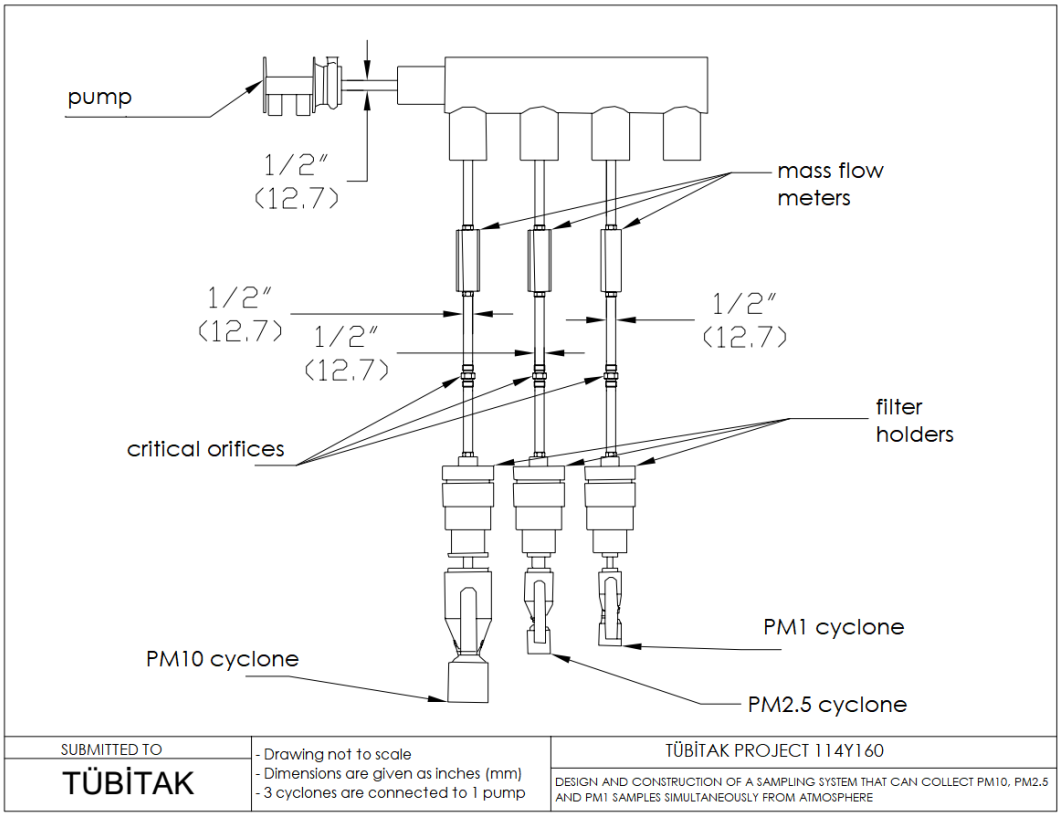

Figure 4.7. Technical drawing of the sampler with critical orifices

As the critical orifice configuration is the final design of the sampler, the sampler was subject to performance tests and following this, the components of the sampler was mounted to the final shelter, which is, durable and resistant to field conditions.

4.3. Variation of air flow rate with respect to various filter types

In this study, stability of air flow rate is a very important parameter, actually, the most important parameter. As previously stated, during the sampling of particles from the atmosphere, the resistance of the filters towards the air flow increases as the pores of the filters are clogged with particles. As a result of this, the flow rate through the filter starts to fall despite the attempts to keep it stable by the flow rate control device (MFC or critical orifice).

In the sampling systems that consists of one single filter, the variation of flow rate with respect to time is acceptable as long as the total volume of air passing through

the filter is monitored with tools like gas meters. However, in size separated sampling systems, like the one in this study, variation in flow rate directly affects the performance of the sampler, due to variation of cyclone cutoff diameters with air flowrate. This fact does apply, not only for the sampler in this study, but also in any type of sampler, where, the collected particle sizes are determined by a size selector like cyclones or pre-impactors.

The most important parameter which influences air flow stability in samplers is the ambient particle concentration. In the cases of high particle load in the air (as in Saharan dust episodes), the filters will be clogged with particles regardless of the sampler type. In addition to particle concentration, some instrumental parameters also influence the performance of the sampler. Pump power, performance of the air flow control unit and the filter type are amongst the instrumental parameters. Powerful pumps and good control units may delay the flow drop but cannot completely prevent. Different filter types have different resistance against air flow. Filters with high air flow resistance have higher tendency of earlier drop in flowrate. For this reason, lower resistance (Δp) is an important criteria in filter selection, yet, not the only concern. Having a low blank value and a reasonable price is also important parameters in filter selection.

Throughout the studies conducted at our department up to now, two type of filters, namely PTTF filters (Teflon) and Nuclepore filters. Teflon filters are made of PTTF (as its name implies), have low trace element blanks, and show low resistance to air flow; however, they are expensive. Nuclepore filters are made up of polycarbonate. Pores are drilled by α-etching, which generates very uniform pore diameters throughout polycarbonate sheet. Electron microscope pictures of PTTF and Nuclepore filters are given in Figure 4.8. Highly uniform pore size in polycarbonate filter is obvious in the figure. Distribution of pore size in PTTF filters are not the same. Pore size in PTTF and other membrane filters (except for Nuclepore) refer to average pore size in the filter. 2.0 μm pore size indicated on the package means that individual pores can have different diameters but the average on the filter is 2.0 μm.

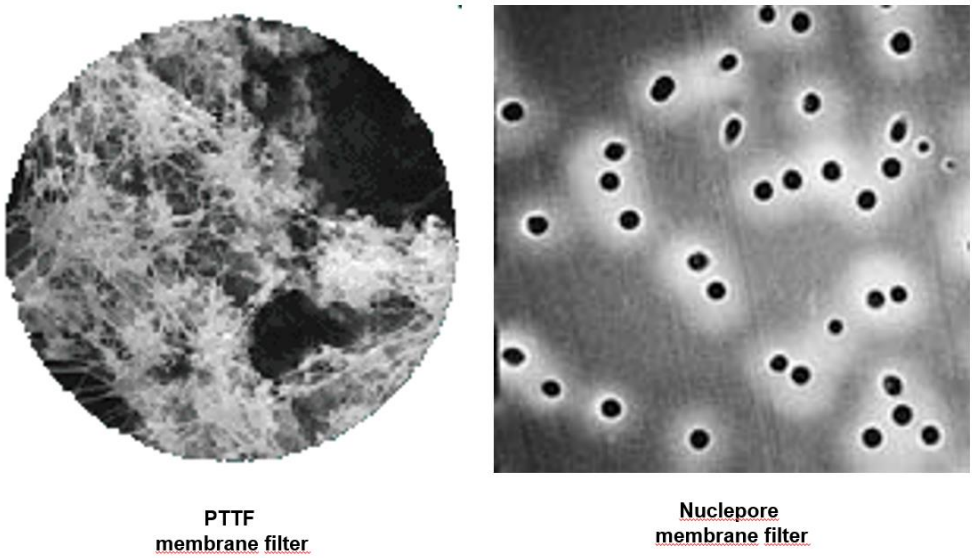

Figure 4.8. Electron microscope pictures of PTTF and Nuclepore filters

Nuclepore filters also have low trace element blanks, and they are significantly cheaper than PTFE filters. However, as pointed before, pressure drop across the filter is high thus, they are more likely to cause flow drop.

In this study, Teflon and Nucleopore filters, which represent two different groups in terms of their resistance to air flow, are used in order to observe the variation of the flow rate in each three channels of the sampler using both type of filters.

The sampler is operated at the station outside the Environmental Engineering building, using Teflon and Nucleopore filters for 72 hours and the air flow rate is monitored with 10 seconds intervals. Variation of air flowrate in time are given in Figure 4.9 and Figure 4.10 for PTTF and polycarbonate filters, respectively.

It is observed that at the end of 72-hour sampling, the flow rate does not vary remarkably when PTTF filter was used. Test sampling started with flow rate of 16.7 LPM and ended with 16.3 LPM. This result corresponds to 2.4% decline in 72 hours, and this percent of variation will not result in a significant change in distribution of collected particles. In conclusion, the trial with PTFE filters yields encouraging results

and shows its capability to collect samples for long durations, even in a relatively polluted atmosphere in Ankara.

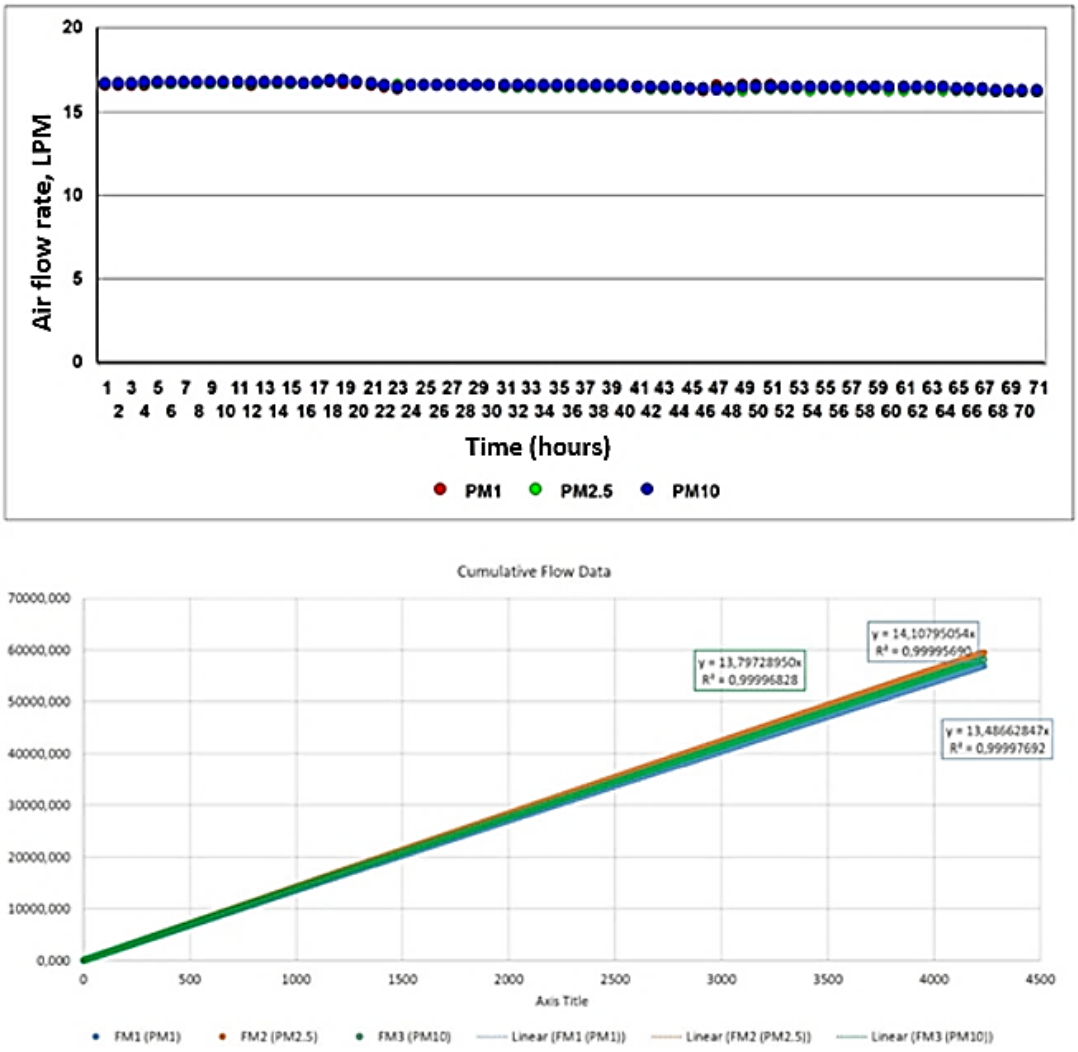

Figure 4.9. Variation of air flowrate wrt time 1: Teflon filter

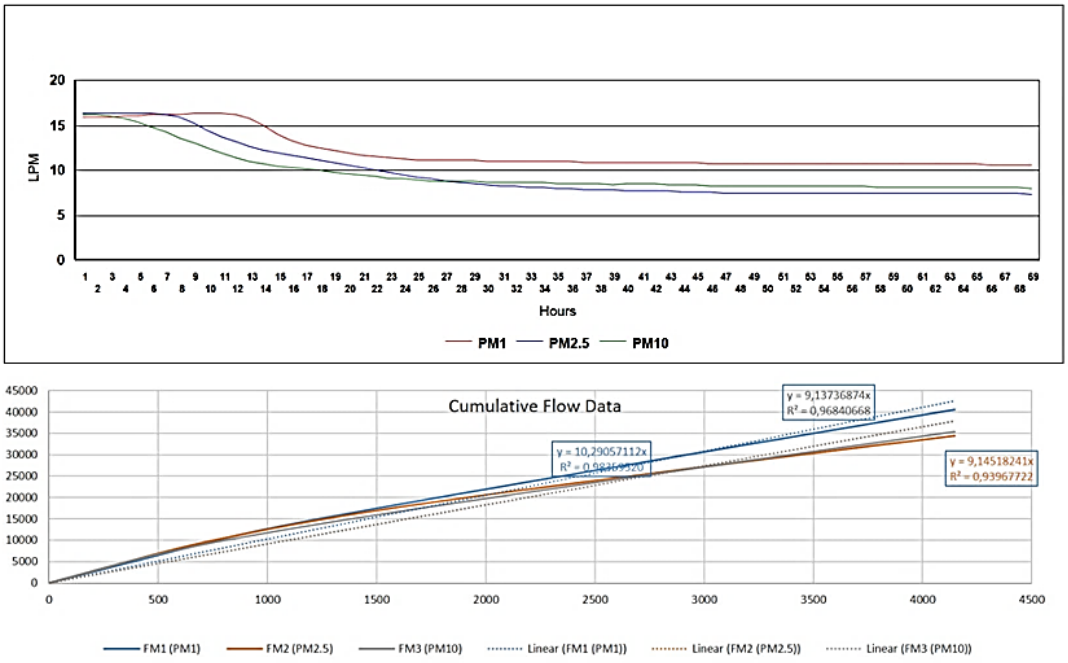

Figure 4.10. Variation of air flowrate wrt time 2: Nucleopore filter

In this procedure, Teflon filters represent the filter group with low resistance to air flow. In other words, the designed system will yield similarly good results with other low resistance filters such as quartz, cellulose fiber, cellulose acetate and nitrate structure filters, thus, can be used safely.

In measurements with Nucleopore filters, however, a stable trend as in Teflon filters could not be retrieved. In this part of the study, the air sampling started with initial flow rate of 16.7 LPM as previous, however, it started to fall after 13 hours in PM_1 channel, 8 hours in $PM_{2.5}$ channel and 4 hours in PM_{10} channel. At the end of 72 hours sampling, flow rates observed in PM_1, $PM_{2.5}$ and PM_{10} are; 11 LPM, 8 LPM and 7 LPM, respectively. According to these results checked on manufacturer's flow rate vs. cutoff diameter charts; PM_1 cyclone eliminates particles greater than 1.5 µm at 11 LPM, while it is supposed to eliminate particles greater than 1 µm. Similarly, in $PM_{2.5}$ channel, at 8 LPM, particles smaller than 10 µm are collected on filters, instead of 2.5 µm and in PM_{10} channel, at 7 LPM, particles smaller than 20 µm are collected instead of 10 µm. These outcomes indicate that Nucleopore filters significantly alters the

characteristics of the sampler and these relatively cheap filters cannot be used in the designed sampler.

Though, it should be noted that these tests were carried out under extreme circumstances. 72 hours is not a typical sampling duration. In 24 hours of sampling, which is more realistic, final flow rates are slightly higher than that of 72 hours, but still not satisfactory, as it cannot remain above 13 LPM, which is intended as lower limit in this study. Furthermore, under higher particle pollution loads than that of Ankara, this decline will begin in a shorter time, which will end up even more altered characteristics of the sampler. Therefore, Nucleopore filters have been concluded inappropriate for the sampler in this study.

As mentioned before, Nucleopore filters have relatively lower cost than Teflon filters, therefore, before eliminating this option, Nucleopore filters were tested for applicability to certain conditions. Two tests were carried out with this purpose. In the first test, the air is sampled from one channel (PM_1) and flow rate is monitored. In the second, all three channels are used but connected to two pumps, instead of one. The variation of flow rate in the first test and the second can be seen in Figure 4.11 and Figure 4.12 respectively.

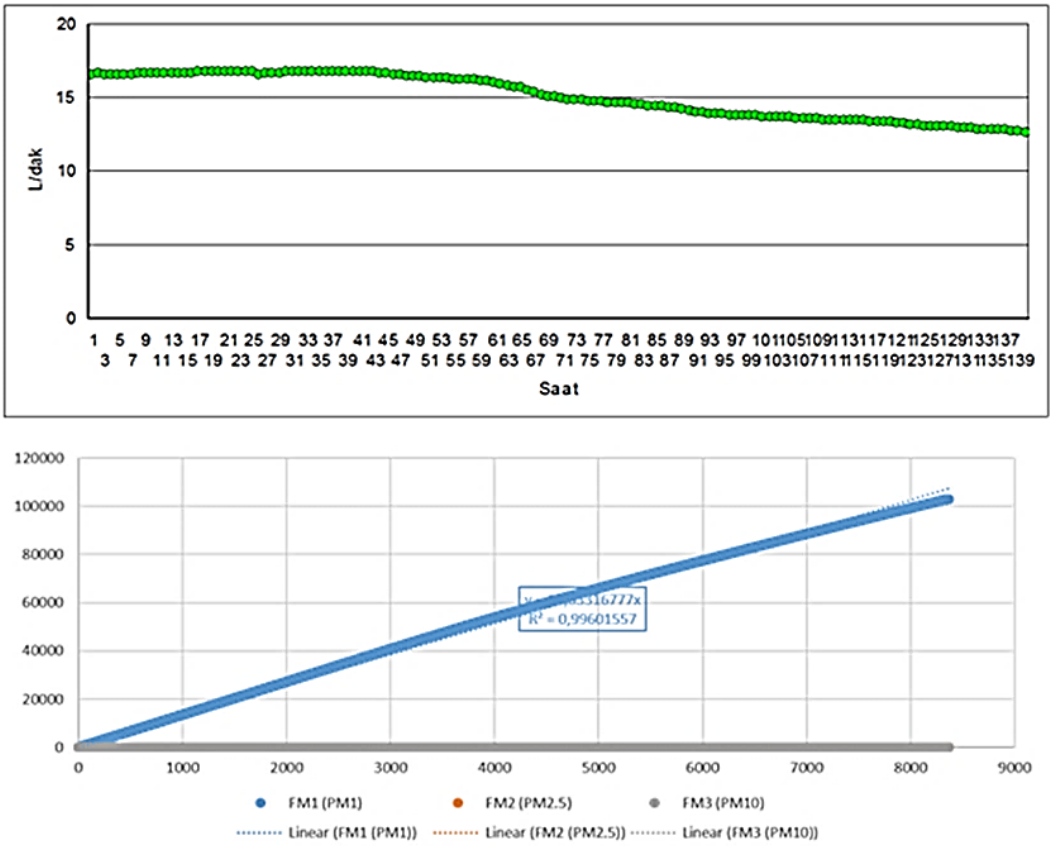

Figure 4.11. Variation of air flowrate wrt time 3: Nucleopore filter, 1 channel and 1 pump

In the test with one channel connected to one pump, the flow rate declines to 13 LPM at the end of 72-hour sampling. Checking from the manufacturer's cutpoint chart for PM_1 cyclone, this flow rate corresponds to 1.2 μm cutpoint diameter. This result is evaluated satisfactory for this study. Therefore, it is considered that Nucleopore filters may be used one channel in sampling studies not exceeding 24 hours.

The second test, with three channels and two pumps, however, did not yield encouraging results. Even though two pumps managed to keep flow rate around 16 LPM for longer duration than single pump, at the end of 24 hours sampling, the flow rate was subject to significant decline.

Results of filter-type tests demonstrated that although Nuclepore filters can be used in one channel when sampling duration not exceeding 24 hours, in general these filters

are not recommended for designed sampler. Teflon and other membrane filters with similar low pressure drop can be reliably used in sampling with this sampler. Teflon filters appears to be the best choice considering their superior blank characteristics.

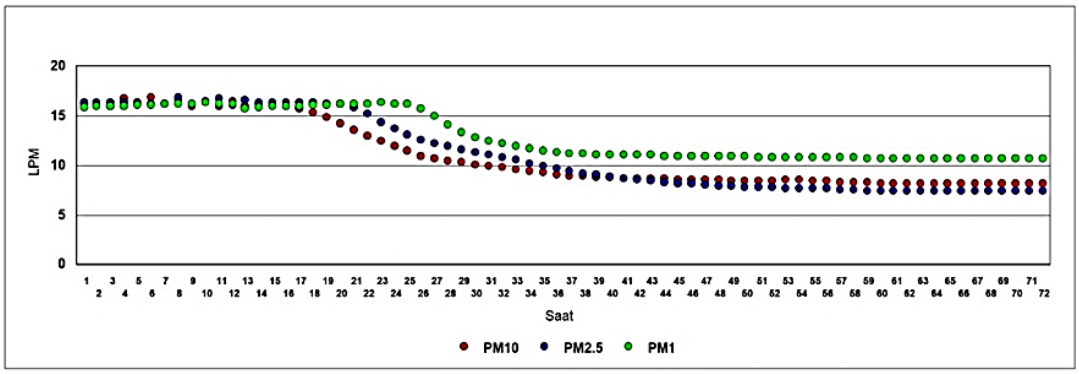

Figure 4.12. Variation of air flowrate wrt time 4: Nucleopore filter, 3 channel and 2 pumps

4.4. Repeatability tests

In this study, repeatability refers to having the same air flow rate at the beginning of each sampling and following the same changing trend through time. To examine the repeatability of the sampling, a test was conducted. In the test, PTFE filters are inserted, and sampler is operated for 1 hour and this procedure is repeated 10 times. The flow rate at each channel with respect to time in 10 second periods was monitored and demonstrated in Figure 4.13.

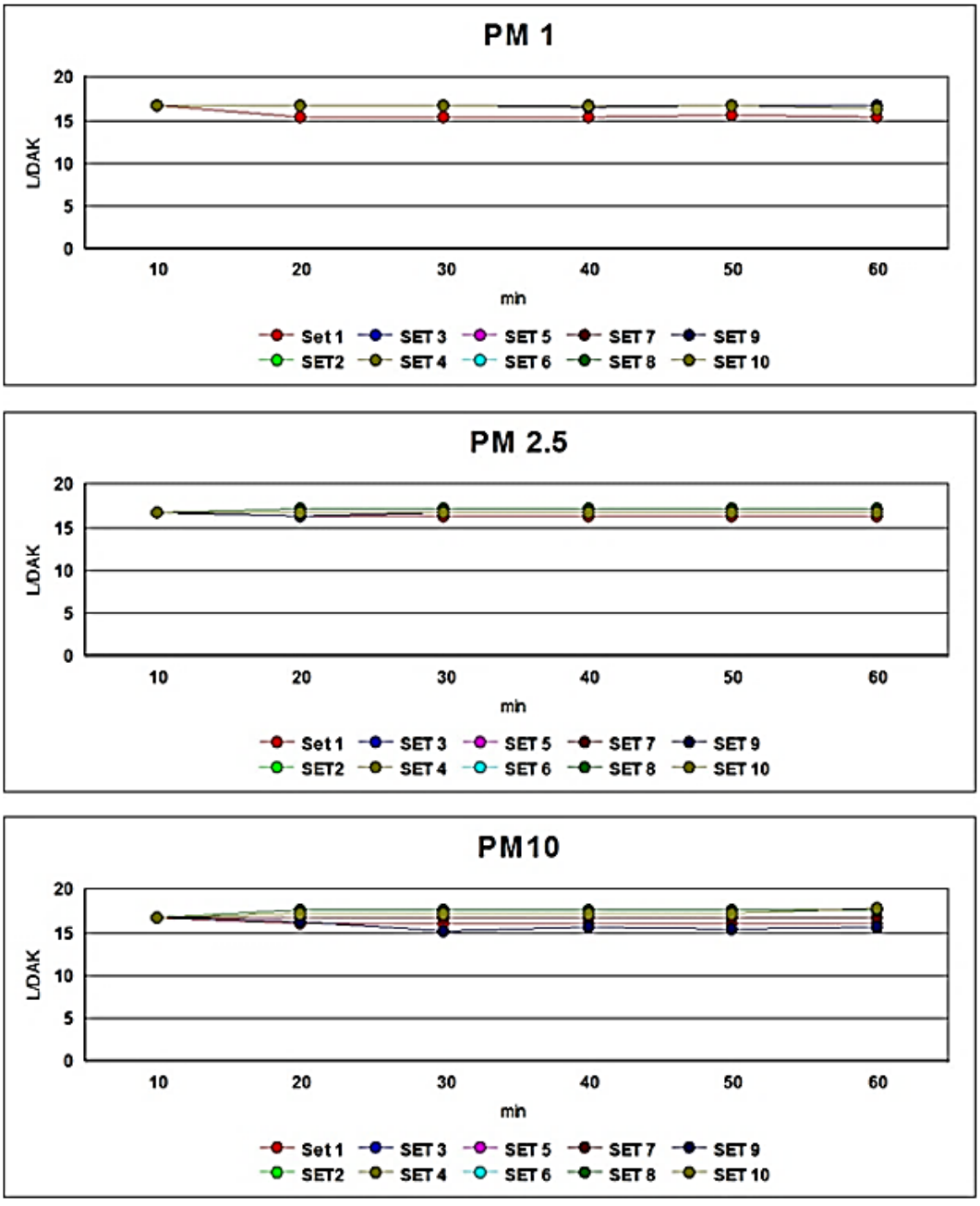

Figure 4.13. Repeatability tests results

As seen in the figure, the sampler has a proper repeatability, as the change in the flow rate at the end of 1 hour is found to be less than 2 percent.

4.5. Construction of data logger and control unit

Every sampler consists of a control module that transfers information from sampler to the user. The most important information in this sampler is the total volume of air that passes through the filter during sampling, as being a main component for calculation of the particulate concentration in the air. Besides, monitoring of air flow rate is also crucial for monitoring of the diameter of the particles collected at each channel of the sampler.

In this study, a control module that can monitor flow rate with 10 second intervals and calculate total air volume based on this data is installed to sampler and data is retrieved through this module. The module receives signals from the mass flow meters at each channel. In the case of power cut, the module reports the time and duration of the cut. The unit is designed and constructed by Dr. Türkay Onacak, Hacettepe University, Environmental Engineering department via a service agreement with our group.

With this unit, the sampling system can be monitored with 10 second intervals. In such sampling, ten second interval is not a widely used integration interval, therefore upon demand, following the finish of the sampling, it is possible to save the total volume of air that passes through the filters during sampling. The view of the module in the sampler cabin can be seen in Figure 4.14.

Figure 4.14. View of the control unit installed on the sampler

The main component of the module is an electronic control card, which is intended to run the control and data reading processes. In this module, 18F452 microcontroller, from the family of PIC (Peripheral Interface Controller), manufactured by MicroChip company is used. A schematic diagram of the controller is shown in Figure 4.15.

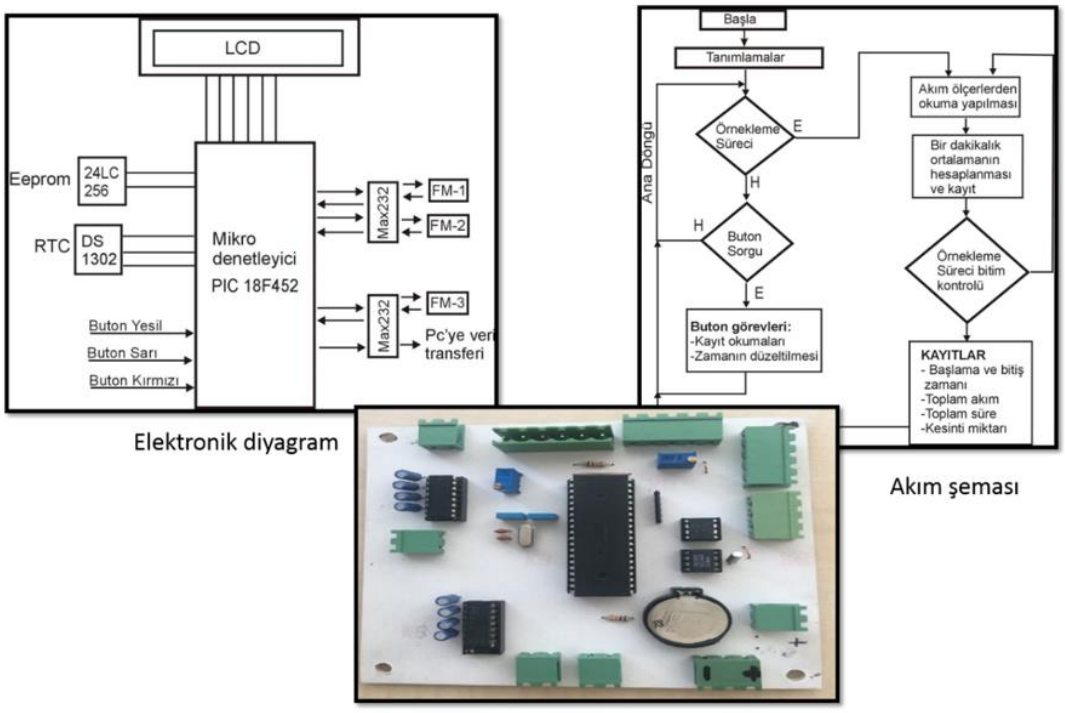

Figure 4.15. Electronic and process flow diagram of the control unit

For determination of the sampling time, an RTC (Real Time Clock) was integrated to the sampler. For this purpose, DS1302 RTC, manufactured by Dallas Semiconductor, was used. For storage of the sampling data, 24LC512 external memory (EEPROM), manufactured by MicroChip, was used. For conversion of RS232 signals to TTL, 2 pieces of MAX232 items was used.

4.5.1. Sampling system micro controller software

The microcontroller, CCS-C PIC was programmed for the specifications of this study.

1- In the main cycle of the control card microcontroller software, sampling process and the buttons are controlled. Software checks whether the sampling

switch is on “1” position and initiates the sampling process if it is “1”. Data coming from mass flowmeters (or MFCs) at every 10 seconds were received and cumulated on previous outcomes. When 6 flow data is received corresponding to 1min data capturing, average of these values constitutes the amount of air that is collected in the last 1 minute. After every minute, this value is added to the previous value so that cumulative volume of air that passes through the filters at any time during the sampling can be seen on display. At the end of 1-day sampling, this value constitutes the daily volume of air withdrawn. A brief formulation of the process are given below.

n1+n2+n3+n4+n5+n6/6=N1 One-minute air volume, L/min

N1+N2+N3+ …… +Nlast Total withdrawn air volume, L/min

2- When sampling switch was brought to “0” position, the signal to microcontroller is ceased and the microcontroller terminates the sampling process and starts saving process. First, sampling start and finish time are saved. Then total amount of flow is read from the mass flow meters and duration of the sampling is saved and number of power cuts, if there is any. After these are complete, it returns to the main menu.
3- Another cycle in microcontroller software is, the check of whether the control buttons are pressed. The assigned task to each button is conducted by the microcontroller upon the buttons are pressed. The tasks of the buttons are explained in detail in the following section.

4.6. Flow rate stability tests

After construction of data log unit, the new sampler has undergone flow rate stability test to ensure proper operation. For this, channels are loaded with filters and the sampler was run to monitor the air flow rate and observe variations caused by different variables, such as sampling duration, filter type and flow rate control device. These studies are conducted in Air Pollution Laboratory of the Environmental Engineering Department.

4.6.1. Flow characteristics of the sampler when mass flow controllers are used in channels

As the 1st phase of the study, the cyclones are connected to mass flow controllers, nuclepore filters are loaded to filter holders and sampler was operated for 72 hours. The variation in flowrate with time is depicted in Figure 4.16.

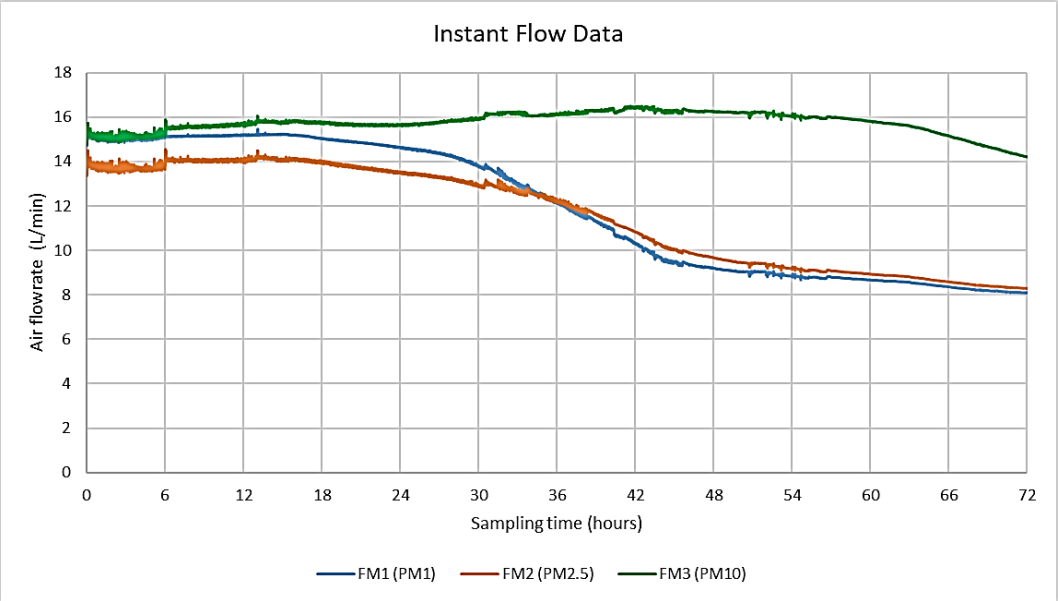

Figure 4.16. 72 hours of sampling with 3 MFCs connected to 1 pump using Nucleopore filters

Flowrate started to drop after 18 hours in $PM_{2.5}$ and PM_1 channels, but it remained constant for a longer time in PM_{10} channel. Flowrate starts to decrease after 60 hours in PM_{10} channel.

Same configuration as above; 3 MFCs with one pump and nucleopore filters, is also run for 24 hours to monitor flow rate for a typical sampling duration and the results are shown in Figure 4.17.

The chart indicates that PM_{10} and PM_1 start with a similar flow rate and the $PM_{2.5}$ with a slightly lower than the other two. Apart from minor fluctuations, all three channels do not undergo significant flow rate drop during 24-hour sampling. However, under field conditions where particle pollution load is higher, this effect is higher.

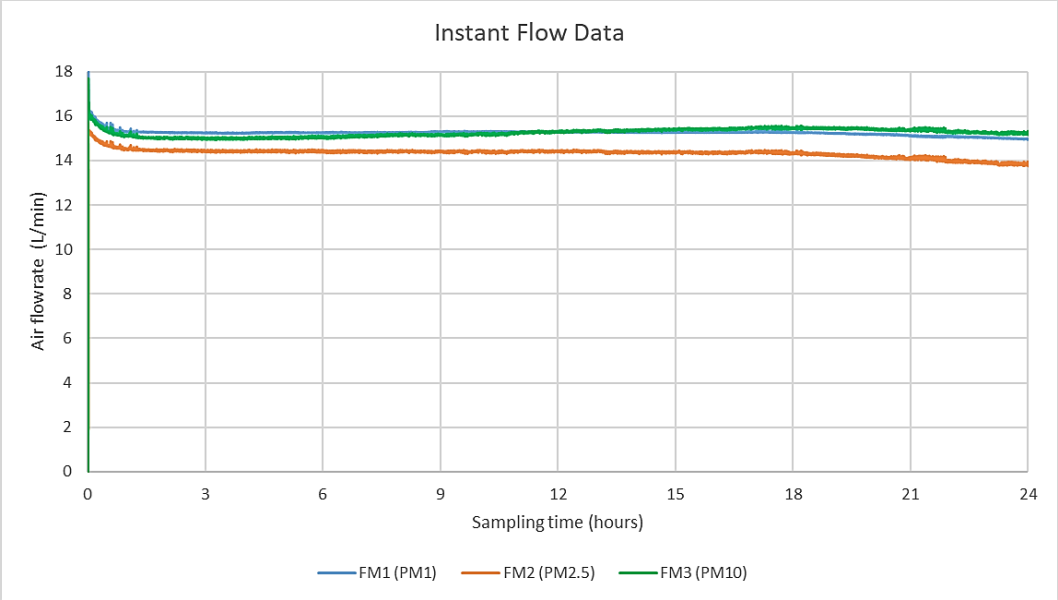

Figure 4.17. 24 hours of sampling with 3 MFCs connected to 1 pump using Nucleopore filters

As for PTFE filters, the same tests are carried out. 3 cyclones are connected to 1 pump and operated for 72 and 24 hours, of which results are shown in Figure 4.18 and Figure 4.19, respectively.

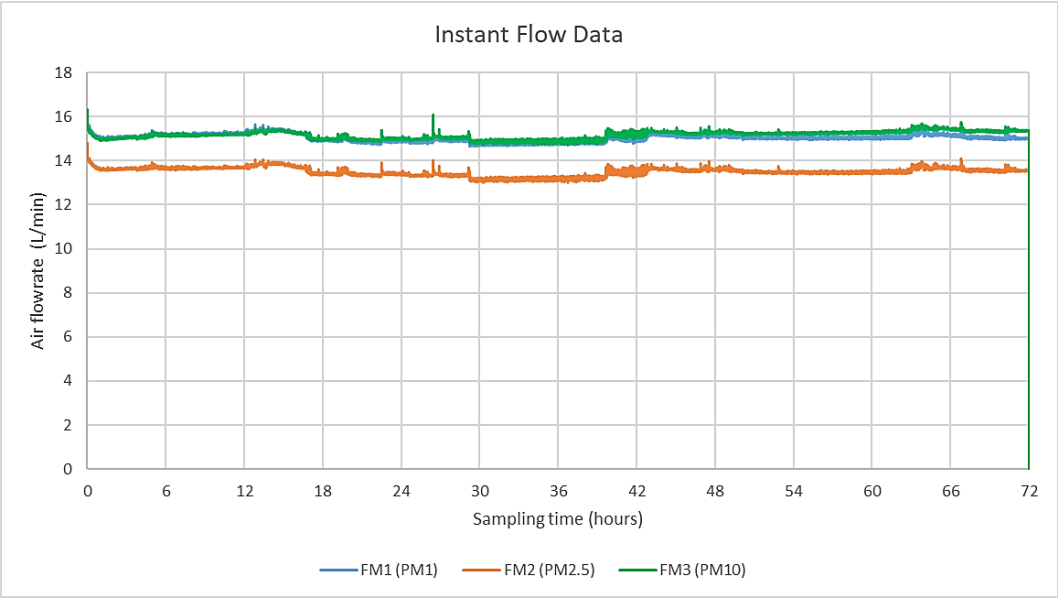

Figure 4.18. 72 hours of sampling with 3 MFCs connected to 1 pump using PTFE filters

Results indicate that Teflon (PTFE) filters have lower resistance to air flow than that of Nucleopore filters, since even at the end of 72 hours, there is no significant flow rate drop is observed in all three channels.

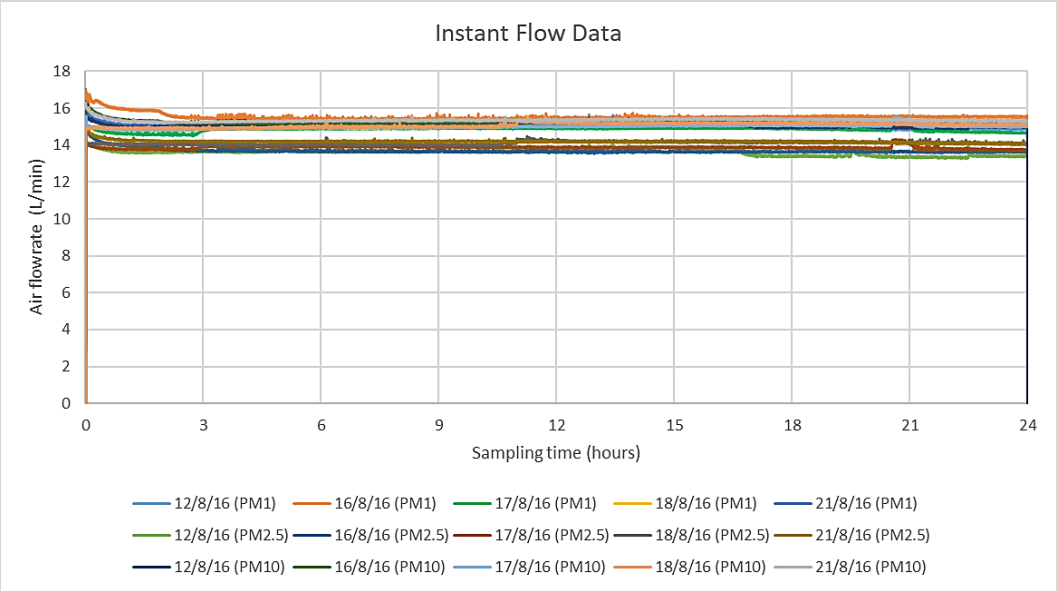

Figure 4.19. 24 hours of sampling with 3 MFCs connected to 1 pump using PTFE filters

24 hours sampling with Teflon filters draw a better sketch of flow rate stability, as shown in Figure 4.19. 5 days of 24-hour sampling flow rate curves are depicted in order to express the variation is minor.

In order to confirm repeatability of the flow rate stability, sampling tests are carried out for 5 days. For this, the sampler is operated for 5 days with 3 MFCs are connected to the pump and the results for each channel is plotted separately in Figure 4.20, Figure 4.21 and Figure 4.22 for PM_1, $PM_{2.5}$ and PM_{10}, respectively. Results indicated that flow rate slightly varies in the first few hours of sampling, however, stable curves that vary narrowly in the rest of the 5-days long sampling period.

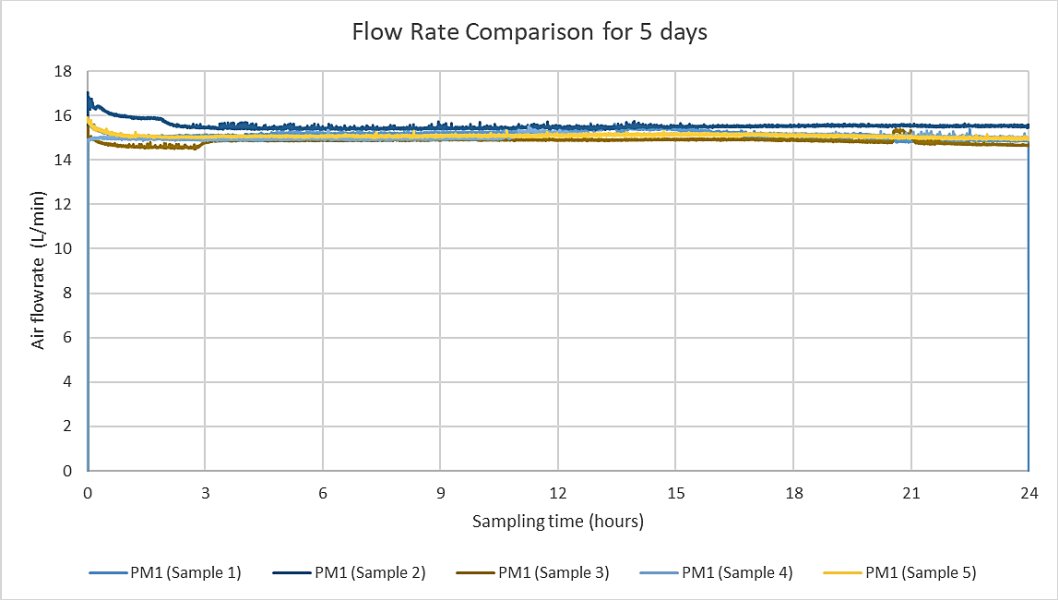

Figure 4.20. Flow comparison for PM_1

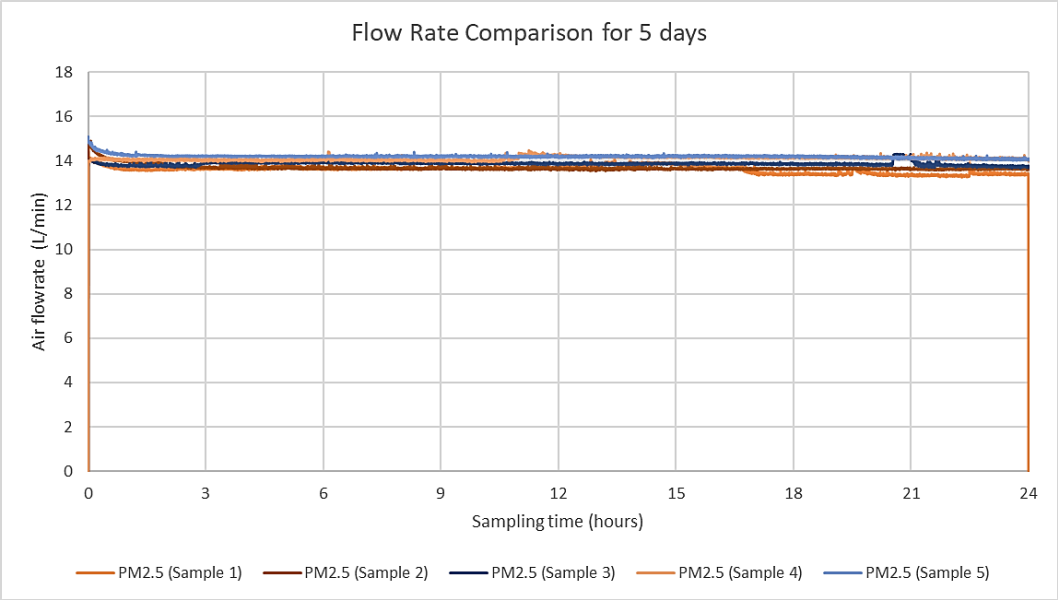

Figure 4.21. Flow comparison for $PM_{2.5}$

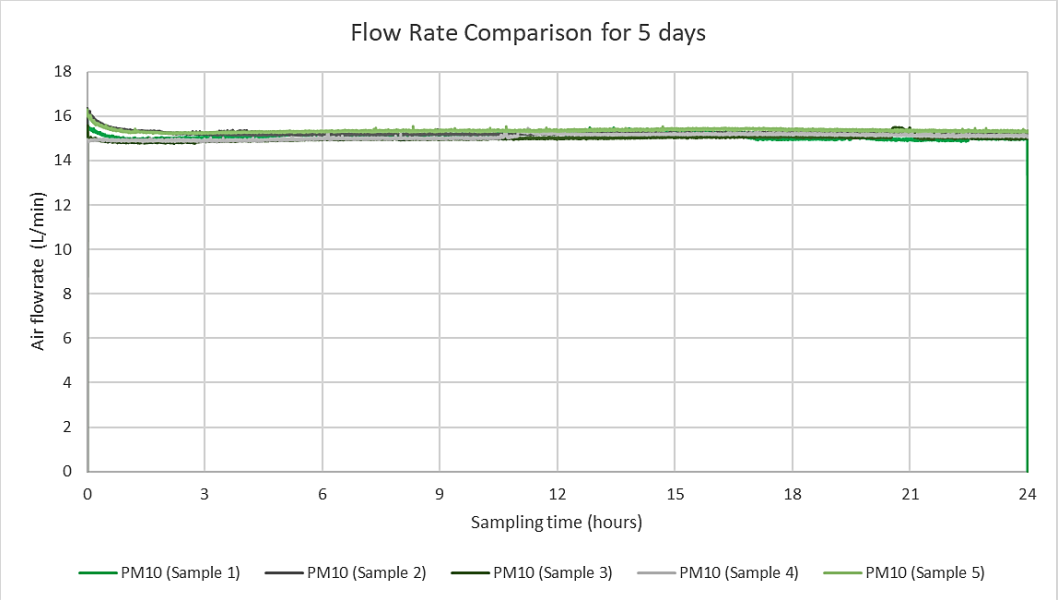

Figure 4.22. Flow comparison for PM_{10}

4.6.2. Sampler configured with critical orifices

After the sampler is operated with mass flow controllers, mass flow controllers are replaced with critical orifices within the scope of the 2nd phase of the study. As critical orifices are solid mechanical devices, a mass flow meter (MFM) is connected to each channel in order to log flow rate data during sampling. Flow rate stability tests are carried out with this configuration as well, of which results are shown as follows.

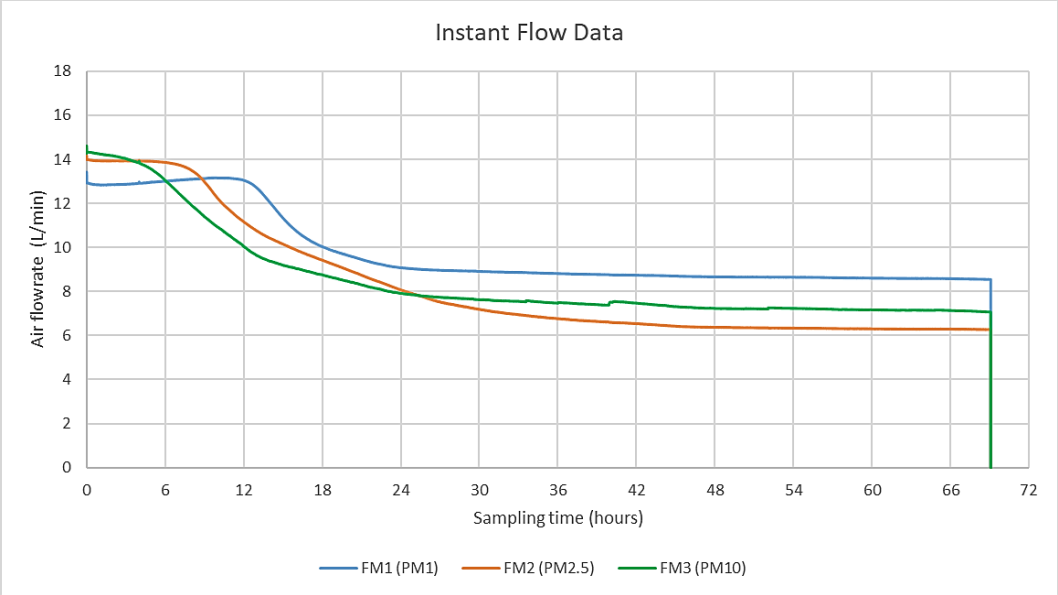

Figure 4.23. 72 hours of sampling with 3 critical orifices on Nucleopore filters

In Figure 4.23, the cyclones are loaded with nucleopore filters and the sampler is run for 72 hours. Flow rates started to drop after first 6 hours for $PM_{2.5}$ and PM_{10}, and after 12 hours for PM_1 channel, due to high resistance of nucleopore filters. Despite the flow rate drop occurred earlier than MFCs, flow rate vs time curves are observed to be much smoother than MFC configuration. This result indicates that critical orifices provide more stable flow rate than mass flow controllers.

In the following trials with nucleopore filters, each cyclone is individually connected to the pump in order to observe flow rate change with respect to time and the pump is run until flow rate drop is observed. As expected, it took much longer when each channel is individually connected to the pump than all three connected to a single pump at the same time.

PM_{10} channel is observed to run for 42 hours with almost no flow rate loss. After that, the flow rate starts to decrease, and the sampling is stopped at 72 hours. For $PM_{2.5}$ channel, flow rate is observed to be stable for the first 42 hours, similar to PM_{10} channel. Later, flow rate starts to decrease at a slower rate than PM_{10}, and finally drops to 10 LPM around 138th hour of the sampling, PM_1 channel starts sampling with lower

flow rate than other two counterparts, however, loses flow rate slower than both PM_{10} and $PM_{2.5}$ channel and finishes sampling with slightly higher flow rate than $PM_{2.5}$ at 138^{th} hour. This pattern is approximately the same as in $PM_{2.5}$ case.

After trials with nucleopore filters, trials with Teflon filters are carried out as well. In the first case all three channels are connected to the pump and operated for 72 hours. Variation in the flow rate is given in Figure 4.24. Results indicate that critical orifice provides smoother flow rate vs time curve as compared to mass flow controllers with the same filter type.

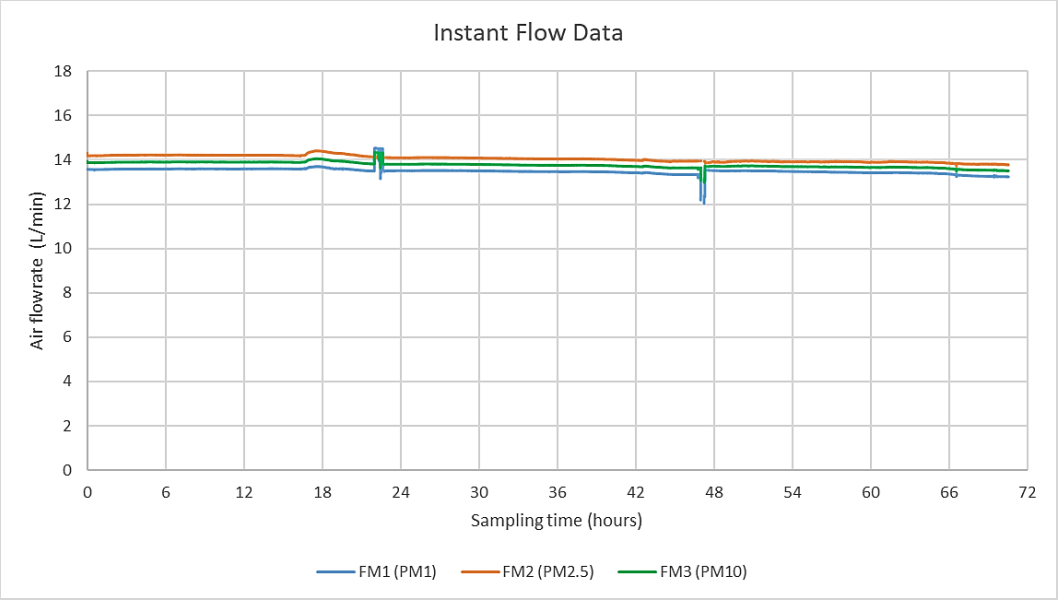

Figure 4.24. 72 hours of sampling with 3 critical orifices on PTTF filters

As in tests with Nuclepore filters the second set of runs were performed with one channel attached to the pump at a time. Variation in air flow rate passing through filter in each channel are given in Figure 4.25, Figure 4.26 and Figure 4.27, for PM_{10}, $PM_{2.5}$ and PM_1 channels respectively. As expected, air flow rate did not change significantly for 24 hours in these runs.

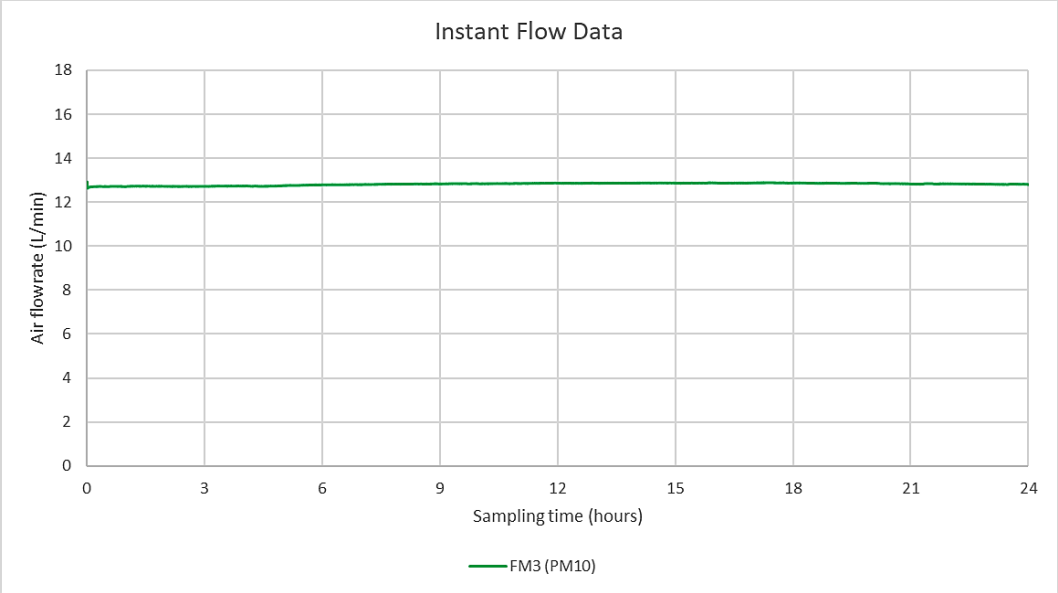

Figure 4.25. 24 hours of sampling with 1 critical orifice on PTFE filter

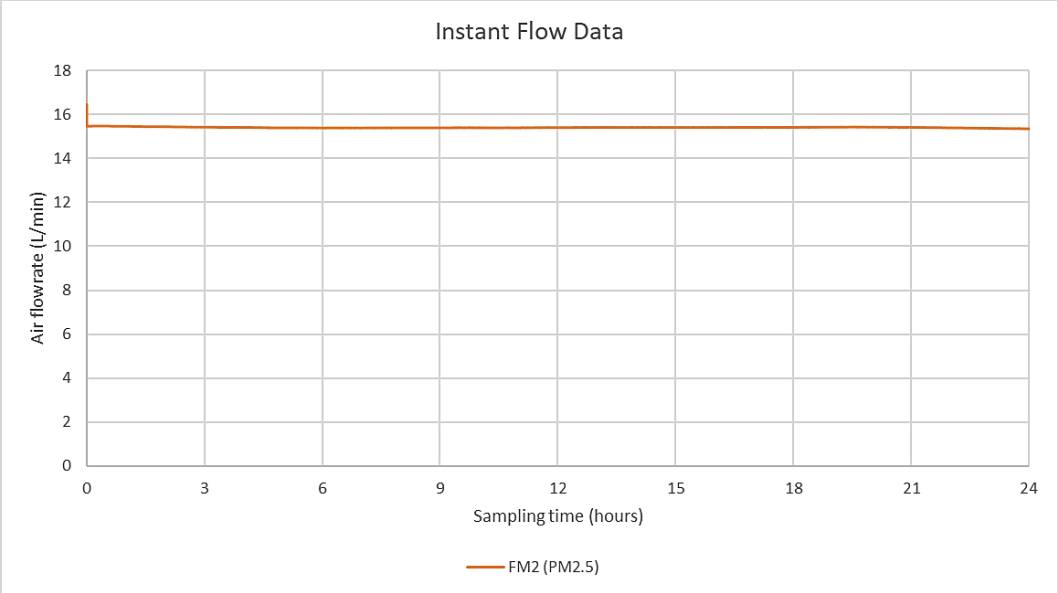

Figure 4.26. 24 hours of sampling with 1 critical orifice on PTFE filter

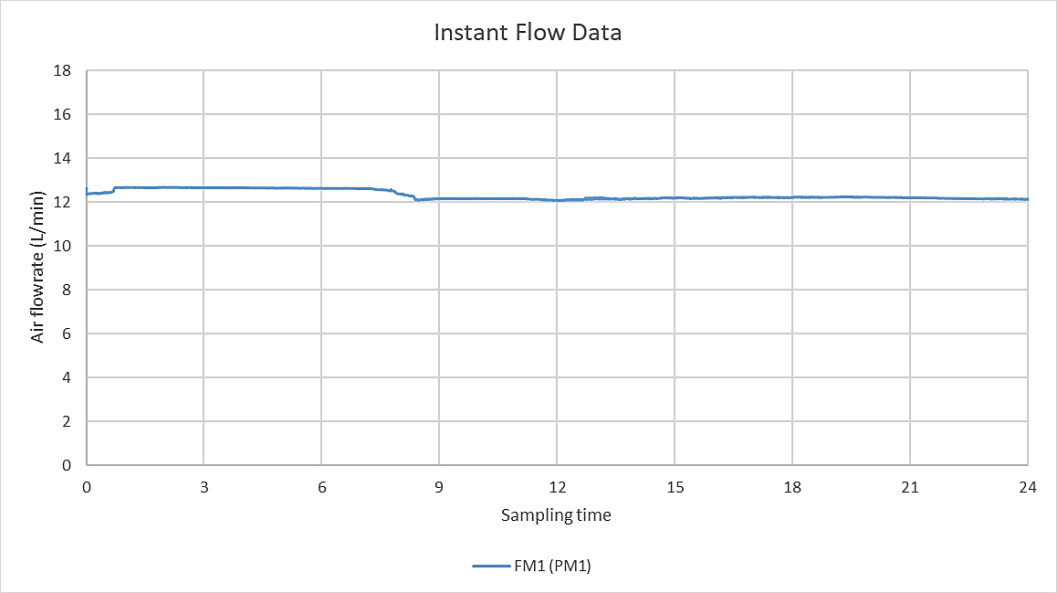

Figure 4.27. 24 hours of sampling with 1 critical orifice on PTFE filter

In order to confirm repeatability of the flow rate stability, sampling tests are carried out for five 24-hour intervals and results for each channel is plotted separately in the following figures. Results indicated that flow rate for each channel varies within a small range (< 5%) in five repeated runs and did not change throughout sampling.

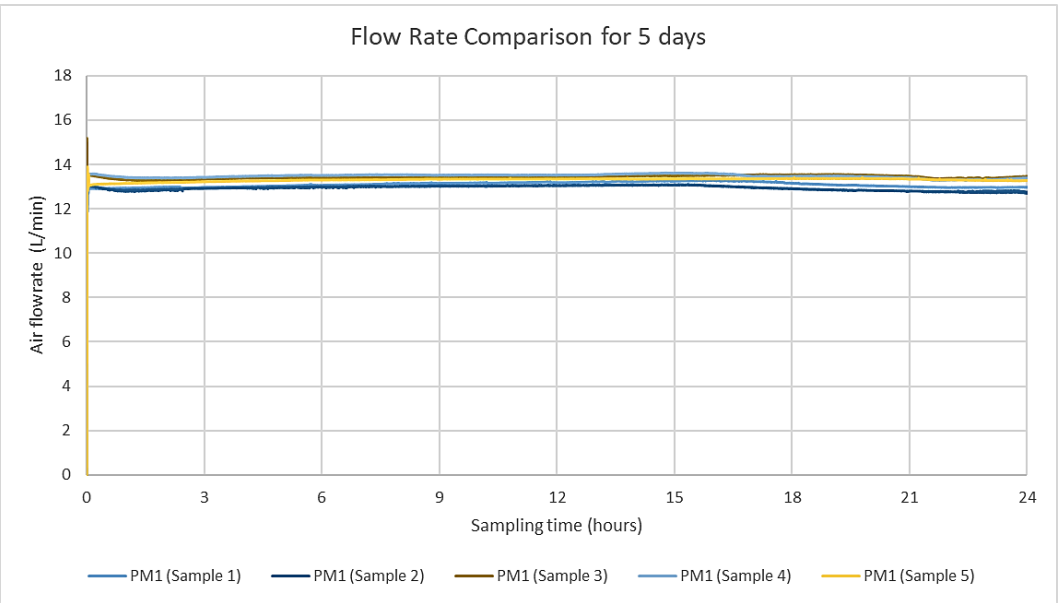

Figure 4.28. Flow comparison for PM_1

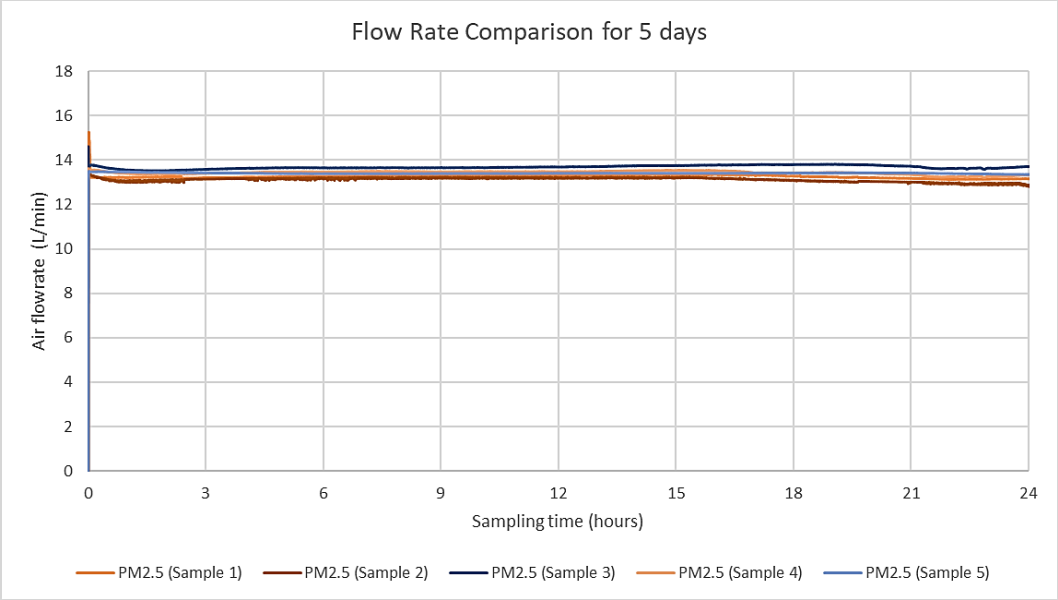

Figure 4.29. Flow comparison for $PM_{2.5}$

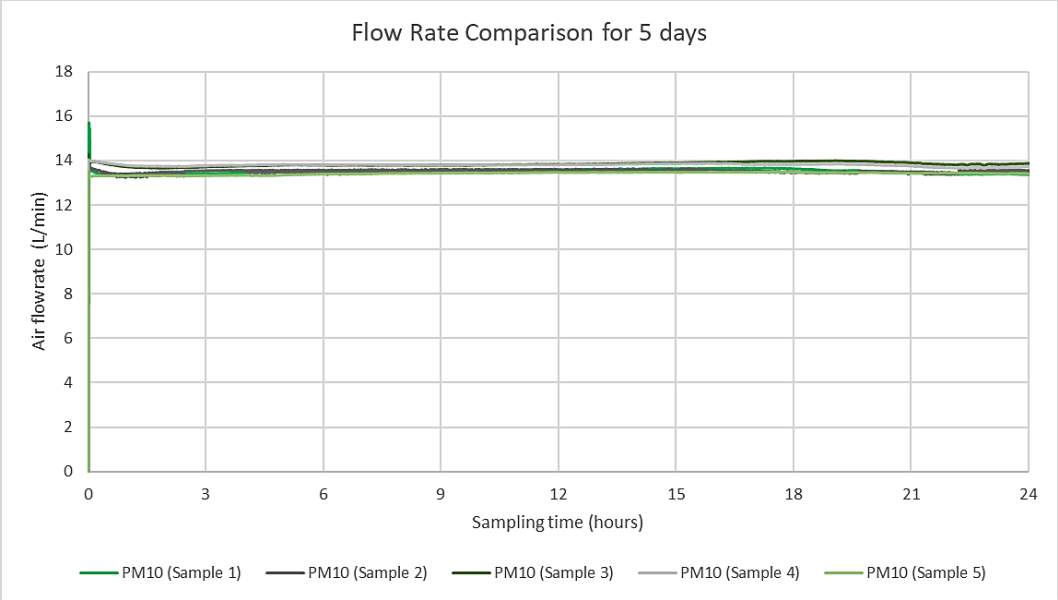

Figure 4.30. Flow comparison for PM_{10}

4.6.3. 1-channel and 3-channel comparison

In order to observe how flow rate is affected by 1-channel configuration and 3-channel configuration, each cyclone is solely connected to the pump and the flow rates are compared for 1-channel and 3-channel configuration for PM_1, $PM_{2.5}$ and PM_{10} cyclones. The procedure is repeated for both MFCs and critical orifices. The results are plotted with respect to particle size in in Figure 4.31 for PM_1, in Figure 4.32. for $PM_{2.5}$ and in Figure 4.33 for PM_{10}.

In Figure 4.31, PM_1 flow rate was observed to oscillate, in 1-channel configuration. MFCs were set to 16.7 L/min, due to fluctuation in the pump, MFC valve opening increases and decreases to sustain the flow rate at 16.7 L/min. In this process, fluctuation is observed between 13th and 21st hours.

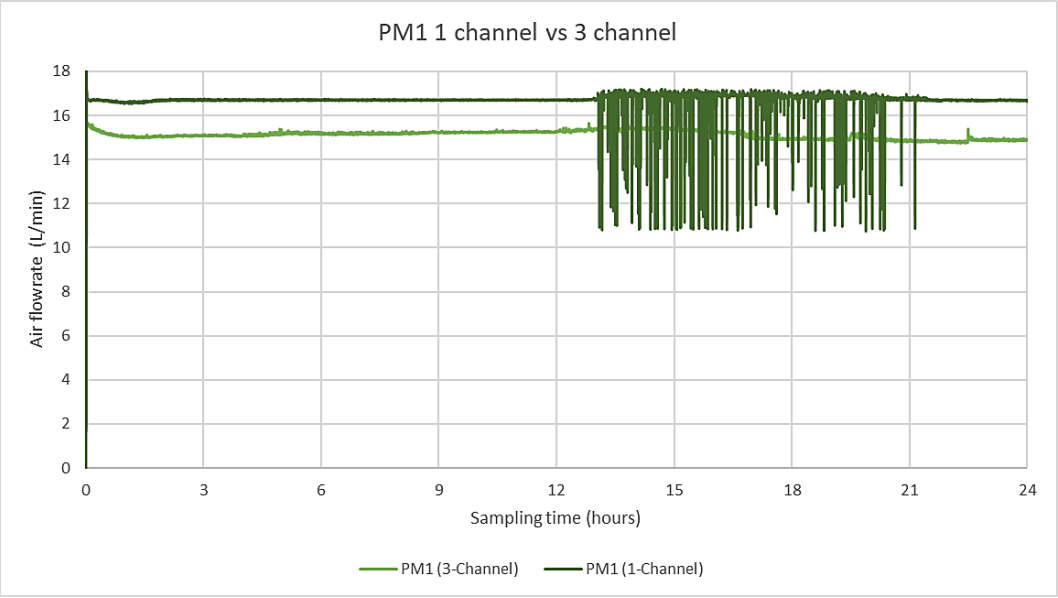

Figure 4.31. 1 channel & 3 channel comparison for PM_1 with MFCs

PM_1 cyclone draws around 1.5 LPM higher flow rate when solely connected than all three connected. Even though PM_1 cyclone maintains flow rate very close to 16.7 LPM, it undergoes substantial fluctuation between 13th – 21st hours of the sampling. These fluctuations were observed in repeated runs and was not observed when critical orifice was used as flow control unit. The reason is not clear, but obviously it is due

to MFC in PM_1 channel. When all cyclones are connected, it draws more stable curve with 1.5 LPM slower flow rate.

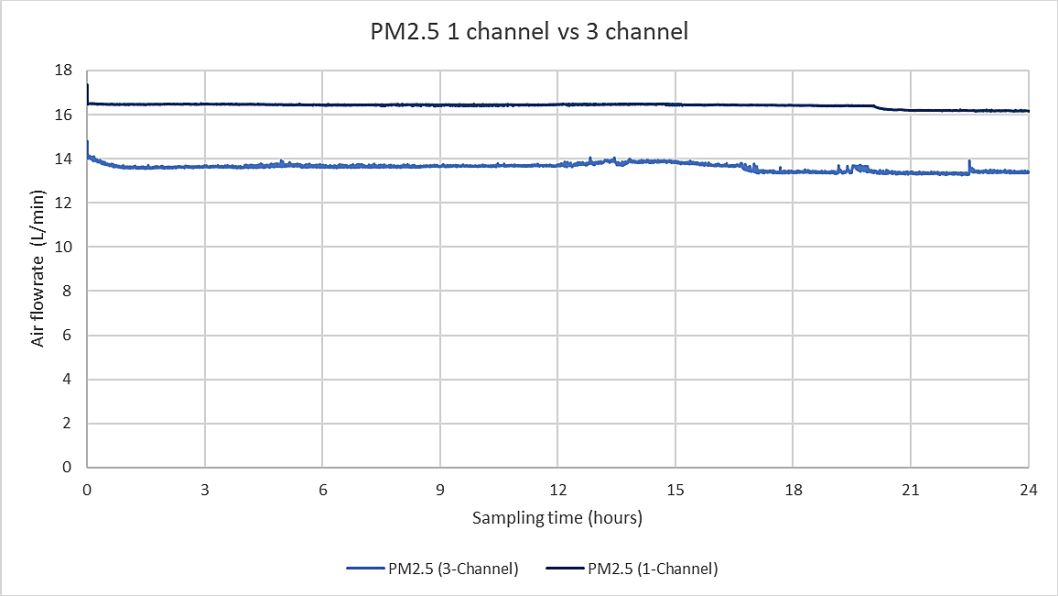

Figure 4.32. 1 channel & 3 channel comparison for $PM_{2.5}$ with MFCs

When comparison is made for $PM_{2.5}$ channel with MFC, flow rate difference is observed to be higher, nearly 2.5 LPM. In 1-channel configuration, $PM_{2.5}$ channel plotted a smooth horizontal curve with a flow rate above 16 LPM. However, in 3-channel configuration, minor fluctuations throughout the sampling are observed. These small fluctuations in both $PM_{2.5}$ and PM_{10} channels are not large enough to effect cutoff diameters of cyclones.

As for PM_{10} channel, a similar trend is observed as $PM_{2.5}$ channel. In 1-channel, PM_{10} draws a smooth horizontal flow rate curve around 16 LPM, whereas in 3-channel, it draws a slightly fluctuating curve at around 15 LPM.

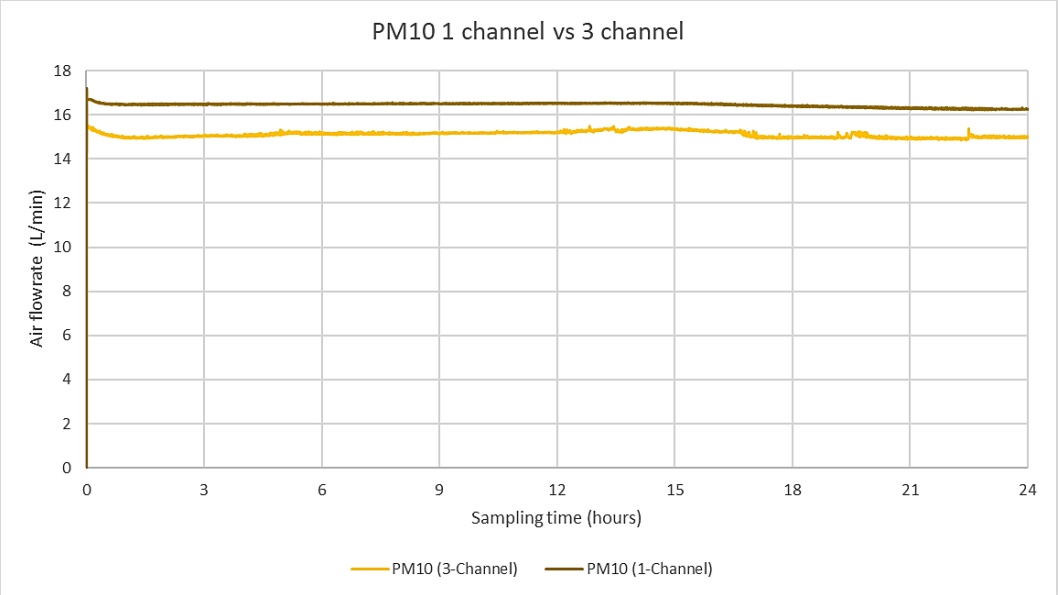

Figure 4.33. 1 channel & 3 channel comparison for PM_{10} with MFCs

In addition to MFCs, 1-channel vs 3-channel comparison is carried out with critical orifices as well.

Figure 4.34 reveals that PM_1 cyclone with critical orifice generates very similar, almost overlapping flow rate curves. Even though flow rates are slightly lower than MFC configuration in both 1-channel and 3 channel, flow rate is observed to be more stable and the curves are smoother. Fluctuations observed when sampler was operated with MFCs in PM_1 channel was not observed when it is operated with critical orifices.

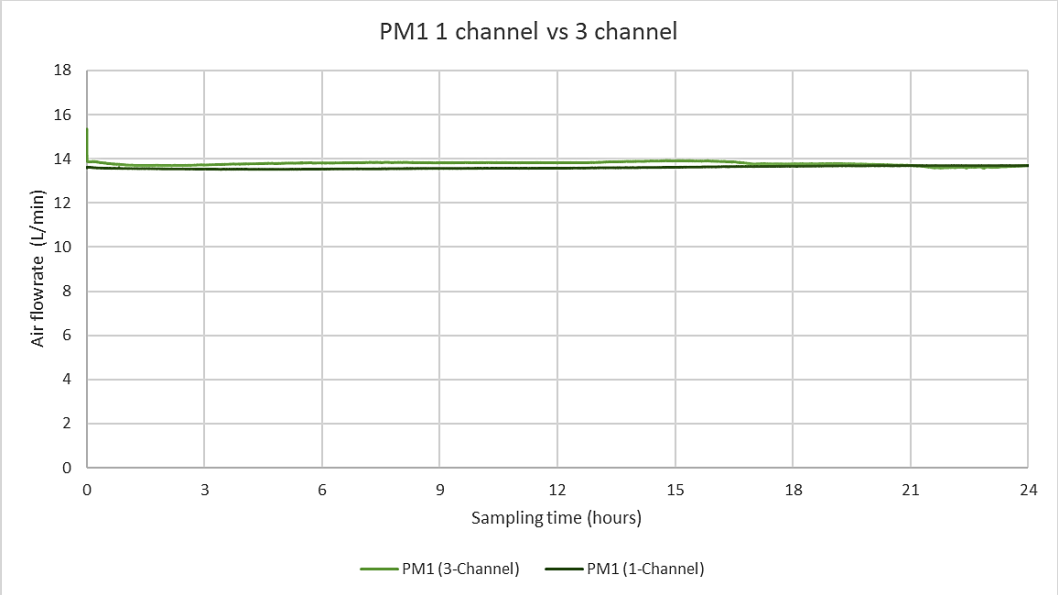

Figure 4.34. 1 channel & 3 channel comparison for PM_1 with critical orifices

$PM_{2.5}$ channel again generates the highest difference between 1-channel and 3-channel configuration, drawing around 15.7 LPM and 14 LPM air respectively, as shown in Figure 4.35. Both configurations plot a steady curve throughout the sampling.

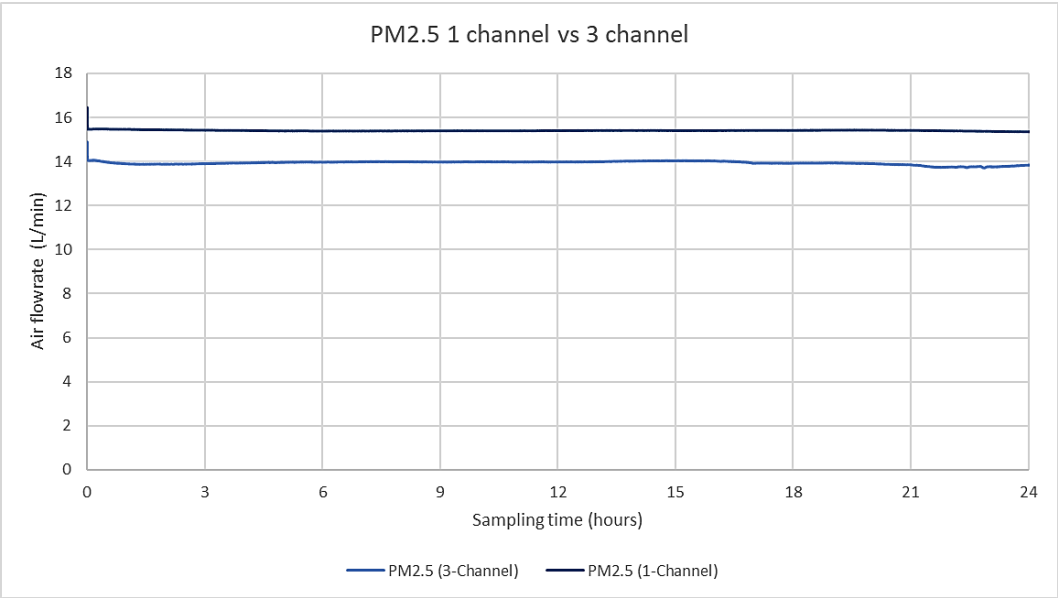

Figure 4.35. 1 channel & 3 channel comparison for $PM_{2.5}$ with critical orifices

Finally, PM_{10} cyclone with critical orifice, draws air at a very similar rate, as shown in Figure 4.36. In both cases, it starts sampling with overlapping curves, however, slight difference occurs due to flow rate decreases slightly in 3-channel configuration, whereas it does not in 1-channel configuration.

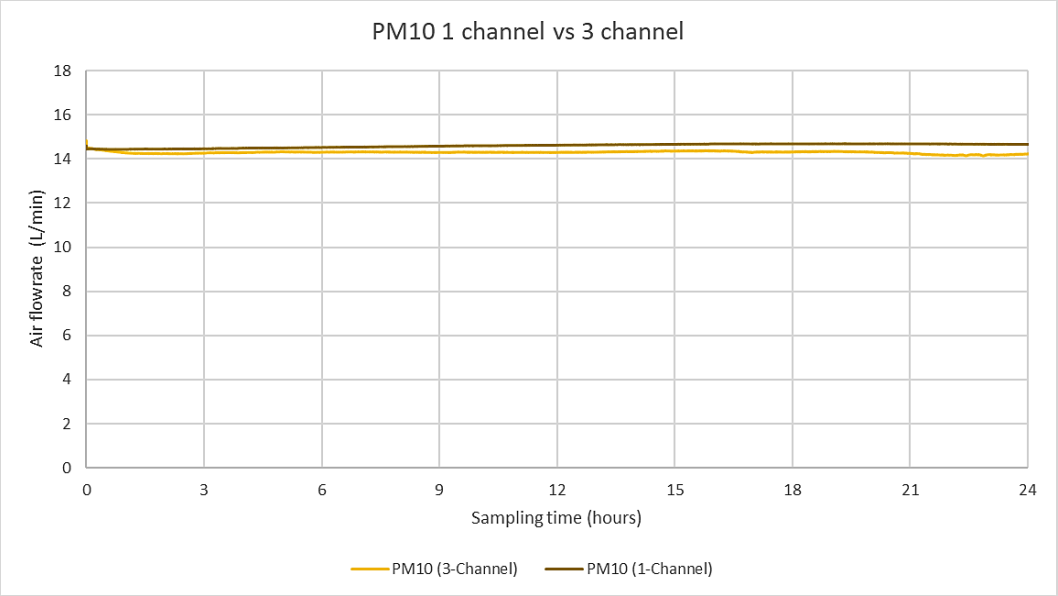

Figure 4.36. 1 channel & 3 channel comparison for PM_{10} with critical orifices

4.7. Assembling of the sampler into a shelter

The final phase ın this study was installation of the components into a shelter to keep the sampler safe and sturdy. Ambient samplers, like the one in this study, should be able operate standalone on the field. Particularly, it should not be affected by meteorological conditions. Considering the sampler consists of substantial amount of electronic hardware, the protection of the sampler from outdoor conditions is of utter importance. The shelter is built in 1.0 m x 1.0 m x 1.5 m dimensions and made of hardened aluminum. The roof of the shelter is built inclined for two reasons; first, to prevent accumulation of rain droplets, second, to prevent the raindrops hit the surface and splash into the cyclones.

In urban areas, the sampling tasks are carried out at 2.0 m elevation, which is known as “nose level”. For this reason, the front face of the sampler is elevated to 2.0 meters

by mounting aluminum profiles to the shelter and the cyclones are placed on this profile, which is at 2.0 m elevation.

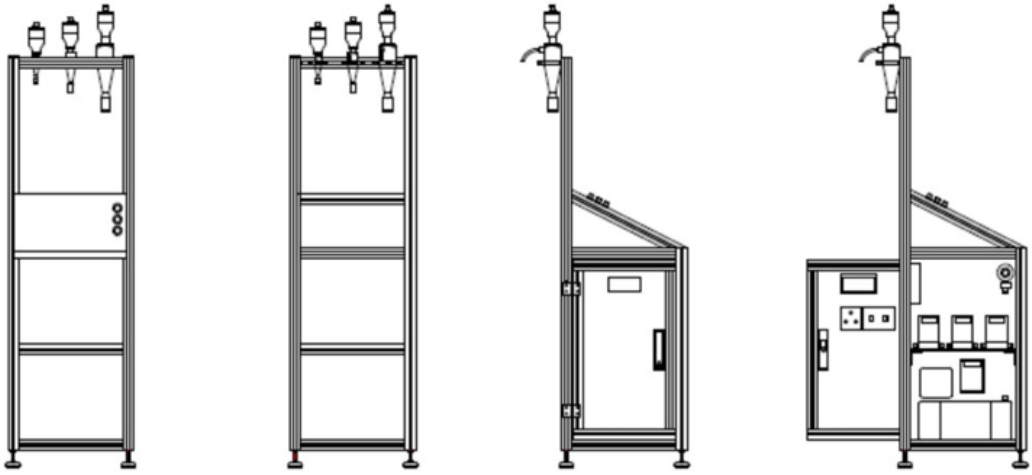

Figure 4.37. Drawing of the sampler shelter

Technical drawing and images of the shelter are depicted in Figure 4.37 and Figure 4.38, respectively

Figure 4.38. Image of the sampling shelter

Pump, mass flowmeters, critical orifices and ½" tubing, excluding the parts of the cyclones, are placed in the shelter. One of the side walls of the shelter is built as a door, which can be opened, and technicians can take action whenever it is needed.

The control unit mentioned in the previous section and the sampling data like air flow rate and total volume of air can be monitored on the display, which is placed on the door. However, the buttons and connections for data transfer to computers are installed inside the shelter to protect them from meteorological conditions, particularly rain. Interior view of the shelter can be seen in Figure 4.39.

Figure 4.39. Sampler constituents installed in the shelter

4.8. Validation studies

How the sampler was designed and effects of various components on air flow passing through filters were discussed in previous sections. However, the ultimate test on usability of sampler in field work is to test it against well-documented samplers that are widely used for aerosol sampling from atmosphere. In this study, the 3-channel sampler designed in this study were tested against a stack filter unit (SFU), two high-

volume samplers, equipped with PM_{10} sampling heads (pre-impactors) (HV-1 and HV-2) and a laser spectrometer (GRIMM, Model 164).

The stack filter unit was designed at the Gent University in Belgium, by Willy Maenhaut in 1994 (Maenhaut et al., 1994), validated and characterized thoroughly (Hopke et al., 1997). SFU found very vide application in aerosol community because of its low cost and capability of sampling coarse and fine particles simultaneously on separate filters. Some of literature where SFU used in sampling are given in Appendix A. High Volume samplers are commercially available samplers that are very widely used throughout the world. In the days, when validation tests were performed, we were also operating a laser spectrometer for a different project. Laser spectrometer is a measurement device that can count particle concentrations in 32 size bins. Particle number concentrations were then converted to mass concentrations (in $\mu g\ m^{-3}$) in PM_1, $PM_{2.5}$ and PM_{10}. Averaging time is 1-min. The laser spectrometer was not particularly run for validation tests. At the same time, we were performing test runs for another TUBITAK project. Data that corresponds to our validation test period were selected and used to compare with PM_1, $PM_{2.5}$ and PM_{10} data generated with new sampler, SFU and Hi-Vols. Actually, the laser spectrometer that is used in this comparison is the only device with which we can compare PM_1 mass concentrations generated with the new sampler.

In this validation exercise, 3-channel sampler, which was designed in this study, was operated side-by-side with a SFU, which collect $PM_{2.5}$ and $PM_{2.5-10}$ particles on separate filters, Grimm Model 164 laser spectrometer and two high volume samplers, both equipped with PM_{10} heads (PM_{10} preimpactor). These five samplers were operated parallel between 08.03.2017 and 31.3.2017. Sampling duration was always 24 hours. However, laser spectrometer was stopped at 25th of March. Samplers were stopped at the same time every morning and they are started at the same time after filters were changed.

Results (particle concentrations) are given in and Figure 4.40. Average PM_{10} concentration measured by our sampler, laser spectrometer, SFU, HV1 and HV2 were 25 ± 10 μg m^{-3}, 26 ± 10, 17 ± 8.3, 21 ± 7.4 and 21 ± 8.9, respectively. PM_{10} concentrations measured by the new sampler agrees nicely with all other samplers used in the test. Statistical tests demonstrated that these five averages are identical with 95% probability ($P < 0.05$)

Table 4.1. *Concentrations of PM_1, $PM_{2.5}$ and PM_{10} measured by different samplers operated side-by-side (concentrations are in $\mu g\ m^{-3}$)*

Date of sampling	*This work*			*SFU*		*Hi-Vol1*	*Hi-Vol2*	*Grimm*		
	PM_1	$PM_{2.5}$	PM_{10}	PM_{10}	$PM_{2.5}$	PM_{10}	PM_{10}	PM_1	$PM_{2.5}$	PM_{10}
8.3.2017	2.8	18	32	21	17	32	34			
9.3.2017	7.2	13	26	25	21	36	40	5.8	12	28
10.3.2017	7.2	18	31	15	12	23	21	9.9	18	37
11.3.2017	3.8	12	22	15	12	17	15	7.1	22	28
13.3.2017	4.9	6.3	7.6	3.5	2.9	12	8.2			
14.3.2017	5.1	7.0	11	4.9	4	9.6	7.6	7.5	7.9	8.6
15.3.2017	10	16	25	12	10	19	17	7.8	8.0	8.7
16.3.2017	11	16	17	15	13	14	12			
17.3.2017	2.8	4.6	9.4	4.3	3.5	6.2	4.9	4.4	20	25
18.3.2017	7.6	12	13	8	7	13	12	7.8	8	11
19.3.2017	8.3	10	14	8	6	18	18	11	12	17
20.3.2017	4.7	8	45	14	11	18	18	11	13	17
21.3.2017	8.6	14	32	21	17	23	26	6.8	9	26
22.3.2017	8.8	12	30	18	15	27	28	9.9	13	36
23.3.2017	6.4	12	29	21	17	21	24	11	14	35
24.3.2017	8.7	17	39	24	20	24	24	9.3	13	34
25.3.2017	13	13	27	22	18	28	29	12	17	39
27.3.2017	9.4	17	27	19	25	21	22	12	15	37
28.3.2017	15	26	47	41	34	33	33			
29.3.2017	7.3	13	32	20	16	30	31			
30.3.2017	6.8	15	22	29	24	27	28			
31.3.2017	7.3	13	21	17	14	19	21			
1.4.2017	8.5	15	12	15	13	14	14			
2.4.2017	7.8	14	18	20	16	20	21			
Average	7.6± 2.9	13 ± 4.4	25 ± 10	17 ± 8.2	14 ± 6.8	21 ± 7.4	21 ± 8.9	8.8± 2.2	13 ± 4.1	26 ± 10

High volume samplers available for comparison were equipped with PM_{10} pre-impactors, but not with $PM_{2.5}$. Consequently, $PM_{2.5}$ concentrations measured with our sampler was compared with $PM_{2.5}$ concentrations measured by SFU and laser spectrometer. Average $PM_{2.5}$ concentration measured in designed sampler was 13 ± 4.4 $\mu g\ m^{-3}$ and corresponding concentration measured by SFU and laser spectrometer were 14 ± 6.8 $\mu g\ m^{-3}$ and 13 ± 4.1, respectively. These numbers also agree very nicely over 23-day sampling period. Similarity between mean concentrations of these three data set is statistically significant with 99% confidence ($P < 0.09$),

PM_1 data generated by the new sampler were compared with corresponding data generated by the laser spectrometer, because the laser spectrometer was the only device that can measure PM_1 concentrations in this country at that time.

Average PM_1 concentration measured by the designed sampler was 7.6 ± 2.9 $\mu g\ m^{-3}$ whereas average PM_1 concentration measured by the laser spectrometer was 8.7 ± 1.9 $\mu g\ m^{-3}$, indicating a very good agreement PM_1 concentrations measured by the two instruments. Student-t test indicated that these two means are identical with 99% probability.

This comparison demonstrates that PM_{10}, $PM_{2.5}$ and PM_1 concentrations measured with new sampler are highly comparable with corresponding measurements with commercially available samplers.

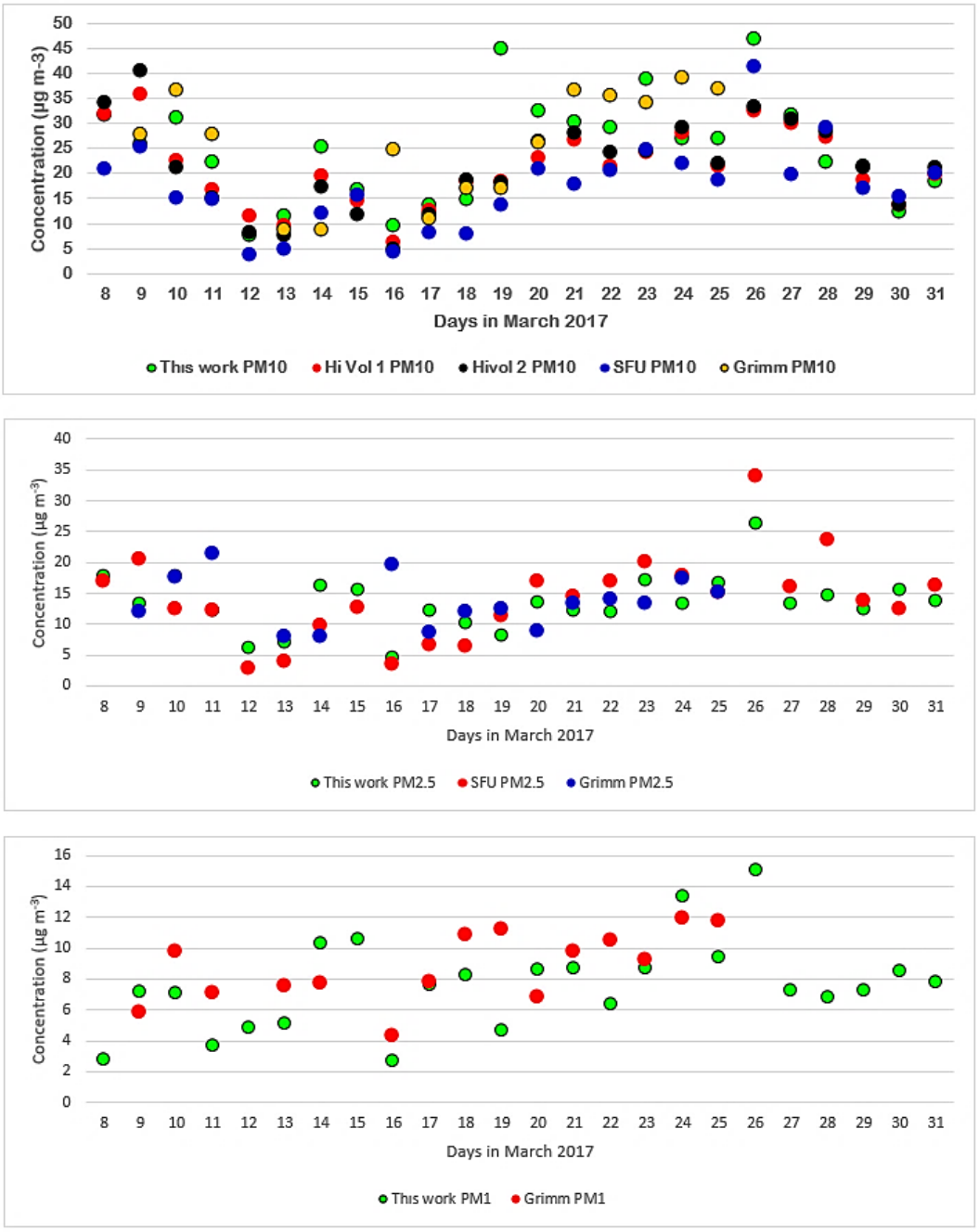

Figure 4.40. Comparison of PM_1, $PM_{2.5}$ and PM_{10} concentrations measured with sampler designed in this study, SFU, two HiVol samplers and Grimm laser spectrometer operated side-by-side in March 2017

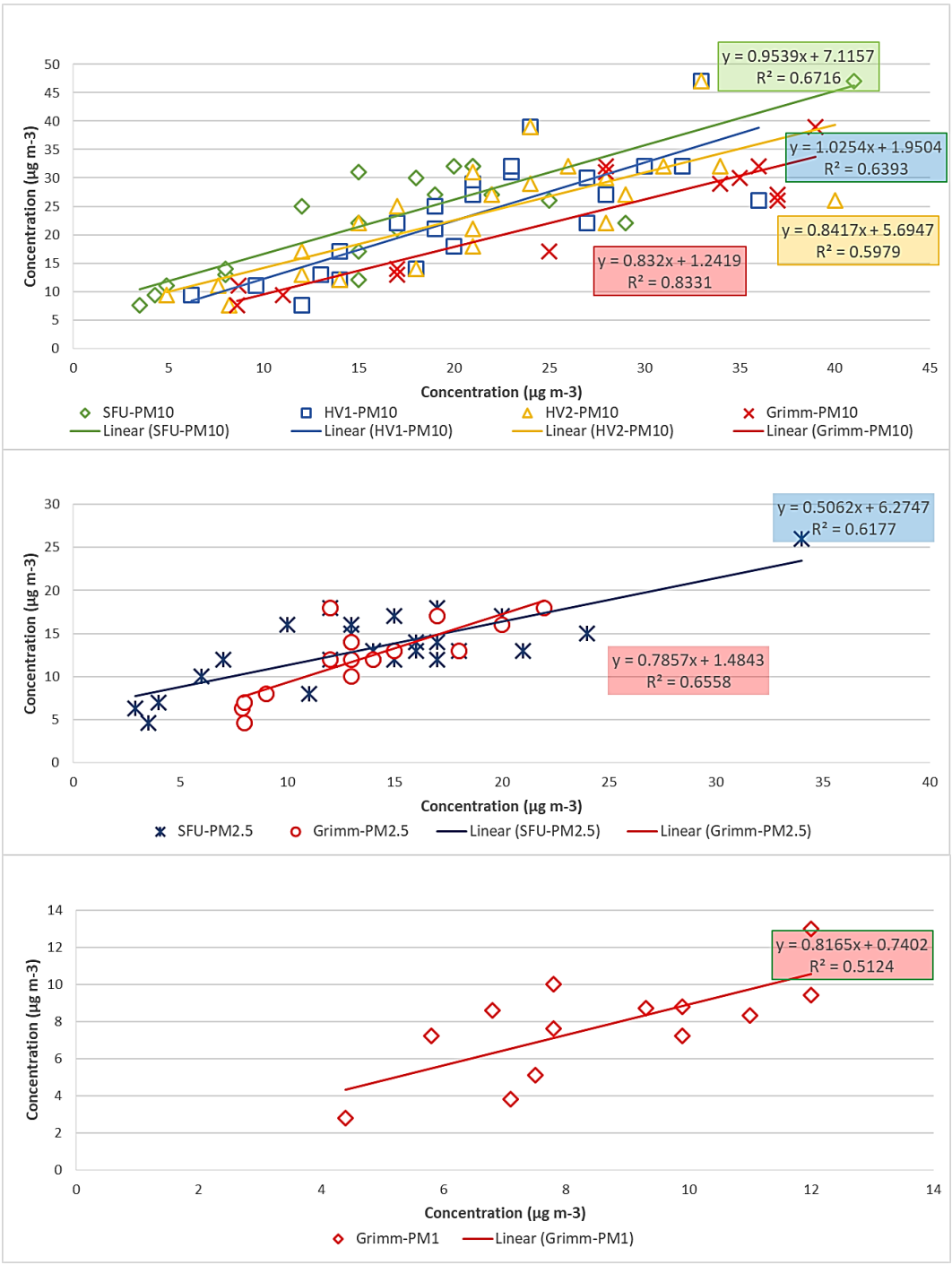

Figure 4.41. Linear regression of PM_1, $PM_{2.5}$ and PM_{10} measured by the new sampler compared to SFU, two HiVol samplers and Grimm laser spectrometer

Day-by-day variation in PM_1, PM_{10} and $PM_{2.5}$ concentrations are given in Figure 4.40. Except for three days, fairly similar PM_{10} concentrations were measured with all samplers. Please note that atmospheric PM_1. PM_{10} and $PM_{2.5}$ concentrations can change by one or two orders-of-magnitude from one day to another. In such a variable system, 13% difference observed between the new sampler and others is considered acceptable. $PM_{2.5}$ data generated by the new sampler is 4% different from corresponding data generated using SFU and 12% different from corresponding data generated by laser spectrometer. The difference between PM_1 data generated with the new sampler and laser spectrometer is <1%. Considering high variability in PM concentrations in the atmosphere, we can safely say that the sampler designed in this study generates similar PM_1, $PM_{2.5}$ and PM_{10} data with commercially available devices that are widely used to collect particle samples from atmosphere.

4.9. Comparison of cost of the sampler developed in this study with available samplers

At the end of performance tests carried out, it has been observed that the sampler developed in this study performs as efficient as commercially available widely known sampler systems. In order to bring its performance to a further extent, its cost is expected to be comparable to that of commercially available samplers.

In this section, the cost of the sampler will be discussed and compared to commercially available devices. Price quotes are received at different times; therefore, costs are given as dollar and euro currency, in order not to mislead due to change in the currency exchange rates. The costs are converted to TL based on The Central Bank currency exchange rates in 2/1/2017. All discussions in this chapter is based on the converted TL costs.

The prices of the main components of the sampler is given in Table 4.2. As it is seen, the costliest item of the sampler is the cyclones; as the PM_{10} cyclone itself costs around 7,000 TL. Although $PM_{2.5}$ and PM_1 cyclones are relatively cheaper, they still cost around 4,000 TL and 3,000 TL respectively. Total cost of the cyclones is estimated to

be 14,000 TL. In addition, filter holders are costly items as well, as they are constructed of Teflon (PTFE). Total burden of the filter holders on the study budget is around 8,200 TL.

Table 4.2 *Prices of the components used in the sampler*

Item	*Unit Price*	*Qty*	*Total Price*	*Total Price (₺)*	*Description*
PM_{10} cyclone	$ 1,915.00	1	$ 1,915.00	6,932.00 ₺	URG-2000-30ENB
PM_1 cyclone	$ 1,063.00	1	$ 1,063.00	3,848.00 ₺	URG-2000-EHB
$PM_{2.5}$ cyclone	$ 885.00	1	$ 885.00	3,204.00 ₺	URG-2000-30EH
Filter holder	$ 762.00	3	$ 2,286.00	8,275.00 ₺	URG-2000-30FG-2
Manifold	$ 792.00	1	$ 792.00	2,867.00 ₺	URG-2000-30HD-1
Critical Orifice	$ 184.00	3	$ 552.00	1,998.00 ₺	Swagelok 6LV-4-VCR-6-DM-055P
MFC	€ 1,150.00	3	€ 3,450.00	13,214.00 ₺	SIERRA model C50L-AL-DD-2-PV2-V1-5POINTCAL-50-C9(0)-50 T8D
Flowmeter	€ 450.00	3	€ 1,350.00	5,171.00 ₺	SIERRA model C50L-AL-DD-2-PV2-V1-5POINTCAL-50-C9(0)-50 T8D
Pump	$ 2,400.00	1	$ 2,400.00	9,192.00 ₺	F&J Specialty products Model DF-1E
Quick connect	12.00 ₺	20	240.00 ₺	240.00 ₺	Eason Pneumatics model PC 1/2 - N03

Item	*Unit Price*	*Qty*	*Total Price*	*Total Price (₺)*	*Description*
Data acquisition system	10,000.00 ₺	1	10,000.00 ₺	10,000.00 ₺	Constructed in Hacettepe University
Encasing	5,000.00 ₺	1	5,000.00 ₺	5,000.00 ₺	Service Procurement
Feedback unit	5,000.00 ₺	1	5,000.00 ₺	5,000.00 ₺	Service Procurement

Along with cyclones and filter holders, mass flow controllers are another high cost equipment in this sampler. Each of them costs around 4,400 TL, which ends up 13,200 TL burden on the budget for all three mass flow controllers. Mass flow meters, on the other side, are relatively cheaper, with a total cost of 5,000 for all three channels. The pump used in this study was readily available in air pollution control laboratory, therefore, no additional expenses were required, however, retail price of the pump is around 9,100 TL.

The service procurement part of the sampler, which includes data acquisition system, encasement of the components into an aesthetically acceptable shelter and data feedback unit, yielded a cost around 20,000 TL.

As mentioned previously, the sampling system was installed in two different configurations. First, the air flow rate through the filters was controlled by mass flow controllers (MFCs). The components used in the sampler in this case and their corresponding costs are given in Table 4.3. The prices and the brands of the items in the table is the same as in the previous table. Construction of this sampler using MFCs costs around 67,772 TL. Cyclones and filter holders constitute 37%, MFCs and the pump constitute 33%, data acquisition and feedback systems constitute 22%, and finally encasement constitutes 7% of total cost of the sampler.

Table 4.3. *Cost of the sampler with MFC configuration*

Item	*Unit Price*	*Qty*	*Total Price*	*Total Price (₺)*	*Description*
PM_{10} cyclone	$ 1,915.00	1	$ 1,915.00	6,932.00 ₺	URG-2000-30ENB
PM_1 cyclone	$ 1,063.00	1	$ 1,063.00	3,848.00 ₺	URG-2000-EHB
$PM_{2.5}$ cyclone	$ 885.00	1	$ 885.00	3,204.00 ₺	URG-2000-30EH
Filter holder	$ 762.00	3	$ 2,286.00	8,275.00 ₺	URG-2000-30FG-2
Manifold	$ 792.00	1	$ 792.00	2,867.00 ₺	URG-2000-30HD-1
MFC	€ 1,150.00	3	€ 3,450.00	13,214.00 ₺	SIERRA model C50L-AL-DD-2-PV2-V1-5POINTCAL-50-C9(0)-50 T8D
Pump	$ 2,400.00	1	$ 2,400.00	9,192.00 ₺	F&J Specialty products Model DF-1E
Quick connect	12.00 ₺	20	240.00 ₺	240.00 ₺	Eason Pneumatics model PC 1/2 - N03
Data acquisition system	10,000.00 ₺	1	10,000.00 ₺	10,000.00 ₺	Constructed in Hacettepe University
Encasing	5,000.00 ₺	1	5,000.00 ₺	5,000.00 ₺	Service Procurement
Feedback unit	5,000.00 ₺	1	5,000.00 ₺	5,000.00 ₺	Service Procurement
Total Cost				**67,772.00 ₺**	

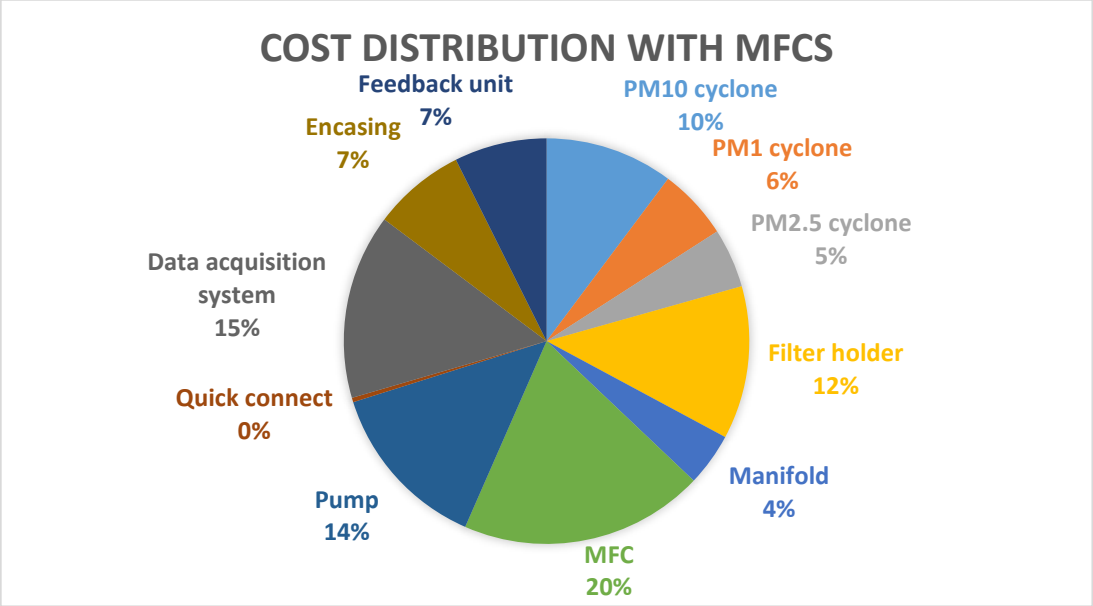

Figure 4.42. Cost distribution of the sampler with MFC configuration

In the case the sampler is constructed with critical orifices, the resulting costs are mentioned in the Table 4.4 below. In this case, total cost is estimated as 56,727 TL. Cyclones and filter holders account for 44% of the cost, whereas critical orifices and the pump account for 20%, data acquisition system account for 27% and encasement account for the remaining 9%. Replacement of MFCs with critical orifices is responsible for deduction of the share of air flow control equipment down to 20%.

Table 4.4. *Cost of the sampler with critical orifice configuration*

Item	*Unit Price*	*Qty*	*Total Price*	*Total Price (₺)*	*Description*
PM_{10} cyclone	$ 1,915.00	1	$ 1,915.00	6,932.00 ₺	URG-2000-30ENB
PM_1 cyclone	$ 1,063.00	1	$ 1,063.00	3,848.00 ₺	URG-2000-EHB
$PM_{2.5}$ cyclone	$ 885.00	1	$ 885.00	3,204.00 ₺	URG-2000-30EH
Filter holder	$ 762.00	3	$ 2,286.00	8,275.00 ₺	URG-2000-30FG-2
Manifold	$ 792.00	1	$ 792.00	2,867.00 ₺	URG-2000-30HD-1

Item	*Unit Price*	*Qty*	*Total Price*	*Total Price (₺)*	*Description*
Critical Orifice	$ 184.00	3	$ 552.00	1,998.00 ₺	Swagelok 6LV-4-VCR-6-DM-055P
Flowmeter	€ 450.00	3	€ 1,350.00	5,171.00 ₺	SIERRA model C50L-AL-DD-2-PV2-V1-5POINTCAL-50-C9(0)-50 T8D
Pump	$ 2,400.00	1	$ 2,400.00	9,192.00 ₺	F&J Specialty products Model DF-1E
Quick connect	12.00 ₺	20	240.00 ₺	240.00 ₺	Eason Pneumatics model PC 1/2 - N03
Data acquisition system	10,000.00 ₺	1	10,000.00 ₺	10,000.00 ₺	Constructed in Hacettepe University
Encasing	5,000.00 ₺	1	5,000.00 ₺	5,000.00 ₺	Service Procurement
Total Cost				**56,727.00 ₺**	

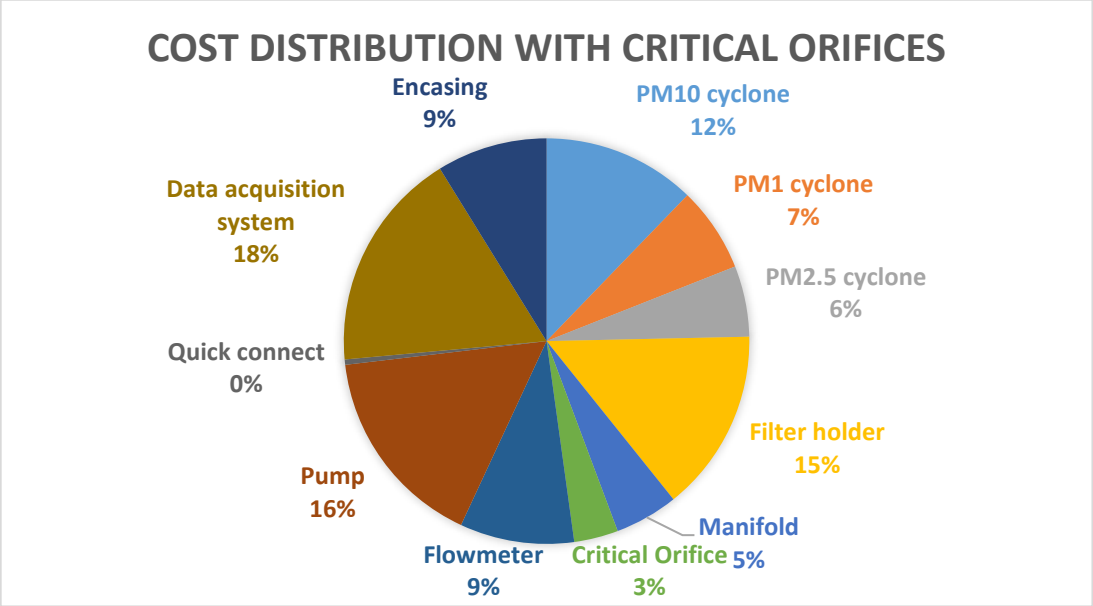

Figure 4.43. Cost distribution of the sampler with critical orifice configuration

Currently, there is no commercially available gravimetric particle sampler device equivalent to the sampler developed in this study (that can collect PM_1, $PM_{2.5}$ and PM_{10} particles simultaneously). For this reason, the cost of the sampler is compared to 3 similar sampler devices that are available on the market. The comparison can be seen in Table 4.5. For the sake of a reliable comparison; all prices are including VAT, as all the expenses within the scope of this study are including VAT.

Table 4.5. *Market research for samplers comparable to the sampler designed in this study*

Item	*Unit Price*	*Qty*	*Total Price*	*Total Price (₺)*	*Description*
Low volume sampler	$ 11,682.00	3	$ 35,046.00	126,866.52 ₺	Tisch model WILBUR
Low volume sampler	$ 24,921.00	3	$ 74,763.00	270,642.06 ₺	Thermo Scientific Model PM10-2025-99
High volume sampler	$ 7,363.00	3	$ 22,089.00	79,962.18 ₺	Thermo Scientific Model PM10-HVS-99

Item	*Unit Price*	*Qty*	*Total Price*	*Total Price (₺)*	*Description*
High volume sampler	$ 8,750.00	3	$ 26,250.00	95,025.00 ₺	Ecotech model HiVol 3000
High volume sampler	$ 9,855.00	3	$ 29,565.00	107,025.30 ₺	Thermo Scientific, model GUV 15HBL
Dichotomous sampler	€ 29,455.00	1	€ 29,455.00	112,812.65 ₺	Thermo Scientific, model Partisol plus

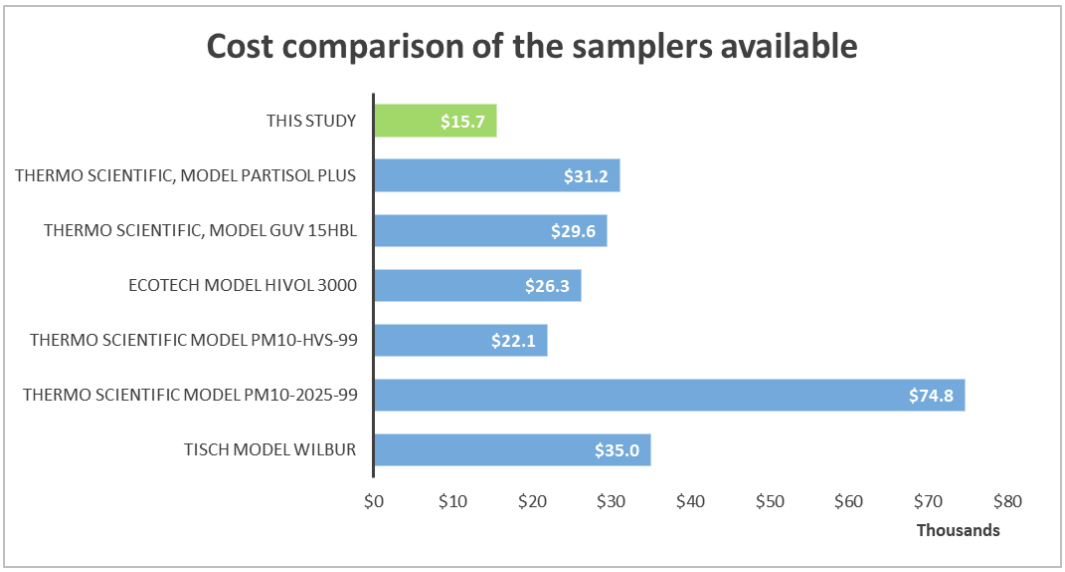

Figure 4.44. Market research for comparable samplers

First group of samplers to be compared is low volume samplers, which collects samples at flow rate as low as 16 LPM. To represent this sampler group, price quotes are acquired from Tisch and Thermo Scientific corporations for their TE-WILBUR and PM10-2025-99 models respectively. Unit prices are; 42,298 TL for Tisch TE-WILBUR sampler and 90,214 TL for Thermo Scientific PM10-2025-99 sampler. The cost of the devices shows a wide variation depending on the construction material of

the devices and the brands. Among these, Tisch sampler has a better price compared to others and represent the price range of a low-vol sampler to be procured at the end of an extensive market research.

One point to be noted in this comparison, none of these devices collect three particle groups simultaneously like the one in this study. During a sampling period, only one particle group at a time can be collected. Therefore, different particles groups should be collected at different times by replacement of the pre-impactor of the sampler for the desired particle group. Or, if simultaneous sampling is required, 3 of these devices are needed. Therefore, the sampler developed in this study compares to 3 low-vol samplers. In this case, Tisch sampler yields a cost of 127,000 TL and Thermo Scientific 270,000 TL. In both options, the cost is much higher than the sampler in this study.

Another sampler group in this comparison is, high volume samplers, which operates at 40 CFM (~70 m^3/h), while low-vol samplers operate at 16.7 LPM (~1 m^3/h). This operational difference results in both advantages and disadvantages. The advantage is, even in short duration samplings, it can collect particles in sufficiently large quantities to be measured by analytical tools. On the other hand, due to extremely high volume of air withdrawn and particles collected, the filter media to be used should be of low resistance to air flow, which restricts options to fiber structure filters such as glass fiber, cellulose fiber, quartz fiber etc. so as to prevent usage of membrane filters, which have greater blank performance. Besides, their motors are not powerful vacuum pumps, therefore, they can operate efficiently in the absence of resistance to air flow, however; in the case of resistance, their flow rate falls more rapidly than low volume samplers. For this, high volume samplers do not offer the best of its performance in highly polluted urban area, whereas, they are very useful in unpolluted rural areas.

As seen in the table, price quotes are given for 3 different models, one of them is manufactured by Ecotech firm, while the remaining two is by Thermo Scientific. While the Ecotech model costs around 95,000 TL, Thermo models cost 80,000 and

107,000 TL. This table reveals that carrying out the sampling of PM_{10}, $PM_{2.5}$ and PM_1 with Hi-Vol samplers cost around twice as much as the sampler developed in this study, neglecting the fact that Hi-Vol sampler with a PM_1 sampling head is quite unlikely to be offered by manufacturers. In addition, considering the excessive energy consumption resulting by 3 pumps -each draw ~1633 m^3/day- and difficulties in handling 3 separate devices, Hi-Vol samplers can be concluded highly inappropriate for the trimodal sampling task in this study.

The most similar commercially available system to the one designed in this study is Dichotomous Sampler, which is a sampling system that works on virtual impactor principle and collects $PM_{2.5}$ and $PM_{2.5\text{-}10}$ particle fractions on separate filters, like SFU. For comparison; price information for Partisol™ model is acquired as around 113,000₺. However, dichotomous sampler needs an additional element for PM_1 fraction. A low volume sampler will complete the particle fraction. Considering the cheapest Low-Vol sampler costs around 43,000₺, the cost of sampling PM_{10}, $PM_{2.5}$ and PM_1 particles result in a total of 156,000₺, which is roughly triple of the sampler developed in this study.

Although not defined as a goal within the scope of this study, a brief cost analysis is presented for the scenario in which the sampler to be designed to collect a single particle group. $PM_{2.5}$ is selected for this scenario. The cost distribution in this case is given in Table 4.6.

Table 4.6. *Cost of the sampler with solely $PM_{2.5}$ sampler configuration*

Item	*Unit Price*	*Qty*	*Total Price*	*Total Price (₺)*	*Description*
$PM_{2.5}$ cyclone	$ 885.00	1	$ 885.00	3,204.00 ₺	URG-2000-30EH
Filter holder	$ 762.00	3	$ 2,286.00	8,275.00 ₺	URG-2000-30FG-2
Manifold	$ 792.00	1	$ 792.00	2,867.00 ₺	URG-2000-30HD-1

Item	*Unit Price*	*Qty*	*Total Price*	*Total Price (₺)*	*Description*
Critical Orifice	$ 184.00	3	$ 552.00	1,998.00 ₺	Swagelok 6LV-4-VCR-6-DM-055P
Flowmeter	€ 450.00	3	€ 1,350.00	5,171.00 ₺	SIERRA model C50L-AL-DD-2-PV2-V1-5POINTCAL-50-C9(0)-50 T8D
Pump	$ 2,400.00	1	$ 2,400.00	9,192.00 ₺	F&J Specialty products Model DF-1E
Quick connect	12.00 ₺	6	72.00 ₺	72.00 ₺	Eason Pneumatics model PC 1/2 - N03
Data acquisition system	10,000.00 ₺	1	10,000.00 ₺	10,000.00 ₺	Constructed in Hacettepe University
Encasing	5,000.00 ₺	1	5,000.00 ₺	5,000.00 ₺	Service Procurement
Total Cost				**35,482.76 ₺**	

Total cost in this case is roughly calculated as 35,500 ₺. Even though this cost is already less than that of commercial low-vol samplers, the real cost will be even less than 35,500 ₺. Since the costs of data acquisition system and encasing is not unit price-based expenditures, the cost in the case of PM_{10}, $PM_{2.5}$ and PM_1 system in calculations. However, in the case this scenario is put into practice, these expenditures will be lower.

CHAPTER 5

CONCLUSION

In this study, a particulate matter (PM) sampler that can collect PM_1, $PM_{2.5}$ and PM_{10} particles simultaneously is constructed, in order to achieve task of sampling multiple particulate matter fractions (and optionally other air pollutants) simultaneously on separate filters at a reasonable cost. This way, lowering budget requirements for sampling tasks and encouraging more research activities in the field and increase competitiveness of the researchers in Turkey in the international area is intended.

General structure of the sampler constructed in this study consists of the following main elements;

- Size selector; 3 cyclones to separate particles in the ambient air PM_1, $PM_{2.5}$ and PM_{10} fractions,
- Collection media; PTFE filters to collect separated particles by each cyclone
- Flow control; critical orifices to control flow at the rate to match with cyclones' cut point diameters,
- Vacuum pump; to supply the system with vacuum needed.

This study is carried out in two phases. In the 1st phase, the sampler is constructed with three cyclones to collect three particle groups separately, mass flow controllers (MFC) and a vacuum pump to draw sample air. In this phase, highest accuracy with the highest technology devices are intended, regardless of costs. The preliminary sampler is installed in a temporary shelter.

In the 2nd phase of the study, mass flow controllers (MFC), which are the most expensive component of the sampler, are replaced with stainless steel critical orifices. After replacement with critical orifices, a data log unit was encoded in order to monitor

air flow rate in each channel, and total volume of air in each channel at the end of sampling. With the aid of this unit, flow rate stability tests are carried out for each variable in the system; MFC configuration vs critical orifice configuration, nucleopore filter vs PTFE filters, 1-channel configuration vs 3-channel configuration. As depicted in Section 4.4, results revealed that critical orifices provided more stable air flow in both filter types. However, as nucleopore filters have higher resistance, flow rate decrease is observed in later hours of sampling. For this reason, PTFE (Teflon®) filters are selected for measurements. In this study, Sartorius 11803--47------N filters, that are of 47 mm diameter and 1.2 μm pore size, are used. Each pack contains 100 filters, which is sufficient for a month of sampling. Among the tests with PTFE filter for 1-channel and 3-channel; 1-channel configuration generated even more stable flow rate curve and average flow rate is observed to be 10 – 15% higher.

Gravimetric analysis of the samples was carried out in the Clean Room, in the Environmental Engineering Department. All filters were conditioned for 24 hours prior to and following the sampling. The filters were weighed using Sartorius MC-5 microbalance scale with 0.001 mg sensitivity in order to determine the mass of particles collected in each channel. Later, PM_1, $PM_{2.5}$ and PM_{10} concentrations were calculated by division of mass to volume of air collected, which are, recorded in the data log unit of the sampler.

After the sampler components were installed to final shelter, the sampler was operated in parallel to a Gent SFU and two high volume samplers with PM_{10} head for 24 days. As discussed in the relevant chapters, the sampler produced consistent results within itself and individual parameters followed similar variation pattern. PM_{10} data by the new sampler is compared against SFU and two Hi-vol samplers. $PM_{2.5}$ data is compared with Grimm EDM 164 laser aerosol spectrometer and SFU. PM_1 data from the new sampler could only be compared with Grimm laser spectrometer, as it was the only sampler (other than the one in this study) that can measure PM_1 data.

The total cost of the final sampler resulted in around 57,000 ₺, (corresponds to around $15,700), which is far cheaper than any of the commercial samplers compared in this study. As stated previously, none of the commercial gravimetric samplers offers 3 particle fractions in one device, as the sampler designed in this study does. By this aspect, the new sampler is unique in its field.

At the end of the study, a particle sampler has been successfully constructed, in order to collect PM_1, $PM_{2.5}$ and PM_{10} particles simultaneously, and with a reasonable cost, therefore, the main purpose of the study has been accomplished.

REFERENCES

Anderson, J. O., Thundiyil, J. G., & Stolbach, A. (2012). Clearing the Air: A Review of the Effects of Particulate Matter Air Pollution on Human Health. *Journal of Medical Toxicology*, *8*(2), 166–175. https://doi.org/10.1007/s13181-011-0203-1

Appel, K. W., Pouliot, G. A., Simon, H., Sarwar, G., Pye, H. O. T., Napelenok, S. L., … Roselle, S. J. (2013). Evaluation of dust and trace metal estimates from the Community Multiscale Air Quality (CMAQ) model version 5.0. *Geoscientific Model Development*, *6*, 883–899. https://doi.org/10.5194/gmd-6-883-2013

Carruthers, D., Carslaw, D., Colvile, R., Richard Derwent OBE, P., Dorling, S., Bernard Fisher, P., … Stevenson, K. (2005). *Particulate Matter in the United Kingdom*. Retrieved from https://uk-air.defra.gov.uk/assets/documents/reports/aqeg/pm-summary.pdf

Cheng, Z., Wang, S., Jiang, J., Fu, Q., Chen, C., Xu, B., … Hao, J. (2013). Long-term trend of haze pollution and impact of particulate matter in the Yangtze River Delta, China. *Environmental Pollution*, *182*, 101–110. https://doi.org/10.1016/j.envpol.2013.06.043

Commission for Environmental Cooperation. (2005). *North American Power Plant Air Emissions*. Retrieved from https://www.etde.org/etdeweb/details_open.jsp?osti_id=20572912

Energy Information Administration. (1999). *Natural Gas 1998 Issues and Trends*. Retrieved from http://www.eia.doe.gov/oil_gas/natural_gas/analysis_publications/

EPA. (1995). *AP 42, Fifth Edition: Compilation of Air Pollutant Emission Factors*. Retrieved from https://www3.epa.gov/ttnchie1/ap42/ch01/final/c01s04.pdf

EPA. (2013). Basic Information Particulate Matter. Retrieved May 24, 2016, from U.S. Environmental Protection Agency website: https://www3.epa.gov/pm/basic.html

EPA. (2015a). *2011 National Emissions Inventory, version 2 Technical Support Document*. Retrieved from https://www.epa.gov/sites/production/files/2015-10/documents/nei2011v2_tsd_14aug2015.pdf

EPA. (2015b). Criteria Air Pollutants. Retrieved May 24, 2016, from U.S. Environmental Protection Agency website: http://www.epa.gov/criteria-air-pollutants

EPA. (2016a). Air Quality and Climate Change Research. Retrieved July 4, 2016, from https://www.epa.gov/air-research/air-quality-and-climate-change-research

EPA. (2016b). Health. Retrieved June 25, 2016, from https://www3.epa.gov/pm/health.html

EPA. (2016c). National Emissions by Source Sector. Retrieved June 15, 2016, from Air Emission Sources website: https://www3.epa.gov/cgi-bin/broker?polchoice=PM&_debug=0&_service=data&_program=dataprog.national_1.sas

EPA. (2016d). Visibility. Retrieved June 30, 2016, from Visibility and Haze website: https://www.epa.gov/visibility/visibility-basic-information

European Commission. (1997). *Ambient air pollution by particulate matter*. Retrieved from http://ec.europa.eu/environment/air/pdf/pp_pm.pdf

Franzi, L. M., Bratt, J. M., Williams, K. M., & Last, J. A. (2011). Why is particulate matter produced by wildfires toxic to lung macrophages? *Toxicology and Applied Pharmacology*, *257*(2), 182–188. https://doi.org/10.1016/j.taap.2011.09.003

Fuzzi, S., Baltensperger, U., Carslaw, K., Decesari, S., Denier Van Der Gon, H., Facchini, M. C., … Gilardoni, S. (2015). Particulate matter, air quality and climate: lessons learned and future needs. *Atmospheric Chemistry and Physics*, *15*, 8217–8299. https://doi.org/10.5194/acp-15-8217-2015

Gertler, A. W. (2005). Diesel vs. gasoline emissions: Does PM from diesel or gasoline vehicles dominate in the US? *Atmospheric Environment*, *39*(13), 2349–2355.

https://doi.org/10.1016/j.atmosenv.2004.05.065

Gilliam, J. H., & Hall, E. S. (2016). *Reference and Equivalent Methods Used to Measure National Ambient Air Quality Standards (NAAQS) Criteria Air Pollutants - Volume I*. https://doi.org/10.13140/RG.2.1.2423.2563

Goli, T. (2017). *Identification and source apportionment of trace elements in urban and suburban area of Ankara*. Ankara M. Sc. Thesis, Middle Est Technical University, Ankara, August 2017.

Grimm Aerosol Technik. (2019). MODEL EDM180. Retrieved February 19, 2019, from https://www.grimm-aerosol.com/products-en/environmental-dust-monitoring/approved-pm-monitor/edm180/

Grythe, H., Ström, J., Krejci, R., Quinn, P., & Stohl, A. (2014). A review of sea-spray aerosol source functions using a large global set of sea salt aerosol concentration measurements. *Atmos. Chem. Phys*, *14*, 1277–1297. https://doi.org/10.5194/acp-14-1277-2014

Hart, D. (2009). BAM-1020 Ambient Particulate Mass Monitor: Keys to Obtaining High Quality Particulate Data Using a PM 2.5 Federal Equivalent Method. Retrieved February 2, 2019, from https://www3.epa.gov/ttnamti1/files/2009conference/Hart.pdf

Hart, K. M., Isabelle, L. M., & Pankow, J. F. (1992). High-Volume Air Sampler for Particle and Gas Sampling. 1. Design and Gas Sampling Performance. https://doi.org/10.1021/es00029a027

Haywood, J., & Boucher, O. (2000). Estimates of the direct and indirect radiative forcing due to tropospheric aerosols: A review. *Reviews of Geophysics*, *38*(4), 513–543. https://doi.org/10.1029/1999RG000078

Hinds, W. C. (1999). *Aerosol technology : properties, behavior, and measurement of airborne particles*. Retrieved from http://aerosol.ees.ufl.edu/atmos_aerosol/section02.html

Hopke, P. K., Xie, Y., Raunemaa, T., Biegalski, S., Landsberger, S., Maenhaut, W., … Cohen, D. (1997). Characterization of the Gent Stacked Filter Unit PM 10

Sampler. *Aerosol Science and Technology*, *27*(6), 726–735. https://doi.org/10.1080/02786829708965507

Houghton, J. T., Ding, Y., Griggs, D. J., Noguer, M., Linden, P. J. van der, Dai, X., … Johnson, C. A. (2001). *Climate Chance 2001: The Scientific Basis*. Retrieved from http://grida.no/climate/ipcc_tar/wg1/pdf/TAR-05.pdf

Hung-Lung, C., & Yao-Sheng, H. (2009). Particulate matter emissions from on-road vehicles in a freeway tunnel study. *Atmospheric Environment*, *43*(26), 4014–4022. https://doi.org/10.1016/j.atmosenv.2009.05.015

Jimoda, L. A. (2012). Effects of Particulate Matter on Human Health, The Ecosystem, Climate and Materials: A Review. *Working and Living Environmental Protection*, *9*(1), 27–44. Retrieved from http://facta.junis.ni.ac.rs/walep/walep201201/walep201201-04.pdf

Kalivitis, N., Kerminen, V.-M., Kouvarakis, G., Stavroulas, I., Bougiatioti, A., Nenes, A., … Mihalopoulos, N. (2015). Atmospheric new particle formation as a source of CCN in the eastern Mediterranean marine boundary layer. *Atmos. Chem. Phys*, *15*, 9203–9215. https://doi.org/10.5194/acp-15-9203-2015

Kerminen, V.-M., Paramonov, M., Anttila, T., Riipinen, I., Fountoukis, C., Korhonen, H., … Petäjä, T. (2012). Cloud condensation nuclei production associated with atmospheric nucleation: a synthesis based on existing literature and new results. *Atmos. Chem. Phys. Atmospheric Chemistry and Physics*, *12*, 12037–12059. https://doi.org/10.5194/acp-12-12037-2012

Kim, K.-H., Kabir, E., & Kabir, S. (2015). A review on the human health impact of airborne particulate matter. *Environment International*, *74*, 136–143. https://doi.org/10.1016/j.envint.2014.10.005

Koçak, E., Öztürk, F., Kılavuz, S. A., İmamoğlu, İ., & Tuncel, G. (2017). Elementel and Organic Carbon Concentrations in Urban and Suburban Ankara Atmospheres: Estimation of Secondary Organic Aerosol. *8th International Atmospheric Symposium, ATMOS2017, Book of Proceedings*, 178–184. İstanbul.

Kuntasal, Ö. O., Kılavuz, S. A., Karman, D., Wang, D., & Tuncel, G. (2013). C5–C12

volatile organic compounds at roadside, residential, and background locations in Ankara, Turkey: Temporal and spatial variations and sources. *Journal of the Air & Waste Management Association*, *63*(10), 1148–1162. https://doi.org/10.1080/10962247.2013.804012

Künzli, N., Kaiser, R., Medina, S., Studnicka, M., Chanel, O., Filliger, P., … Sommer, H. (2000). Public-health impact of outdoor and traffic-related air pollution: a European assessment. *The Lancet*, *356*(9232), 795–801. https://doi.org/10.1016/S0140-6736(00)02653-2

Langmann, B. (2013). Volcanic Ash versus Mineral Dust: Atmospheric Processing and Environmental and Climate Impacts. *ISRN Atmospheric Sciences*, *2013*(ii), 1–17. https://doi.org/10.1155/2013/245076

Lewis, R., & Schwartz, E. (2004). Sea Salt Aerosol Production: Mechanisms, Methods, Measurements and Models—A Critical Review. *American Geophysical Union Geophysical Monograph Series*, *152*, 413. https://doi.org/10.1029/GM152

Liberti, A. (1975). Modern Methods for Air Pollution Monitoring. *Analytical Chemistry*, 519–534. https://doi.org/10.1016/B978-0-408-70730-5.50007-7

Lundgren, D. a., Hlaing, D. N., Rich, T. a., & Marple, V. a. (1996). Data from a Trichotomous Sampler. *Aerosol Science and Technology*, *25*(3), 353–357. https://doi.org/10.1080/02786829608965401

Ma, C.-J., & Kim, K.-H. (2014). Preliminary Study on the Cloud Condensation Nuclei (CCN) Activation of Soot Particles by a Laboratory-scale Model Experiments. *Asian Journal of Atmospheric Environment*, *8*(4), 175–183. https://doi.org/10.5572/ajae.2014.8.4.175

Maenhaut, W., Francois, F., & Cafmeyer, J. (1994). *The "Gent" Stacked Filter Unit (SFU) Sampler for the Collection of Atmospheric Aerosols in Two Size Fractions: Description and Instructions for Installation and Use*. Retrieved from http://www.iaea.org/inis/collection/nclcollectionstore/_public/25/054/25054927.pdf

Malm, W. C. (1999). *Introduction to Visibility*. Retrieved from https://www.epa.gov/sites/production/files/2015-05/documents/introvis.pdf

Marple, V., Lundgren, D., & Olson, B. (2014). A PM1.0/2.5/10 Trichotomous Virtual Impactor Based Sampler: Design and Applied to Arid Southwest Aerosols—Part II: Application to Arid Southwest Aerosols. *KONA Powder and Particle Journal*, *31*(31), 2–9. https://doi.org/10.14356/kona.2014001

Mccammon, C. S., Denver, N. /, Office, F., & Woebkenberg, M. L. (1998). *General Considerations for Sampling Airborne Contaminants*. Retrieved from https://www.cdc.gov/niosh/docs/2003-154/pdfs/chapter-d.pdf

Merikanto, J., Spracklen, D. V, Mann, G. W., Pickering, S. J., & Carslaw, K. S. (2009). Impact of nucleation on global CCN. *Atmos. Chem. Phys. Atmospheric Chemistry and Physics*, *9*, 8601–8616. Retrieved from www.atmos-chem-phys.net/9/8601/2009/

Monahan, E. C., Spiel, D. E., & Davidson, K. L. (1986). A Model of Marine Aerosol Generation Via Whitecaps and Wave Disruption. In Edward C Monahan & G. Mac Niocaill (Eds.), *Oceanic Whitecaps: And Their Role in Air-Sea Exchange Processes* (pp. 167–174). https://doi.org/10.1007/978-94-009-4668-2_16

National Research Council. (2010). *Global Sources of Local Pollution*. https://doi.org/10.17226/12743

Nemery, B., Hoet, P. H., & Nemmar, A. (2001). The Meuse Valley fog of 1930: an air pollution disaster. *The Lancet*, Vol. 357, pp. 704–708. https://doi.org/10.1016/S0140-6736(00)04135-0

NSW EPA. (2013). Sources of particulate pollution. Retrieved June 12, 2016, from NSW EPA initiatives website: http://www.epa.nsw.gov.au/aqms/pmsourcesreg.htm

O'Dowd, C. D., Facchini, M. C., Cavalli, F., Ceburnis, D., Mircea, M., Decesari, S., … Putaud, J.-P. (2004). Biogenically driven organic contribution to marine aerosol. *Nature*, *431*(7009), 676–680. https://doi.org/10.1038/nature02959

O'Keefe Controls Co. (2010). Precision Orifices Plus Fluid Control Products.

Retrieved September 30, 2019, from http://www.okcc.com/PDF/cat 11 Rev 7_web.pdf

Omidvarborna, H., Kumar, A., & Kim, D. S. (2014). Characterization of particulate matter emitted from transit buses fueled with B20 in idle modes. *Journal of Environmental Chemical Engineering*, *2*(4), 2335–2342. https://doi.org/10.1016/j.jece.2014.09.020

Park, J.-M., Rock, J. C., Wang, L., Seo, Y.-C., Bhatnagar, A., & Kim, S. (2009). Performance evaluation of six different aerosol samplers in a particulate matter generation chamber. *Atmospheric Environment*, *43*(2), 280–289. https://doi.org/10.1016/j.atmosenv.2008.09.028

Parkinson, K. J., & Day, W. (1979). The Use of Orifices to Control the Flow Rate of Gases. *Journal of Applied Ecology*, *16*(2), 623–632. Retrieved from https://www.jstor.org/stable/pdf/2402536.pdf

Passant, N. R., Peirce, M., Rudd, H. J., Scott, D. W., Marlowe, I., & Watterson, J. D. (2002). UK Particulate and Heavy Metal Emissions from Industrial Processes. Retrieved June 26, 2016, from AEAT-6270 Issue 2 website: https://uk-air.defra.gov.uk/assets/documents/reports/empire/AEAT6270Issue2finaldraft_v2.pdf

Perraud, V., Bruns, E. A., Ezell, M. J., Johnson, S. N., Yu, Y., Alexander, M. L., … Finlayson-Pitts, B. J. (2012). Nonequilibrium atmospheric secondary organic aerosol formation and growth. *Proceedings of the National Academy of Sciences*, *109*(8), 2836–2841. https://doi.org/10.1073/pnas.1119909109

Queensland Government. (2013). High and Low Volume Air Samplers. Retrieved May 9, 2016, from Collecting and measuring airborne particles website: https://www.qld.gov.au/environment/pollution/monitoring/air-pollution/samplers/

Queensland Government. (2017). Airborne particles. Retrieved February 10, 2019, from http://www.qld.gov.au/environment/pollution/monitoring/air/

Radke, L. F., Hegg, D. A., Hobbs, P. V, Nance, J. D., Lyons, J. H., Laursen, K. K., … Ward, D. E. (1991). Particulate and Trace Gas Emissions from Large Biomass

Fires in North America. In *Global Biomass Burning: Atmospheric, Climatic, and Biospheric Implications* (pp. 219–220). Retrieved from http://www.fs.fed.us/psw/publications/riggan/psw_1991_riggan001(radke).pdf

Robert, M. A., VanBergen, S., Kleeman, M. J., & Jakober, C. A. (2007). Size and composition distributions of particulate matter emissions: part 1--light-duty gasoline vehicles. *Journal of the Air & Waste Management Association (1995)*, *57*(12), 1414–1428. Retrieved from http://www.ncbi.nlm.nih.gov/pubmed/18200926

Seinfeld, J. H., & Pandis, S. N. (2006). *Atmospheric chemistry and physics : from air pollution to climate change* (2nd ed.). Hoboken, NJ: John Wiley & Sons, Inc.

Stockham, L. W., & Plante, M. D. (2004). *CRITICAL ORIFICE THEORY, DESIGN AND IMPLEMENTATION*. Retrieved from https://apps.dtic.mil/dtic/tr/fulltext/u2/a449633.pdf

Thermo Scientific. (n.d.). Beta Attenuation Technology for Particulate Matter Measurement - TR. Retrieved February 10, 2019, from https://www.thermofisher.com/tr/en/home/industrial/environmental/environmental-learning-center/air-quality-analysis-information/beta-attenuation-technology-particulate-matter-measurement.html

ThermoScientific. (2015). Partisol 2025i Dichotomous Sequential Air Sampler. Retrieved July 3, 2016, from Partisol™ 2025i-D Dichotomous Sequential Air Sampler website: https://www.thermofisher.com/order/catalog/product/2025ID?ICID

Timms, C. (2012). Great Smog 60 years on: "New laws needed to clean London's air." *BBC News*. Retrieved from http://www.bbc.com/news/uk-england-london-20269309

Tisch Environmental. (2014). TE-WILBUR Low Volume FRM Sampler. Retrieved February 8, 2019, from https://tisch-env.com/low-volume-air-sampler/

UCSUSA. (2015). Aerosol particles and climate. Retrieved July 4, 2016, from http://www.ucsusa.org/global_warming/science_and_impacts/science/aerosol

s-and-global-warming-faq.html#bf-toc-1

Urbanski, S. P., Hao, W. M., & Baker, S. (2009). Chemical Composition of Wildland Fire Emissions. *Developments in Environmental Science*, *8*. https://doi.org/10.1016/S1474-8177(08)00004-1

Voiland, A. (2010). Aerosols: Tiny Particles, Big Impact. Retrieved June 15, 2016, from The Earth Observatory website: http://earthobservatory.nasa.gov/Features/Aerosols/

Washington State Department of Ecology. (2017). *PM 2.5 and PM 10 Beta Attenuation Monitor Operating Procedure*. Retrieved from https://fortress.wa.gov/ecy/publications/documents/1702005.pdf

Westervelt, D. M., Pierce, J. R., & Adams, P. J. (2014). Analysis of feedbacks between nucleation rate, survival probability and cloud condensation nuclei formation. *Atmos. Chem. Phys*, *14*, 5577–5597. https://doi.org/10.5194/acp-14-5577-2014

Whitby, K. T. (1978). The physical characteristics of sulfur aerosols. *Atmospheric Environment (1967)*, *12*(1–3), 135–159. https://doi.org/10.1016/0004-6981(78)90196-8

World Health Organisation. (2003). *Health Aspects of Air Pollution with Particulate Matter, Ozone and Nitrogen Dioxide*. Retrieved from http://www.euro.who.int/__data/assets/pdf_file/0005/112199/E79097.pdf

World Health Organisation. (2014). Ambient (outdoor) air quality and health. In *WHO*. Retrieved from World Health Organization website: http://www.who.int/mediacentre/factsheets/fs313/en/

Zhang, C., Yao, Q., & Sun, J. (2005). Characteristics of particulate matter from emissions of four typical coal-fired power plants in China. *Fuel Processing Technology*, *86*(7), 757–768. https://doi.org/10.1016/j.fuproc.2004.08.006

Zhao, H., Che, H., Zhang, X., Ma, Y., Wang, Y., Wang, H., & Wang, Y. (2013). Characteristics of visibility and particulate matter (PM) in an urban area of Northeast China. *Atmospheric Pollution Research*, *4*(4), 427–434.

https://doi.org/10.5094/APR.2013.049

APPENDICES

A. Literature where SFU was used in sampling of atmospheric particles

1. Szramowiat-Sala, K., Korzeniewska, A., Sornek, K., Marczak, M., Wierońska, F., Berent, K., Gołaś, J., Filipowicz, M. The properties of particulate matter generated during wood combustion in in-use stoves (2019) Fuel, 253, pp. 792-801.

2. Lestiani, D.D., Santoso, M., Kurniawati, S., Sari, D.K., Kusmartini, I., Manurung, A., Riadi, A. Chemical Composition of Fine Particulate Matter from Peat Forest Fires at Palangka Raya and Its Dispersion using HYSPLIT (2019) IOP Conference Series: Earth and Environmental Science, 303 (1), art. no. 012035, .

3. Kurniawati, S., Santoso, M., Lestiani, D.D., Atmodjo, D.P.D., Sari, D.K., Kusmartini, I. Identification of Potential Source Location of Sulfur at Urban Area Bandung using Conditional Probability Function (CPF) (2019) IOP Conference Series: Earth and Environmental Science, 303 (1), art. no. 012042,

4. Santoso, M., Lestiani, D.D., Kurniawati, S., Damastuti, E., Kusmartini, I., Prakoso, D., Dimas, Triyambodo, Rita Elemental Composition of Particulate Matter Air Pollution Collected Around Industrial Area in East Java (2019) IOP Conference Series: Earth and Environmental Science, 303 (1), art. no. 012036,

5. Ranjan, R., Indolfi, M., Ferrara, M.A., Sirleto, L. Implementation of a nonlinear microscope based on stimulated raman scattering (2019) Journal of Visualized Experiments, 2019 (149), art. no. e59614,

6. Begum, B.A., Hopke, P.K. Identification of sources from chemical characterization of fine particulate matter and assessment of ambient air quality in Dhaka, Bangladesh (2019) Aerosol and Air Quality Research, 19 (1), pp. 118-128.

7. Zheng, C., Hong, Y., Liu, S., Yang, Z., Chang, Q., Zhang, Y., Gao, X. Removal and Emission Characteristics of Condensable Particulate Matter in an Ultralow Emission Power Plant (2018) Energy and Fuels, 32 (10), pp. 10586-10594.

8. Malafronte, L., Morel, B., Pohjoranta, A. Online Total Harmonic Distortion Analysis for Solid Oxide Fuel Cell Stack Monitoring in System Applications (2018) Fuel Cells, 18 (4), pp. 476-489.

9. Sempere, F., Winter, P., Waalkens, A., Hühnert, N., Cranshaw, I., Beigi, B., Thorpe, R.B. Treatment of discontinuous emission of sewage sludge odours by a full scale biotrickling filter with an activated carbon polishing unit

10. Tahri, M., Benchrif, A., Bounakhla, M., Benyaich, F., Noack, Y. Seasonal variation and risk assessment of PM2.5 and PM2.5-10 in the ambient air of Kenitra, Morocco (2017) Environmental Science: Processes and Impacts, 19 (11), pp. 1427-1436.

11. Kim, H.-W., Kim, K.-H., Park, H.-S. Life cycle impact assessment of the environmental infrastructures in operation phase: Case of an industrial waste incineration plant (2017) Environmental Engineering Research, 22 (3), pp. 266-276.

12. Seneviratne, S., Handagiripathira, L., Sanjeevani, S., Madusha, D., Waduge, V.A.A., Attanayake, T., Bandara, D., Hopke, P.K. Identification of sources of fine particulate matter in Kandy, Sri Lanka (2017) Aerosol and Air Quality Research, 17 (2), pp. 476-484.

13. Li, M., Wang, C., Cen, K., Ni, M., Li, X. PCDD/F emissions during startup and shutdown of a hazardous waste incinerator

14. Owoade, K.O., Hopke, P.K., Olise, F.S., Adewole, O.O., Ogundele, L.T., Fawole, O.G. Source apportionment analyses for fine (PM2.5) and coarse (PM2.5–10) mode particulate matter (PM) measured in an urban area in southwestern Nigeria (2016) Atmospheric Pollution Research, 7 (5), pp. 843-857.

15. Parthasarathy, K., Sahu, S.K., Pandit, G.G. Comparison of two receptor model techniques for the size fractionated particulate matter source apportionment (2016) Aerosol and Air Quality Research, 16 (6), pp. 1497-1508.

16. Orogade, S.A., Owoade, K.O., Hopke, P.K., Adie, D.B., Ismail, A., Okuofu, C.A. Source apportionment of fine and coarse particulate matter in industrial areas of Kaduna Northern Nigeria (2016) Aerosol and Air Quality Research, 16 (5), pp. 1179-1190.

17. Furu, E., Katona-Szabo, I., Angyal, A., Szoboszlai, Z., Török, Zs., Kertész, Zs. The effect of the tramway track construction on the aerosol pollution in Debrecen, Hungary (2015) Nuclear Instruments and Methods in Physics Research, Section B: Beam Interactions with Materia

18. Rahman, S.A., Hamzah, M.S., Elias, M.S., Salim, N.A.A., Hashim, A., Shukor, S., Siong, W.B., Wood, A.K. A long term study on characterization and source apportionment of particulate pollution in klang valley, kuala Lumpur

19. Rahim, F.L.M., Hassim, M.H., Mokhtar, M.M. Environmental assessment of ashes generated from medical waste incineration (2015) Chemical Engineering Transactions, 45, pp. 1699-1704.

20. Ezeh, G.C., Obioh, I.B., Asubiojo, O.I., Chiari, M., Nava, S., Calzolai, G., Lucarelli, F., Nuviadenu, C. The complementarity of PIXE and PIGE techniques: A case study of size segregated airborne particulates collected from a Nigeria city (2015) Applied Radiation and Isotopes, 103, pp. 82-92.

21. Adebiyi, F.M., Ezeh, G.C., Adeyemi, F.A., Obioh, I.B. Trace elements in particulate matter of ambient air at petroleum filling stations (2015) Toxicological and Environmental Chemistry, 97 (7), pp. 847-856.

22. Owoade, K.O., Hopke, P.K., Olise, F.S., Ogundele, L.T., Fawole, O.G., Olaniyi, B.H., Jegede, O.O., Ayoola, M.A., Bashiru, M.I. Chemical compositions and source identification of particulate matter (PM2.5 and PM2.5–10) from a scrap iron and steel smelting industry along the Ife–Ibadan highway, Nigeria (2015) Atmospheric Pollution Research, 6 (1), pp. 107-119.

23. Ezeh, G.C., Obioh, I.B., Asubiojo, O.I., Chiari, M., Nava, S., Calzolai, G., Lucarelli, F., Nuviadenu, C.K. Elemental compositions of PM 10-2.5 and PM 2.5 aerosols of a nigerian urban city using ion beam analytical techniques (2014) Nuclear Instruments and Methods in Physics Research, Section B: Beam Interactions with Materials and Atoms, 334, pp. 28-33.

24. Siddique, N., Waheed, S. Source apportionment using reconstructed mass calculations (2014) Journal of Environmental Science and Health - Part A Toxic/Hazardous Substances and Environmental Engineering, 49 (4), pp. 463-477.

25. Chen, M.-W., Lin, T.-C., Wang, L.-C., Chang-Chien, G.-P. The PCDD/f removal efficiency of a medical waste incinerator dual-bag filter system (2014) Aerosol and Air Quality Research, 14 (4), pp. 1223-1231.

26. Ni, Z., Dong, F., Yang, Y., Pang, T., Wu, B., Zhang, Z., Zeng, Z. Study on measurement of flue gas velocity and particulate concentration by optical method (2014) Zhongguo Jiguang/Chinese Journal of Lasers, 41 (1), art. no. 0108002, .

27. Jin, X.-C., Zhang, G.-Y., Xiao, C.-J., Huang, D.-H., Yuan, G.-J., Yao, Y.-G., Wang, X.-H., Hua, L., Wang, P.-S., Ni, B.-F. Source apportionment of PM2.5 in Xinzhen, Beijing using PIXE and XRF (2014) Yuanzineng Kexue Jishu/Atomic Energy Science and Technology, 48 (7), pp. 1325-1330.

28. Silva, A.V., Almeida, S.M., Oliveira, C.M., Miranda, A.M. Chemical characterization of ambient suspended particles in an urban area affected by industrial activities (2014) WIT Transactions on Ecology and the Environment, 181, pp. 635-646.

29. Maenhaut, W., Karnieli, A., Andreae, M.O. Ten-year study of fine aerosol at Sde Boker, Israel, using PIXE: Time trends, seasonal variation, correlations, and source areas for anthropogenic elements (2014) Nuclear Instruments and Methods in Physics Research, Section B: Beam Interactions with Materials and Atoms, 318 (PART A), pp. 119-124.

30. Abiye, O.E., Obioh, I.B., Ezeh, G.C. Elemental characterization of urban particulates at receptor locations in Abuja, north-central Nigeria (2013) Atmospheric Environment, 81, pp. 695-701.

31. Sandeep, P., Saradhi, I.V., Pandit, G.G. Seasonal variation of black carbon in fine particulate matter (PM 2.5) at the tropical coastal city of Mumbai, India (2013) Bulletin of Environmental Contamination and Toxicology, 91 (5), pp. 605-610.

32. Santoso, M., Lestiani, D.D., Markwitz, A. Characterization of airborne particulate matter collected at Jakarta roadside of an arterial road (2013) Journal of Radioanalytical and Nuclear Chemistry, 297 (2), pp. 165-169.

33. Lestiani, D.D., Santoso, M., Trompetter, W.J., Barry, B., Davy, P.K., Markwitz, A. Determination of chemical elements in airborne particulate matter collected at Lembang, Indonesia by particle induced X-ray emission (2013) Journal of Radioanalytical and Nuclear Chemistry, 297 (2), pp. 177-182.

34. Tahri, M., Bounakhla, M., Zghaïd, M., Benchrif, A., Zahry, F., Noack, Y., Benyaïch, F. TXRF characterization and source identification by positive matrix factorization of airborne particulate matter sampled in Kenitra City (Morocco) (2013) X-Ray Spectrometry, 42 (4), pp. 284-289.

35. Tahri, M., Bounakhla, M., Zghaïd, M., Noack, Y., Benyaïch, F., Benchrif, A. Evaluation of airborne particulate matter pollution in Kenitra City, Morocco [Avaliação da poluição de material particulado de aviação em Kenitra, Marrocos] (2013) Revista Ambiente e Agua, 8 (1), pp. 38-47.

36. Siddique, N., Jawad, M., Waheed, S. Instrumental neutron activation analysis for the study of size-fractionated airborne particulate matter samples (2013) Radiochimica Acta, 101 (4), pp. 273-277.

37. Tahir, N.M., Suratman, S., Fong, F.T., Hamzah, M.S., Latif, M.T. Temporal distribution and chemical characterization of atmospheric particulate matter in the eastern coast of Peninsular Malaysia (2013) Aerosol and Air Quality Research, 13 (2), pp. 584-595.

38. Obioh, I.B., Ezeh, G.C., Abiye, O.E., Alpha, A., Ojo, E.O., Ganiyu, A.K. Atmospheric particulate matter in Nigerian megacities (2013) Toxicological and Environmental Chemistry, 95 (3), pp. 379-385.

39. De Arespacochaga, N., Pérez, L., Benito, S., Pérez, A., Cortina, J.L., McPhail, S. Performance of a biogas-powered SOFC pilot plant: Description of the biogas treatment and optimisation of the fuel cell operational conditions (2013) EFC 2013 - Proceedings of the 5th European Fuel Cell Piero Lunghi Conference, pp. 327-328.

40. Lestiani, D.D., Santoso, M., Kurniawati, S., Markwitz, A. Characteristic of airborne particulate matter samples collected from two semi industrial sites in Bandung, Indonesia (2013) Indonesian Journal of Chemistry, 13 (3), pp. 271-277.

41. Owoade, O.K., Fawole, O.G., Olise, F.S., Ogundele, L.T., Olaniyi, H.B., Almeida, M.S., Ho, M.-D., Hopke, P.K. Characterization and source identification of airborne particulate loadings at receptor site-classes of Lagos Mega-City, Nigeria (2013) Journal of the Air and Waste Management Association, 63 (9), pp. 1026-1035.

42. Siddique, N., Jawad, M., Waheed, S. Work place air particulate monitoring of automobile workshops for public health and safety (2013) Journal of Radioanalytical and Nuclear Chemistry, 295 (1), pp. 179-190.

43. Santoso, M., Dwiana Lestiani, D., Hopke, P.K. Atmospheric black carbon in PM2.5 in Indonesian Cities (2013) Journal of the Air and Waste Management Association, 63 (9), pp. 1022-1025.

44. Félix, P.M., Almeida, S.M., Pinheiro, T., Sousa, J., Franco, C., Wolterbeek, H.T. Assessment of exposure to metals in lead processing industries (2013) International Journal of Hygiene and Environmental Health, 216 (1), pp. 17-24.

45. Ofosu, F.G., Hopke, P.K., Aboh, I.J.K., Bamford, S.A. Biomass burning contribution to ambient air particulate levels at Navrongo in the Savannah zone of Ghana (2013) Journal of the Air and Waste Management Association, 63 (9), pp. 1036-1045.

46. Waheed, S., Jaafar, M.Z., Siddique, N., Markwitz, A., Brereton, R.G. PIXE analysis of PM 2.5 and PM 2.5-10 for air quality assessment of Islamabad, Pakistan: Application of chemometrics for source identification (2012) Journal

of Environmental Science and Health - Part A Toxic/Hazardous Substances and Environmental Engineering, 47 (13), pp. 2016-2027.

47. Tahri, M., Bounakhla, M., Bouh, H.A., Benyaich, F., Noack, Y., Essaid, B. Application of nuclear analytical techniques (XRF and NAA) to the evaluation of air quality in Moroccan cities - Case of Meknes city (2012) Carpathian Journal of Earth and Environmental Sciences, 7 (2), pp. 231-238.

48. Siddique, N., Waheed, S., Daud, M., Markwitz, A., Hopke, P.K. Air quality study of Islamabad: Preliminary Results (2012) Journal of Radioanalytical and Nuclear Chemistry, 293 (1), pp. 351-358.

49. Yahiaoui, F., Benrachedi, K., Belamri, M. Air pollution by fraction particulate matters PM10, PM2.5 in the site of algiers centers (2012) Asian Journal of Chemistry, 24 (3), pp. 1033-1037.

50. Ezeh, G.C., Obioh, I.B., Asubiojo, O.I., Abiye, O.E. PIXE characterization of PM10 and PM2.5 particulates sizes collected in Ikoyi Lagos, Nigeria (2012) Toxicological and Environmental Chemistry, 94 (5), pp. 884-894.

51. Villeneuve, J., Palacios, J.H., Savoie, P., Godbout, S. A critical review of emission standards and regulations regarding biomass combustion in small scale units (<3MW) (2012) Bioresource Technology, 111, pp. 1-11.

52. Xiao, C., Zhang, G., Huang, D., Ni, B., Liu, C., Qin, Y., Sun, H., Wang, P., Tian, W. Preliminary study on air pollution source identification in Xinzhen, Beijing, using NAA and PIXE (2012) Journal of Radioanalytical and Nuclear Chemistry, 291 (1), pp. 95-100.

53. Almeida, S.M., Silva, A.V., Freitas, M.C., Marques, A.M., Ramos, C.A., Silva, A.I., Pinheiro, T. Characterization of dust material emitted during harbour activities by k0-INAA and PIXE (2012) Journal of Radioanalytical and Nuclear Chemistry, 291 (1), pp. 77-82.

54. Tu, L.-K., Wu, Y.-L., Wang, L.-C., Chang-Chien, G.-P. Distribution of polybrominated dibenzo-p-dioxins and dibenzofurans and polybrominated diphenyl ethers in a coal-fired power plant and two municipal solid waste incinerators (2011) Aerosol and Air Quality Research, 11 (5), pp. 596-615.

55. Huggins, F.E., Galbreath, K.C., Eylands, K.E., Van Loon, L.L., Olson, J.A., Zillioux, E.J., Ward, S.G., Lynch, P.A., Chu, P. Determination of nickel species in stack emissions from eight residual oil-fired utility steam-generating units (2011) Environmental Science and Technology, 45 (14), pp. 6188-6195.

56. Mansouri, N., Firouzbakhsh, M., Hesami, Z. Determination of aerosol emission and bag filter efficiency in fire-proof products industries (2011) Iran Occupational Health, 8 (2), pp. 5-13.

57. Ogawa, H., Dahl, P.J., Suzuki, T., Kai, P., Takai, H. A microbiological-based air cleaning system using a two-step process for removal of ammonia in discharge air from a pig rearing Building (2011) Biosystems Engineering, 109 (2), pp. 108-119.

58. Rahman, S.A., Hamzah, M.S., Wood, A.K., Elias, M.S., Salim, N.A.A., Sanuri, E. Sources apportionment of fine and coarse aerosol in Klang Valley, Kuala Lumpur using positive matrix factorization (2011) Atmospheric Pollution Research, 2 (2), pp. 197-206.

59. Santoso, M., Lestiani, D.D., Mukhtar, R., Hamonangan, E., Syafrul, H., Markwitz, A., Hopke, P.K. Preliminary study of the sources of ambient air pollution in Serpong, Indonesia (2011) Atmospheric Pollution Research, 2 (2), pp. 190-196.

60. Seneviratne, M.C.S., Waduge, V.A., Hadagiripathira, L., Sanjeewani, S., Attanayake, T., Jayaratne, N., Hopke, P.K. Characterization and source apportionment of particulate pollution in Colombo, Sri Lanka (2011) Atmospheric Pollution Research, 2 (2), pp. 207-212.

61. Žitnik, M., Kastelic, A., Rupnik, Z., Pelicon, P., Vaupetič, P., Bučar, K., Novak, S., Samardžija, Z., Matsuyama, S., Catella, G., Ishii, K. Time-resolved measurements of aerosol elemental concentrations in indoor working Environments (2010) Atmospheric Environment, 44 (38), pp. 4954-4963.

62. Themelis, N.J. Chlorine sources, sinks, and impacts in wte power plants (2010) 18th Annual North American Waste-to-Energy Conference, NAWTEC18, pp. 77-84.

63. Razos, P., Christides, A. An investigation on heavy metals in an industrial area in Greece (2010) International Journal of Environmental Research, 4 (4), pp. 785-794.

64. Ait Bouh, H., Benyaich, F., Bounakhla, M., Noack, Y., Zahry, F., Tahri, M. Atmospheric particulate matter characterisation in meknes city [Caracterisations de la matiere particulaire atmospherique dans la ville de meknes] (2010) Physical and Chemical News, 54, pp. 47-54.

65. Mkoma, S.L., Wang, W., Maenhaut, W. Seasonal variation of water-soluble inorganic species in the coarse and fine atmospheric aerosols at Dar es Salaam, Tanzania (2009) Nuclear Instruments and Methods in Physics Research, Section B: Beam Interactions with Materials and Atoms, 267 (17), pp. 2897-2902.

66. Farinha, M.M., Verburg, T.G., Freitas, M.C., Wolterbeek, H.Th. Local and regional sources as given by aerosol measurements and biomonitoring at Sado estuary area, Portugal (2009) Journal of Radioanalytical and Nuclear Chemistry, 281 (2), pp. 299-305.

67. Jasan, R.C., Plá, R.R., Invernizzi, R., Dos Santos, M. Characterization of atmospheric aerosol in Buenos Aires, Argentina (2009) Journal of Radioanalytical and Nuclear Chemistry, 281 (1), pp. 101-105.

68. Mkoma, S.L., Maenhaut, W., Chi, X., Wang, W., Raes, N. Chemical composition and mass closure for PM10 aerosols during the 2005 dry season at a rural site in Morogoro, Tanzania (2009) X-Ray Spectrometry, 38 (4), pp. 293-300.

69. Zghaid, M., Noack, Y., Bounakla, M., Benyaich, F. Atmospheric particulate pollution in Kenitra (Morocco) [Pollution atmosphérique particulaire dans la ville de Kenitra (Maroc)] (2009) Pollution Atmospherique, (203), pp. 313-324.

70. Dos Santos, M., Gómez, D., Dawidowski, L., Gautier, E., Smichowski, P. Determination of water-soluble and insoluble compounds in size classified airborne particulate matter (2009) Microchemical Journal, 91 (1), pp. 133-139.

71. Mkoma, S.L., Maenhaut, W., Chi, X., Wang, W., Raes, N. Characterisation of PM10 atmospheric aerosols for the wet season 2005 at two sites in East Africa (2009) Atmospheric Environment, 43 (3), pp. 631-639.

72. Jones, J.K., Mashek, J.W., Gifford, J.B. Multi-pollutant control project at Cholla unit 4 (2008) Air and Waste Management Association - 7th Power Plant Air Pollutant Control 'Mega' Symposium 2008, 2, pp. 863-877.

73. Jasiulionis, R., Rožkov, A. The solubility of the aerosol, 137Cs and 60Co carrier, in the Ignalina Nuclear Power Plant region (2008) Applied Radiation and Isotopes, 66 (12), pp. 1992-1998.

74. Cushing, K.M., Grubb, W.T., Corina, B.V., Chang, R.L. Long-term COHPAC baghouse performance at Alabama Power Company's E. C. Gaston Units 2 & 3 (2008) Air and Waste Management Association - 7th Power Plant Air Pollutant Control 'Mega' Symposium 2008, 2, pp. 1040-1055.

75. Pitea, D., Bortolami, M., Collina, E., Cortili, G., Franzoni, F., Lasagni, M., Piccinelli, E. Prevention of PCDD/F formation and minimization of their emission at the stack of a secondary aluminum casting plant (2008) Environmental Science and Technology, 42 (19), pp. 7476-7481.

76. Tsopelas, F., Tsakanika, L.-A., Ochsenkühn-Petropoulou, M. Extraction of arsenic species from airborne particulate filters-Application to an industrial area of Greece (2008) Microchemical Journal, 89 (2), pp. 165-170.

77. Santoso, M., Hopke, P.K., Hidayat, A., Diah Dwiana L. Sources identification of the atmospheric aerosol at urban and suburban sites in Indonesia by positive matrix factorization (2008) Science of the Total Environment, 397 (1-3), pp. 229-237.

78. Almeida, S.M., Freitas, M.C., Pio, C.A. Neutron activation analysis for identification of African mineral dust transport (2008) Journal of Radioanalytical and Nuclear Chemistry, 276 (1), pp. 161-165.

79. Yang, W.-T., Ni, B.-F., Wang, P.-S., Tian, W.-Z., Sun, A.-H., Shen, L., Xiao, C.-J., Zhang, G.-Y., Gao, D.-H., Liu, C.-X., Huang, D.-H., Zhou, S.-C., Hu, L., Lu, P. Element composition analysis of airborne particulate matter (PM10

and PM2.5) by instrument neutron activation analysis (2007) Yuanzineng Kexue Jishu/Atomic Energy Science and Technology, 41 (2), pp. 228-231.

80. England, G.C., Watson, J.G., Chow, J.C., Zielinska, B., Chang, M.-C.O., Loos, K.R., Hidy, G.M. Dilution-based emissions sampling from stationary sources: Part 2—gas-fired combustors compared with other fuel-fired systems (2007) Journal of the Air and Waste Management Association, 57 (1), pp. 79-93.

81. Jones, J.K. Multi-pollutant control project at hunting ton unit 2 (2006) Proceedings of the EPA-DOE-EPRI-A and WMA Power Plant Air Pollutant Control Mega Symposium 2006, 3, pp. 1177-1189.

82. Vieira, B.J., Biegalski, S.R., Freitas, M.C., Landsberger, S. Atmospheric trace metal characterization in industrial area of Lisbon, Portugal (2006) Journal of Radioanalytical and Nuclear Chemistry, 270 (1), pp. 55-62.

83. Ocskay, R., Salma, I., Wang, W., Maenhaut, W. Characterization and diurnal variation of size-resolved inorganic water-soluble ions at a rural background site (2006) Journal of Environmental Monitoring, 8 (2), pp. 300-306.

84. Chung, Y.-S., Kim, S.-H., Moon, J.-H., Kim, Y.-J., Lim, J.-M., Lee, J.-H. Source identification and long-term monitoring of airborne particulate matter (PM2.5/PM10) in an urban region of Korea (2005) Journal of Radioanalytical and Nuclear Chemistry, 267 (1), pp. 35-48.

85. Chung, Y.-S., Kim, S.-H., Moon, J.-H., Kim, Y.-J., Lim, J.-M., Lee, J.-H. Analysis of urban dust (PM2/PM10-2) in Daejeon city by instrumental neutron activation analysis (2005) Journal of Radioanalytical and Nuclear Chemistry, 267 (1), pp. 95-107.

86. Al-Momani, I.F., Daradkeh, A.S., Haj-Hussein, A.T., Yousef, Y.A., Jaradat, Q.M., Momani, K.A. Trace elements in daily collected aerosols in Al-Hashimya, central Jordan (2005) Atmospheric Research, 73 (1-2), pp. 87-100.

87. Freitas, M.C., Almeida, S.M., Reis, M.A., Ventura, M.G. Neutron activation analysis: Still a reference method for air particulate matter measurements (2004) Journal of Radioanalytical and Nuclear Chemistry, 262 (1), pp. 235-239.

88. Athari, M., Sohrabpour, M., Shahriari, M., Rostami, S. Elemental characterization of TSP and two size fractions of airborne particulate matter from Tehran by INAA and AAS (2004) Journal of Radioanalytical and Nuclear Chemistry, 260 (2), pp. 351-356.

89. Lei, C., Landsberger, S., Basunia, S., Tao, Y. Study of PM 2.5 in Beijing suburban site by neutron activation analysis and source apportionment (2004) Journal of Radioanalytical and Nuclear Chemistry, 261 (1), pp. 87-94.

90. Begum, B.A., Kim, E., Biswas, S.K., Hopke, P.K. Investigation of sources of atmospheric aerosol at urban and semi-urban areas in Bangladesh (2004) Atmospheric Environment, 38 (19), pp. 3025-3038.

91. Kane, L., Romanow, S., Meche, H. New developments: Continuous emissions monitoring system (2004) Hydrocarbon Processing, 83 (2 SECTION 1), p. 98.

92. Farinha, M.M., Freitas, M.C., Almeida, S.M. Air quality control monitoring at an urban and industrialized area (2004) Journal of Radioanalytical and Nuclear Chemistry, 259 (2), pp. 203-207.

93. Záray, G., Óvári, M., Salma, I., Steffan, I., Zeiner, M., Caroli, S. Determination of platinum in urine and airborne particulate matter from Budapest and Vienna (2004) Microchemical Journal, 76 (1-2), pp. 31-34.

94. Solyar, B.Z., Glazov, L.Sh., Liberzon, I.M., Aladysheva, E.Z., Knyaz'kov, A.L., Nikitin, A.A., Kirillov, D.V., Zaitsev, A.V., Kazakov, A.K., Danilov, N.A. Replacement of electrofilters in an external cyclone system for dust removal from regeneration stack gases on the 1A/1M unit (2003) Chemistry and Technology of Fuels and Oils, 39 (6), pp. 326-329.

95. Chung, Y.-S., Moon, J.-H., Park, K.-W., Kim, S.-H., Lee, J.-H., Lee, K.-Y. Airborne particulates (PM2.5/PM10) monitoring in Korea by instrumental neutron activation analysis (2002) Journal of Radioanalytical and Nuclear Chemistry, 254 (1), pp. 117-128.

96. Costa, C.J., Marques, A.P., Freitas, M.C., Reis, M.A., Oliveira, O.R. A comparative study for results obtained using biomonitors and PM10 collectors in Sado Estuary (2002) Environmental Pollution, 120 (1), pp. 97-106.

97. Maenhaut, W., De Ridder, D.J.A., Fernández-Jiménez, M.-T., Hooper, M.A., Hooper, B., Nurhayati, M. Long-term observations of regional aerosol composition at two sites in Indonesia (2002) Nuclear Instruments and Methods in Physics Research, Section B: Beam Interactions with Materials and Atoms, 189 (1-4), pp. 259-265.

98. Maenhaut, W., Schwarz, J., Cafmeyer, J., Chi, X. Aerosol chemical mass closure during the EUROTRAC-2 AEROSOL Intercomparison 2000 (2002) Nuclear Instruments and Methods in Physics Research, Section B: Beam Interactions with Materials and Atoms, 189 (1-4), pp. 233-237.

99. Tries, M.A., Holloman, R.L., Bobek, L.M. Predicted responses for a particulate detection system in a continuous stack monitör (2002) Health Physics, 83 (4), pp. 558-566.

100. Cao, L., Tian, W., Ni, B., Zhang, Y., Wang, P. Preliminary study of airborne particulate matter in a Beijing sampling station by instrumental neutron activation analysis (2002) Atmospheric Environment, 36 (12), pp. 1951-1956.

101. John, A.C., Kuhlbusch, T.A.J., Fissan, H., Schmidt, K.-G. Size-fractionated sampling and chemical analysis by total-reflection X-ray fluorescence spectrometry of PMx in ambient air and emissions (2001) Spectrochimica Acta - Part B Atomic Spectroscopy, 56 (11), pp. 2137-2146.

102. Wada, E.T., Sterling, A.M. Development and evaluation of a mass spectrometer-based continuous emission monitor for volatile organic compound emmissions from combustion devices (2001) Waste Management, 21 (5), pp. 477-482.

103. Zandaryaa, S., Gavasci, R., Lombardi, F., Fiore, A. Nitrogen oxides from waste incineration: Control by selective non-catalytic reduction (2001) Chemosphere, 42 (5-7), pp. 491-497.

104. Yang, S., Dong, J., Cheng, B. Characteristics of air particulate matter and the sources in urban and rural area of Beijing, China (2000) Journal of Environmental Sciences, 12 (4), pp. 402-409.

105. Yatin, M., Tuncel, S., Aras, N.K., Olmez, I., Aygun, S., Tuncel, G. Atmospheric trace elements in Ankara, Turkey: 1. factors affecting chemical composition of fine particles (2000) Atmospheric Environment, 34 (8), pp. 1305-1318.

106. Gaikwad, R.P. Symposium offers latest in air emissions control: Other technologies: Evaluate PM2.5 controls (1999) Power, 143 (6), p. 76.

107. Carter, S.R. Removing VOCs from air streams (1999) Chemical Engineering and Technology, 22 (8), p. 638.

108. Chung, Y.S., Moon, J.H., Chung, Y.J., Cho, S.Y., Kang, S.H. Study on air pollution monitoring in Korea using low volume air sampler by instrumental neutron activation analysis (1999) Journal of Radioanalytical and Nuclear Chemistry, 240 (1), pp. 79-94.

109. Aldape, F., Hernández-Méndez, B., Flores M, J. Manganese survey in airborne particulate matter from a mining area at Hidalgo State, Mexico (1999) Nuclear Instruments and Methods in Physics Research, Section B: Beam Interactions with Materials and Atoms, 150 (1-4), pp. 363-369.

110. Parr, R.M., Smodiš, B. Health-related monitoring and assessment of airborne particulate matter: An overview of recent IAEA programs (1999) Biological Trace Element Research, 71-72, pp. 169-179.

111. Alves, L.C., Reis, M.A., Freitas, M.C. Air particulate matter characterisation of a rural area in Portugal (1998) Nuclear Instruments and Methods in Physics Research, Section B: Beam Interactions with Materials and Atoms, 136-138, pp. 941-947.

112. Alves, L.C., Reis, M.A., Freitas, M.C., Gouveia, M.A. Elemental Analysis of Particulate Matter and Source Identification in Lisbon (1998) X-Ray Spectrometry, 27 (5), pp. 313-320.

113. Hopke, P.K., Xie, Y., Raunemaa, T., Biegalski, S., Landsberger, S., Maenhaut, W., Artaxo, P., Cohen, D. Characterization of the gent stacked filter unit pm10 sampler (1997) Aerosol Science and Technology, 27 (6), pp. 726-735.

114. Imhoff, Robert E., Brown, Craig Measuring particle and speciated gas-phase Hg in plumes from coal-fired steam plants (1996) Proceedings of the Air & Waste Management Association's Annual Meeting & Exhibition, pp. 14pp.

115. Matz, G., Mnchmeyer, W., Walte, A. Automated analysis of PAH in emissions with thermal desorption and GC/MS (1996) Journal of Automatic Chemistry, 18 (3), p. 101.

116. Maenhaut, W., François, F., Cafmeyer, J., Okunade, O. Size-fractionated aerosol composition at Gent, Belgium. Results from a one-year study (1996) Nuclear Instruments and Methods in Physics Research, Section B: Beam Interactions with Materials and Atoms, 109-110, pp. 476-481.

117. Otten, P., Injuk, J., Van Grieken, R. Elemental concentrations in atmospheric particulate matter sampled on the North Sea and the English Channel (1994) Science of the Total Environment, The, 155 (2), pp. 131-149.

118. Nudo, Lori Capturing heavy metals (1993) Pollution Engineering, 25 (14), pp. 80-82.

119. Rogers, C.F., Watson, J.G., Jr., Mathai, C.V. Design and Testing of a New Size Classifying Isokinetic Sequential Aerosol Sampler (1989) Journal of the Air Pollution Control Association, 39 (12), pp. 1569-1576.

120. Gillette, D.A., Clayton, R.N., Mayeda, K., Sridhar, K. Tropospheric aerosols from some major dust storms of the southwestern United States. (1978) Journal of Applied Meteorology, 17 (6), pp. 832-845.

B. Data logger system user manual

The particle sampler device is initiated by pushing the power switch to “1” position, so that the device receives power. At this stage, the sampling switch, which is black, should stay on “0” position in order not to initiate sampling immediately it receives power.

After the power switch is on, the main menu is displayed after 2 seconds of intro screen.

The main menu view:

AA/GG SS:DD:ss (date and time)

YESIL = KAYITLAR

KIRMIZI = SAAT-AYAR

DURUM=0 XXXXX

Initiation of sampling: In order to start sampling, pushing the sampling switch to “1” position is sufficient. When it is in “1” position, the pump is connected to power and starts to operate.

Display view during the sampling:

BAS= AA/GG SS:DD:ss

FM1=XX.XXX SAY=0-6

FM2=XX.XXX SAN=XX

FM3=XX.XXX TOP=XXXXX

In the first line, start and finish date and time are displayed. In the following 3 three lines, 10 seconds flow data from each mass flow meter is displayed. “SAY” stands for the number of the 10 second interval (0 – 6), “SAN” displays the seconds in the current minute, and “TOP” reveals the total minutes throughout the sampling.

Termination of the sampling: Sampling can be finished any time by pushing the sampling switch to “0” position. Following the first 1-minute cycle is complete, the microcontroller terminates the sampling and returns to main menu display.

Power cut: In the case of power source is down, the system resumes the sampling process as soon as the power is back on.

Reading the records: The green button is pressed while on main menu and the records menu is displayed.

Records display view:

SON KAYIT NO= XXX

KIRMIZI= TARIH

SARI= SONUCLAR

YESIL= ESKI SONUCLAR

In this menu, the most recent sampling information is displayed.

Sampling history display view:

KAYIT NO= XXX

BAS= YY/AA/GG SS:DD (Sampling start time and date)

BIT= YY/AA/GG SS:DD (Sampling finisg time and date)

KESSAY= XXX SARI=GERI

KESSAY: Reveals the number of power cuts during the sampling

By pressing the yellow button, the device will return to previous menu (records display).

In the records menu, the results can be seen by pressing yellow button.

Results display view:

FM1=XXXXX.XXX

FM2=XXXXX.XXX

FM3=XXXXX.XXX

TOP= XXXXX KIR=GERI

In the first three lines, the outcomes gathered from each flow meter is displayed. These values represent the total volume of air withdrawn by each channel during the sampling, in liters. In the last line, “TOP” represents the duration of the sampling, in minutes. In this menu, the red button returns to records menu.

Reading the previous records: In the records menu, green button allows to display previous sampling records.

Previous records display

KAYIT NO= XXX

KIRMIZI= TARIH

SARI= SONUCLAR

YESIL= Eski Kayıt

Record number is decreased by pressing the green button, until the desired record number is reached. In each record number, the red button allows to display the time and date of the sampling and the yellow button allows to display the results of the sampling, as explained before.

Setting time: In the case time needs to be set, it can be conducted by pressing red button on main menu. Following the explanations on display, the time can be set to reflect the real time.